Effects of Wet Mat Curing Time and Earlier Loading on Long-Term Durability of Bridge Decks: Fracture, Flexural Strength and Shrinkage

Authors: Sanjaya Senadheera, Randall Scott Phelan, Aruna Amarasiri, and Hari Aamidala

Notice

Technical Report Documentation Page

1. Report No.: FHWA/TX -09-2116-4B	2. Government Accession No.:	3. Recipient's Catalog No.:
4. Title and Subtitle: Effects of Wet Mat Curing Time and Earlier Loading on Long-Term Durability of Bridge Decks: Fracture, Flexural Strength and Shrinkage		5. Report Date: January 2009
		6. Performing Organization Code:
7. Author(s): Sanjaya Senadheera, Randall S. Phelan, Aruna Amarasiri, Hari Aamidala		8. Performing Organization Report No. 0-2116-4B
9. Performing Organization Name and Address: Texas Tech University College of Engineering Box 41023 Lubbock, Texas 79409-1023		10. Work Unit No. (TRAIS):
		11. Contract or Grant No. : Project 0-2116
12. Sponsoring Agency Name and Address Texas Department of Transportation Research and Technology P. O. Box 5080 Austin, TX 78763-5080		13. Type of Report and Period Cover: Final Report 04/07/99 - 08/31/04
		14. Sponsoring Agency Code:
15. Supplementary Notes: This study was conducted in cooperation with the Texas Department of Transportation and the Federal Highway Administration		

Abstract: There is increasing pressure from owners, contractors, and the public to open bridge decks sooner to full traffic loads. As a result, a set of criteria or guidelines is needed to determine when concrete bridge decks can safely be opened. Today, current practice allows many bridge decks and concrete pavements to be opened to traffic once a desired compressive strength is achieved from a representative field-cast test cylinder. Though generally untrue, many believe that this strength value serves as a measure of the durability of the placed concrete. In a collaborative research effort between Texas Department of Transportation and researchers at Texas Tech University, studies were undertaken to collect research data that could potentially lead to the development of new guidelines as to when bridge decks can be open to (a) construction traffic and (b) full traffic without sacrificing concrete durability. This report presents detailed findings of three tests – fracture, flexural strength and shrinkage.

17. Key Words: concrete, bridge, deck, durability, curing, wet mat, vehicle loading, early loading		Distribution Statement No restrictions. This report available to the public through the National Technical Information Service, Springfield, Virginia 22616 www.ntis.gov	
19. Security Classif. (of this report) Unclassified	20. Security Classif. (of this page) Unclassified	21. No. of Pages 128	22. Price

Form DOT F 1700.7 (8-72)

EFFECTS OF WET MAT CURING TIME AND EARLIER LOADING ON LONG-TERM DURABILITY OF BRIDGE DECKS: FRACTURE, FLEXURAL STRENGTH AND SHRINKAGE

by

Sanjaya Senadheera, Randall S. Phelan,

Hari Aamidala and Aruna Amarasiri

Report 0-2116-4B

conducted for the

by the

CENTER FOR MULTIDISCIPLINARY RESEARCH IN TRANSPORTATION

TEXAS TECH UNIVERSITY

September 2009

AUTHOR'S DISCLAIMER

The contents of this report reflect the views of the authors who are responsible for the facts and the accuracy of the data presented herein. The contents do not necessarily reflect the official view of policies of the Texas Department of Transportation or the Federal Highway Administration. This report does not constitute a standard, specification, or regulation.

PATENT DISCLAIMER

There was no invention or discovery conceived or first actually reduced to practice in the course of or under this contract, including any art, method, process, machine, manufacture, design or composition of matter, or any new useful improvement thereof, or any variety of plant which is or may be patentable under the patent laws of the United States of America or any foreign country.

ENGINEERING DISCLAIMER

Not intended for construction, bidding, or permit purposes.

TRADE NAMES AND MANUFACTURERS' NAMES

The United States Government and the State of Texas do not endorse products or manufacturers. Trade or manufacturers' names appear herein solely because they are considered essential to the object of this report.

Table of Contents

<center>List of Tables</center>

List of Figures

CHAPTER I

INTRODUCTION

This report presents detailed findings from research project 0-2116 that are related to cracking of concrete. Topics covered include concrete fracture including fatigue fracture, flexural strength and shrinkage. These topics have been investigated for selected concrete mixtures used by TxDOT with regard to their influence to the duration of wet curing of concrete.

1.1 FRACTURE

1.1.1 Research Objectives

Bridge decks are commonly constructed for the Texas Department of Transportation (TxDOT) by overlaying a layer of concrete on pre-cast deck panels. The concrete used for the overlay typically have compressive strengths between 5,500 and 7,000 psi at 28-day age, contains fly ash or slag, air-entrained, has a 3-4 in. slump and a water-cement ratio between 0.41 and 0.46. According to the current TxDOT specifications (Texas Department of Transportation, 1993a, 1993b), the concrete has to be cured using wet mats for eight days if it contains Type I cement, and for 10 days if it contains Type I/II cement, fly ash or ground granulated blast-furnace slag (ggbs), and vehicular traffic is allowed on the bridge two days after the mats have been removed. There could be significant benefits in opening newly constructed bridge decks to early traffic, which includes quick cessation of disruption to traffic, especially in urban areas and major traffic corridors. Research was carried out at Texas Tech University to determine whether there are any long-term detrimental effects of curtailing curing earlier than currently required by TxDOT and allowing vehicles to traverse the bridge shortly thereafter. As a part of the research, the fracture properties of several medium-strength concrete mixes cured for various durations were investigated. Concrete that is weak in fracture could possibly crack extensively, leading to deterioration of the slabs and allowing the ingress of chlorides from de-icing salts to the reinforcing bars. The results presented in this report stem from this research. This report essentially comprises of findings from experimentation carried out specifically for the determination of fracture properties of bridge deck concrete, and further experimentation designed to follow up on ideas that developed as the work progressed. In addition to fracture and fatigue-fracture properties, the flexural strength and absorption-desorption characteristics of concretes were obtained. The purpose of this research was to obtain data that would compliment and clarify some of the main thrusts of the investigations.

1.1.2 The Variation of Fracture Properties of Medium-Strength Concrete with Duration of Curing and Age

Concrete from San Antonio, El Paso, Pharr, Fort Worth, Atlanta, and Lubbock districts in Texas were used in this study. Fracture properties were obtained at 7-day age and 16-day age, while fatigue fracture properties were obtained at 10-day age and 28-day age. For the experimentation carried out at 7-day age and 10-day age, specimens cured for 4 days and 7 days were tested, while for testing carried out at 16-day age, specimens cured for 2, 4, 8, and 14 days were tested. To obtain size independent fracture properties, three sizes of notched cylinders were used, while the fatigue testing was predominantly carried out on a single size of specimen. Bazant's size-effect law was then used to determine the fracture parameters that best fit the fracture data. The fracture parameters as given by the Jenq-Shah model were also calculated from the size-effect parameters using theoretical correlations.

1.1.3 Investigation of Current Fracture Testing Philosophies

During the experimentation described above, several research ideas were developed and further investigations were performed to follow up on these. These investigations are described in the following paragraphs.

1. Bazant's size-effect law and Jenq and Shah's two-parameter model were considered as choices for the standard for characterizing fracture in concrete. Each model has its own strengths and weaknesses, and given the current discussion among experts in the field, their equivalence is of great interest. Though the fracture toughness, K_{Ic}, is used in both models, the size-effect law uses the size of the fracture process zone, c_f as an additional parameter, while the two-parameter model uses the critical crack-tip opening displacement, $CTOD_c$, for the same. There are theoretical relations between c_f and $CTOD_c$ of which the accuracy can be examined. A good match between the results obtained from both models indicates that it is advantageous to have both models as standards.

2. The size-effect method requires that several sizes of specimens be tested to obtain the parameters that define behavior in fracture. On the other hand, the two-parameter model can be used with specimens of a single size. A decision has to be made by the researcher which size to use in testing. The size that gives the best match with the data obtained from the size-effect law can possibly be the most attractive. This study was designed to determine the size of notched cylinder that is best for this purpose.

3. RILEM standards for the size-effect method (RILEM, 1990a) specify that the specimens of different sizes should be of the same thickness. It is thought that this scheme of dimensioning specimens leads to smaller specimens drying out faster upon the curtailing of curing. An alternative scheme of making specimens progressively "thinner"

with increasing size is proposed by which it can be assured that all specimens cure and dry in a similar manner. The accuracy of data obtained using the proposed scheme is examined herein.

4. The reason the scheme of keeping the thickness constant has not come under criticism so far is that most testing is carried out on specimens continuously moist-cured until a few hours before the time of testing. This practice is contrary to construction practices where curing is carried out for only a limited period of time. Any study carried out on effects of curtailed curing will be affected by the dissimilarity of curing and drying between specimens of different size. A concern in the proposed alternative scheme is the possibility of larger, thinner specimens failing at lower loads than they should because of buckling type effects. This experimental investigation delves into whether there are such effects.

5. In the case of testing using the two-parameter model, the specimen has to be unloaded and reloaded after the peak load has been reached to obtain the effective crack length at failure. The RILEM recommendations (RILEM, 1990b) use both the unloading and reloading compliances to estimate the effective crack length. The personal experience of the author is that the reloading compliance could be significantly affected by slow crack growth. Since the size-effect law gives an independent estimate of the fracture properties it will be possible to ascertain the accuracy of using one or both compliances.

The bulk of research carried out on fracture of concrete has focused on specimens made from coarse aggregate of limited size. The proposed research will use aggregate up to ¾ inch in size to better represent normal concrete.

1.2 FLEXURE

At the time of this research, TxDOT used the 7-day flexural strength as a criterion to evaluate the suitability of concrete for bridge decks. This research project conducted a large number of flexural strength tests on concrete beams cast using several concrete mixes often used by TxDOT in bridge decks. The wet curing durations used were 0, 2, 4, 8, 10 and 14 days. The detailed experimental plan, the results and the findings are outlined in the following chapters of this report.

1.3 SHRINKAGE

1.3.1 Introductory Background

The tendency of concrete to crack has been historically accepted as inevitable. Thus, typically structures have been designed based primarily on strength. This has been true even for concrete bridge decks, though the deterioration and decay of bridge decks has

focused attention on long-term durability in the design of these structures. To truly improve the durability of concrete bridge decks, a good understanding of the behavior of the materials is needed.

Recent studies show that concrete deck cracking is primarily the result of shrinkage caused by drying and by various other factors [Carden and Ramey 1999; French et al. 1999; Issa 1999; Kwak 2000]. The increased concern over the economy of designing heavy structures has resulted in use of high strength concrete. However, with the use of high strength concrete having high modulus of elasticity, cracks at an earlier age have become more common [Weiss 1999]. This increased cracking potential may be attributed to increased brittleness, increased stiffness, decreased creep relaxation, and higher autogenous shrinkage. The increase in autogenous shrinkage is attributed to the use of low water to cementitious material ratio (w/c) in the high strength concrete thereby leading to bridge deck cracking. Stresses caused by heavy traffic volume may further aggravate the deck cracking. However, as will be discussed later, applied stress is not the only cause leading to cracking in concrete.

Concrete has relatively low tensile strength compared to its compressive strength. Thus, though concrete performs well in compression it can easily crack in tension. Concrete undergoes a variety of volumetric changes depending on its constituent materials, curing conditions, and its temperature. These properties of concrete have a significant effect on pore moisture (internal pore relative humidity) and hence on the volume change in concrete. Internal movement of moisture is also substantially affected by the moisture and temperature changes in the surrounding environment.

Apart from the factors described above, the size of the structural member and applied stresses affect shrinkage stresses. All these factors lead to increase in shrinkage stress development even before any external loads were applied. These tensile stresses developed due to shrinkage being greater than the tensile strength of concrete, results in cracking of concrete. Figure 1.1 shows a schematic diagram indicating the development of tensile strength and shrinkage stresses with age. Concrete is expected to crack when the shrinkage stress exceeds the tensile strength of concrete, as indicated by the point of intersection of the curves.

Concrete can be considered as volumetrically stable if it remains at a constant moisture and temperature environment. However, concrete is a composite material in which aggregate is bound by a binder which is the hydrated cementitious material. This binder is formed due to the chemical hydration reaction between water and cementitious materials. The hydration reaction results in a change of internal moisture content even in constant ambient moisture and temperature conditions.
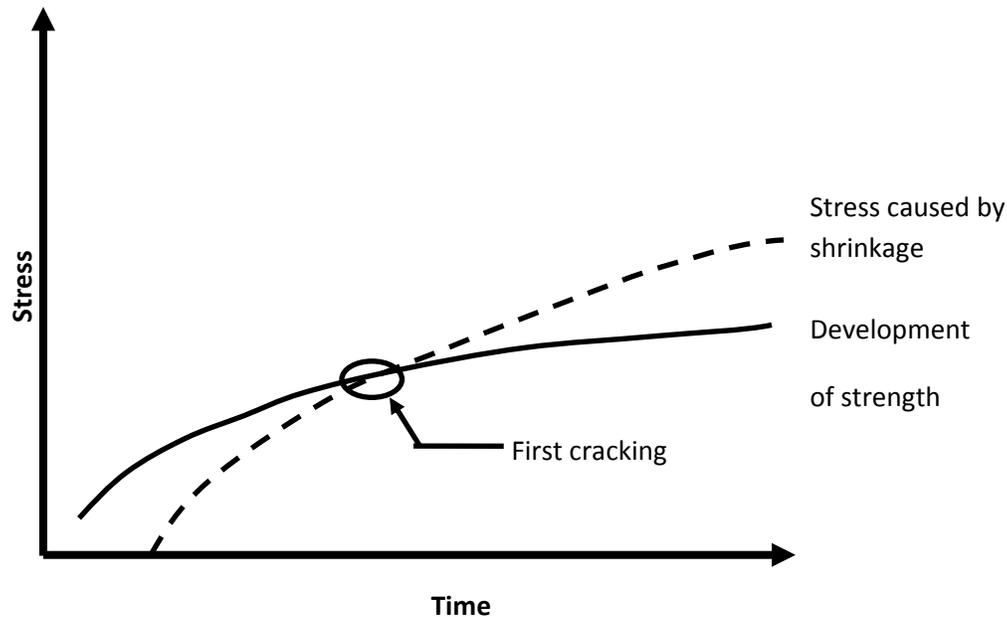
Figure 1.1 Effect of shrinkage and tensile strength development on cracking

Dominant factors affecting transverse cracking in bridge decks are longitudinal end restraint, girder stiffness, deck thickness, concrete shrinkage, concrete modulus of elasticity and ambient air temperature at deck placement [French et al. 1999]. According to the results of earlier research, restrained concrete deck shrinkage is the leading cause of bridge deck cracking [Altoubat 2001; French et al. 1999; Rogalla 1995]. This stresses the need for a good understanding of the effect of concrete shrinkage and restraint on cracking of bridge decks. When concrete is free to shrink or expand without any restraint, it does so without serious consequences. However, bridge decks are often exposed to a certain amount of restraint resulting in significant tensile stresses. These tensile stresses, combined with low fracture resistance of concrete result in cracking.

The increased concern of the effect of shrinkage of concrete on structures has led to several recent theoretical and experimental studies [Shah et al. 1997; Koenders 1997; Altoubat 2001]. Cracks provide a path for corrosive agents to enter the concrete, thereby accelerating the deterioration of reinforcing steel in bridge decks. Cracking can also lead to deterioration of pavements incurring greater costs of repair. Deck cracking and the quality of the top one to two inches of deck concrete has been found to have a significant effect on the durability of concrete bridge decks [Carden and Ramey 1999]. The quality of curing considerably affects the properties of this top layer of deck concrete and, therefore, has a definite impact on the durability of the bridge deck.

Increased concern of early-age cracking in bridge decks and persistent pressure from the public for early opening of bridge decks to full traffic loads has led to the study of curing durations based on potential based on the potential of concrete to shrink and tensile strength. As discussed previously, historically, concrete compressive strength was considered the sole design criterion, and in many cases this continues to be true even today. Current practice typically allows many bridge decks to be opened to traffic once the desired compressive strength is achieved. In general, the required compressive strength is considered to be obtained once field-cast cylinders reach he required strength. Again, though strength typically has been considered to be the primary criterion for assessing the quality of the concrete, other criteria are required to fully understand the durability of the placed concrete. For example, since early-age deterioration can reduce the useful life of the structure, an increased need to better understand the durability of concrete decks has developed.

Shrinkage cracking in concrete depends on several factors including the rate and magnitude of free shrinkage, degree of structural restraint and fracture resistance. Though no standard testing procedure exists to assess the potential for cracking, several researchers have used the ring-test [Weiss 1999] and restrained shrinkage tests [Altoubat 2001; Koenders 1997; Sule 2003].

In this research a variety of bridge deck mixes were tested for free or unrestrained shrinkage. As discussed previously, in a structure under restraint, free shrinkage causes cracks. Free shrinkage strain alone does not provide sufficient information to characterize the behavior of restrained concrete. Therefore additional tests have been conducted to obtain the tensile strength and elastic modulus for different concrete mixes in order to predict the age of first shrinkage induced crack under full restraint. However, the degree of restraint in bridge decks is difficult to evaluate, thus the accurate prediction of shrinkage cracking is complicated. Also, with numerous other factors that are difficult or impossible to assess completely, such as actual mix composition, curing temperatures, finishing techniques, etc., combined with the varying degrees of restraint, typically prevents accurate prediction of shrinkage cracking. Nevertheless, the approach used in this research will give relative prediction of age of shrinkage induced first crack. This information can be used to better understand the effects of curing on shrinkage induced cracking and to compare different curing durations.

1.3.2 Curing Practices

In Texas, the requirement for wet-mat curing is 8 days for decks with Type I and III cements and 10 days for decks with Type II and I/II cements and for mix designs with fly ash [TxDOT 1993]. According to the 1993 Texas Standard Specifications at least 14 days should be given after the last slab concrete has been in place for construction traffic on

structures with a maximum of ¾ ton vehicles and 21 days may be given for other construction traffic or for the full traffic [TxDOT 1993].

Increased congestion of traffic during the construction and repair work on highways has led to the need for early opening of bridge decks to traffic. Attempting to decrease the time of construction and repair has been the focus of numerous researchers. Research conducted by TxDOT has led to incorporation of the *special provisions to Item 420 – Concrete Structures* into standard practice. These special provisions, adopted in 1998, allow the opening of the bridge deck to full traffic much sooner than the 21 days as required by the 1993 specifications. According to these special provisions, once the concrete is cured sufficiently, the deck is allowed to dry for one day to let it prepare for the surface treatment and an additional day was typically allowed for any required surface treatment [TxDOT 1998]. The bridge deck is then opened to full traffic if the design compressive strength is gained. In general the compressive strength is determined using site cast concrete cylinder specimens.

As a result, bridge decks in Texas are currently opened to full traffic in 10 to 12 days after the concrete is placed, leading to a significant decrease in the time of congestion on the highways. Although this current practice reduces the number of days before full traffic load is allowed on bridge decks compared to 1993 specifications it does not reduce the number of wet mat curing days. This thesis is particularly aimed at investigating the effect of different curing durations on the early age strength development in order to assess the resistance of concrete to shrinkage induced cracking. As the conclusion of this study, a better understanding of the effects of curing on long term durability of bridge decks is expected.

1.3.3 Objectives and Scope

Different tests have been conducted to investigate the time-dependent development of material properties including free shrinkage, modulus of elasticity in compression and split tensile strength tests for several bridge deck mix designs in Texas. The tensile strength approach was adopted as it was considered to be the best available approach to study the effects of curing duration on shrinkage cracking potential of concrete. The concrete mixes used in this reserach were the mostly commonly used in different climatic zones in Texas. They had varying w/c ratios, cement contents, air contents, and varying types and contents of cementitious materials. The different tests conducted and measurements taken for these different mixes are shown in Table 1.1.

Table 1.1 Tests Conducted on Different TxDOT District Mixes

	Free Shrinkage Tests	Weight & Temperature Measurements	Modulus of Elasticity Test	Split Tensile Test
Atlanta	✓			
Houston	✓			
El Paso	✓		✓	✓
San Antonio	✓		✓	✓
Pharr	✓	✓		
Fort Worth	✓	✓	✓	✓
Lubbock	✓	✓	✓	✓

✓ shows that, that particular test was performed on the TxDOT district mix
✓

The free shrinkage strains were used to compare different curing durations for all the mixes shown in Table 1.1. Prediction of age of first shrinkage induced crack was only possible for El Paso, San Antonio, Fort Worth, and Lubbock district mixes, as the modulus of elasticity and tensile strength data was not available for other district mixes. The test plan, different tests conducted, results and findings are discussed in the following chapters of this report

The predicted ages of first shrinkage induced cracks for the four district mixes i.e. El Paso, San Antonio, Fort Worth, and Lubbock was used to understand the effect of curing on shrinkage-induced cracks in concrete bridge decks. It is anticipated that the knowledge gained through this work can be used to optimize the number of curing days and age required before full traffic can be allowed on bridge decks in Texas.

Chapter 2 of this report provides detailed information on the experimental program for all three tests outlined above. Chapter 3 provides the results and a discussion of them and Chapter 4 summarizes the key findings and the conclusions.

CHAPTER II

EXPERIMENTAL PROCEDURES

2.1 FRACTURE

This chapter is subdivided as follows: Section 2.1.1 contains the details of the procedure used to find the fracture properties of concretes using the size-effect law. The procedure has been modified from the one give by RILEM (1990a) to accommodate the change in specimen geometry from notched beams to notched cylinders. Section 2.1.2 contains the experimental procedure to be used in determining the fracture parameters as defined by the Jenq-Shah model. Section 2.1.3 details the mix designs examined, while section 2.1.4 and section 2.1.5 explains the procedures used in the production and curing of test specimens respectively. The methodologies used in carrying out the tests are provided in section 2.1.6.

2.1.1 Size-Effect Method

The basic relationships that will be used can be expressed by the following equations. For a comparison of the stress levels at failure between the different sizes of specimens to be carried out, a nominal stress at failure must be defined as

$$\sigma_{Nu} = c_n \left(\frac{P_u}{bd} \right).$$

(2.1)

In the case of the notched cylinder, the nominal stress can be set equal to the maximum principal tensile stress generated in a full cylinder (without a notch) by setting $c_n = 2/\pi$ and

$$\sigma_{Nu} = \left(\frac{2P_u}{\pi bd} \right).$$

(2.2)

According to the size-effect law,

$$\sigma_{Nu} = \frac{K_{Ic}}{\sqrt{k^2(\alpha_0)d + 2k(\alpha_0)k'(\alpha_0)c_f}}.$$

(2.3)

By rearranging,

$$\left(\frac{1}{\sigma_{Nu}}\right)^2 = \frac{k^2(\alpha_0)d}{K_{Ic}^{\ 2}} + \frac{2k(\alpha_0)k'(\alpha_0)c_f}{K_{Ic}^{\ 2}} \ . \tag{2.4}$$

It should be noted that Equation 2.4 is valid only for the size ranges where a reversal of the size-effect has not taken place, as it sometimes does for notched cylinders (Bazant and Planas, 1998). Several alternative equations have been proposed for $k(\ )$ for notched cylinders. Petroski and Odrovic (1986) suggested

$$k(\alpha) = (0.9566 + 0.6779\alpha - .9932\alpha^2 + 2.6773\alpha^3)\sqrt{\frac{\pi\alpha}{2}} \tag{2.5}$$

The value of α, which is the ratio of the width of the notch to the diameter of the cylinder, was 1/6 for all the cylinders reported herein. The values shown in Table 2.1 were obtained using the above equations for this value of α. It should be noted that $g(\alpha) = k^2(\alpha)$, and $g'(\alpha) = 2k(\alpha).k'(\alpha)$.

Table 2.1. Values of Stress Intensity Functions as Given by Several Authors

Reference	$k(\alpha)$	$k'(\alpha)$	$g(\alpha)$	$g'(\alpha)$
Petroski and Odrovic	0.539492	1.910095	0.291052	2.060964
Tang et al.	0.532922	1.856264	0.284005	1.978487
Bazant et al.	0.519065	1.785399	0.269428	1.853475

Concrete specimens being tested in fracture are loaded with bearing strips at the load points to avoid localized crushing. Unlike in three-point bending test of beams, the width of the loading strips affects the magnitude of the stress intensity factor generated at the crack-tip in notched cylinders (Tang, 1994). Therefore, the function $k(\alpha)$ in the case of the notched cylinder is dependent on the ratio (β) between the loading strip width and diameter of cylinder, and it is taken into account in Equation 2.6, which is adapted from the work by Tang (1994).

$$k(\alpha, \beta) = \sqrt{\frac{\pi\alpha}{2}}(L_0(\beta) + L_1(\beta)\alpha + L_2(\beta)\alpha^2 + L_3(\beta)\alpha^3) \tag{2.6}$$

The values for L_0, L_1, L_2, and L_3 for a number of values of β have been obtained by Tang using FEA. The ASTM specification for obtaining the tensile strength of concrete using the split-cylinder test on un-notched specimens (ASTM, 2000c) recommends a loading strip width to cylinder diameter ratio of $\frac{1}{6}$, while some researchers (Bazant and Planas, 1998) recommend that the above ratio should be kept at about $\frac{1}{12}$, principally because at larger values of β, a secondary load peak can occur after the fracturing of the specimen

that is sometimes higher than the original fracture load. The values that the constants L_0, L_1, L_2, and L_3 take for two values of β given by Tang are shown in Table 2.2.

Table 2.2 L_0, L_1, L_2 and L_3 for Two Common Values of $\tilde{\beta}$

B	L_0	L_1	L_2	L_3
0.167	0.959471	-0.03088	1.495833	-0.32986
0.083	0.983712	0.086919	1.065829	0.521401

As explained in the description of the experimental procedure, . had not been kept a constant for all specimen sizes reported herein, causing a correction to be required to the ultimate load before the size-effect law can be used. If the average of the values of   for the three specimen sizes tested is $_{avg}$, the experimental failure loads need to be corrected to what can be expected if the strip width is . . $_{avg}$. Thus, if the actual strip used in testing a particular size of specimen was narrower than it needs to be, the failure load has to be increased by a factor, and vice versa. The nominal stress at failure of a specimen of size d, and a bearing strip width to cylinder diameter ratio of $_{avg}$, is found by

$$\sigma_{Nu.avg} = \frac{K_{If}}{\sqrt{g'(\alpha_0, \beta_{avg})c_f + g(\alpha_0, \beta_{avg})d}} \ . \tag{2.7}$$

If the bearing strip width to cylinder diameter ratio actually used in the test for the size d_i was $_i$, then the expected nominal stress at failure of that specimen is given by

$$\sigma_{Nu} = \frac{K_{If}}{\sqrt{g'(\alpha_0, \beta_i)c_f + g(\alpha_0, \beta_i)d_i}} \ . \tag{2.8}$$

By dividing (2.7) by (2.8), the correction factor to be applied to normalize the failure load to a cylinder with bearing strip width to cylinder diameter ratio of $_{avg}$ is given by

$$CF = \frac{\sqrt{g'(\alpha_0, \beta_i)c_f + g(\alpha_0, \beta_i)d_i}}{\sqrt{g'(\alpha_0, \beta_{avg})c_f + g(\alpha_0, \beta_{avg})d_i}} \ . \tag{2.9}$$

This correction factor can be used to increase or decrease the failure loads obtained experimentally to what can be expected if a cylinder with bearing strip width to cylinder diameter ratio of $_{avg}$ were used. The correction improved the fit of the data to the size-effect law considerably.

Though the correction is theoretically exact, an iterative solution is required because the correction factor includes the size of the fracture process zone c_f. This correction factor could possibly be used to re-examine data from any previous studies where different values of ̤ have been used. The correction changed the nominal stress at failure by about 5% in some cases, but affected the derived values of K_{If} and c_f much more significantly. The peak loads that have been obtained from testing can be used to determine the fracture parameters according to the preceding methodology. The original test method is for notched beams (RILEM, 1990a), but is easily adapted to notched cylinders. The basis is a plot of ordinates Y_j against the abscissas X_j, where j is an index which changes from 1 to n, the number of specimens, and

$$Y_j = \left(\frac{\pi b d_j}{2P_j} \right)^2 \qquad (2.10)$$

$$X_j = d_j. \qquad (2.11)$$

where P_j is the failure load of the specimen j.

Such a plot is shown in Figure 2.1.
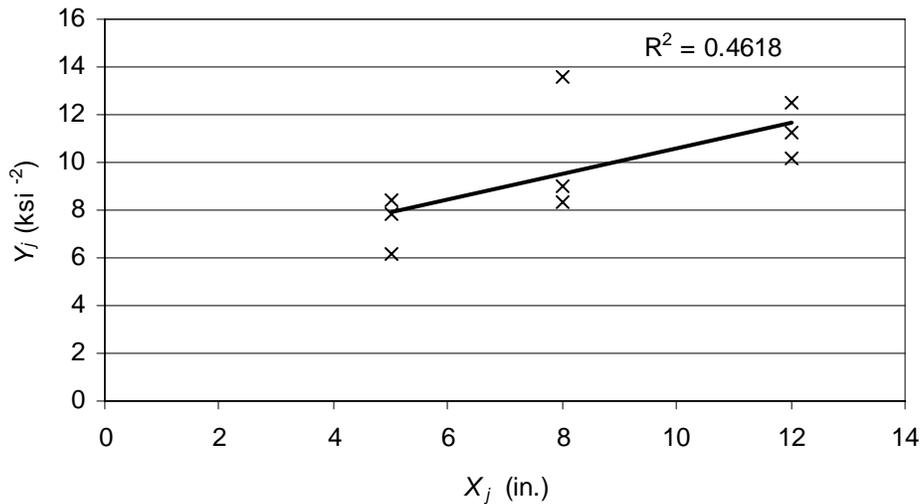
Figure 2.1 Example of Plot Generated from Size-Effect Test

Now the slope and the intercept of the regression line can be determined for $Y = AX + C$ as

$$A = \frac{\sum_j (X_j - \overline{X})(Y_j - \overline{Y})}{\sum_j (X_j - \overline{X})^2} \qquad (2.12)$$

$$C = \overline{Y} - A\overline{X}, \qquad (2.13)$$

where

$$\overline{X} = \frac{1}{n}\sum_j X_j \qquad (2.14)$$

$$\overline{Y} = \frac{1}{n}\sum_j Y_j. \qquad (2.15)$$

$(\overline{X}, \overline{Y})$ is the centroid of all the data points. The plot has to be visually checked to determine whether it is approximately linear. If it is not, there may be some testing errors in the data, or in the case of notched cylinders, there may have been a reversal of the size-effect.

The properties in fracture when the fracture process zone is unaffected by the proximity of the boundaries can now be found by

$$G_f = \frac{g(\alpha_0)}{E_c A} \qquad (2.16)$$

$$c_f = \frac{g(\alpha_0)}{g'(\alpha_0)}\left(\frac{C}{A}\right) \qquad (2.17)$$

and the critical crack-tip opening displacement, as defined in the Jenq-Shah model

$$\delta_c = (32 G_f c_f / \pi E_c)^{0.5}. \qquad (2.18)$$

2.1.2 Jenq and Shah Model

The procedure for determination of fracture parameters K_{IC} and $CTOD_C$ for mortar and concrete is given by RILEM (1990b), and utilizes notched beams tested in three-point bending. Therefore, as notched cylinders were used for the research reported here, the procedure had to be amended, though it was followed as closely as possible. Four specimens are required to be tested for each material. In the case of notched beams, the recommendations specify that thickness of the specimens tested be between 3.15± 0.20 in., the loaded span 23.62 ± 0.39 in., and the depth 5.91 ± 0.20 in., for concrete with aggregate sizes up to one inch. The notch, which can be pre-cast or saw-cut, has to be less than 0.20 inches in width, and the notch-to depth ratio is fixed at1/3. The specimens, once taken out of their molds, should be kept in a moist-curing room with 100 % relative humidity and 73.4 ± 3.6^o F, until about four hours before testing. Obviously, for a study on the effects of different periods of curing, the above curing regimen cannot be followed. It is preferable to have a closed-loop testing machine with the CMOD as the feedback signal to achieve a stable fracture, though the recommendations allow a relatively stiff machine to be used without CMOD control. The CMOD and load has to be recorded continuously during the test.

The rate of loading has to be such that the peak load is reached in about five minutes. Once the load drops below the peak to about 95% of the value at the peak, loading and unloading shall be carried out to determine the compliance (CMOD per unit load). The loading and unloading cycle shall be completed in about one minute.

The Young's modulus can be calculated from the initial compliance of the specimen. RILEM recommendations provide equations that can be used for this purpose, but they are not applicable to the notched cylinders utilized in this research. Tang (1994) carried out a FEA to determine the behavior of the notched cylinder in fracture, as predicted by the Jenq and Shah model, and the results can be used for this purpose. The dimensions that need to be entered into the FEA are shown in Figure 2.2.

Tang (1994) found the coefficients L_0, L_1, L_2, and L_3 of Equation 2.6 by using FEA and their results are presented in Table 2.3.

Table 2.3 Coefficients L_0, L_1, L_2, and L_3 (Tang, 1994).

Varia-Ble	t/R							
	0	0.06	0.1	0.14	0.2	0.22	0.25	0.28
L_0	0.99105	0.98755	0.98097	0.97108	0.94496	0.93529	0.91372	0.89583
L_1	0.14083	0.11363	0.06784	-0.00078	-0.06851	-0.11528	-0.10632	-0.18147
L_2	0.86510	0.96689	1.1365	1.3937	1.6235	1.7587	1.6933	1.9171
L_3	0.88375	0.70175	0.39258	-0.06557	-0.66022	-0.92033	-1.0549	-1.4674
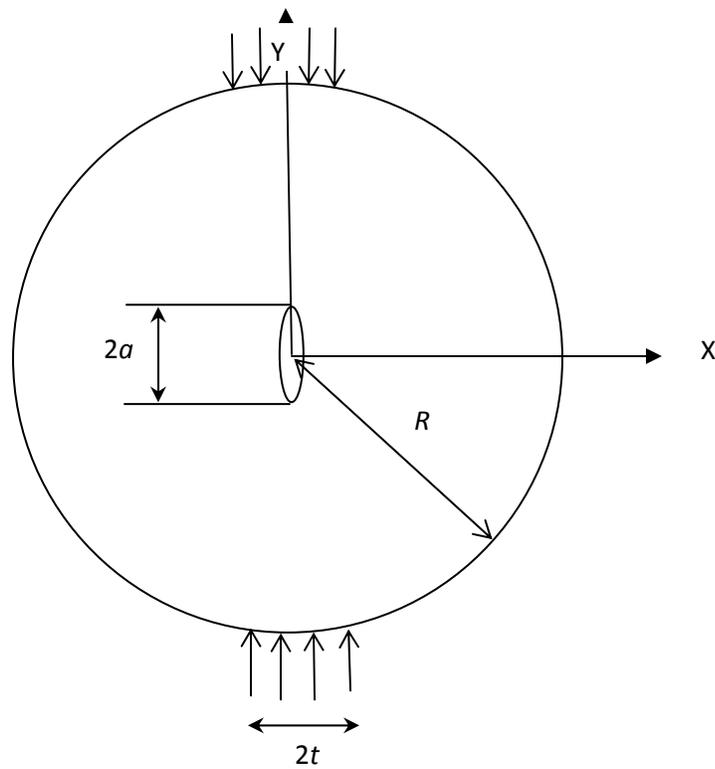
Figure 2.2 The Geometry Used in the Analysis by Tang (1994).

The CMOD under load as given by Tang et al. (1996) is

$$CMOD = \frac{\alpha P}{E'b} M(\alpha, \beta) \qquad (2.19)$$

where $E' = E$ for plane stress and $E' = E/(1-\nu)$ for plane strain. E is the elastic modulus, and ν Poisson's ratio, and M is expressed as a function of $\alpha = a/R$ as

$$M(\alpha, \beta) = A_0(\beta) + A_1(\beta)\alpha + A_2(\beta)\alpha^2 + A_3(\beta)\alpha^3. \qquad (2.20)$$

A_0, A_1, A_2, and A_3 are functions of β, and are listed in Table 2.4

Table 2.4 Coefficients A_0, A_1, A_2, and A_3 (Tang et. al, 1996)

Coeff.	t/R							
	0	0.06	0.1	0.14	0.2	0.22	0.25	0.28
A_0	1.2571	1.2515	1.2408	1.2252	1.1886	1.1754	1.1516	1.1239
A_1	0.2680	0.2512	0.2290	0.1914	0.1542	0.1098	0.07282	0.04530
A_2	0.57080	0.63067	0.70934	0.83742	0.97529	1.1008	1.2116	1.2866
A_3	2.4428	2.3305	2.1591	1.8980	1.4825	1.2666	0.99640	0.75190

Henceforth, the ratio between the CMOD and the crack opening at any point in the crack (Figure 2.3) is found by

$$\frac{COD(y)}{CMOD} = \sqrt{\left(1 - \frac{y}{a}\right)\left[1 + \frac{y}{a}S\left(\alpha, \frac{t}{R}, \frac{y}{a}\right)\right]} \qquad (2.21)$$

where

$$S\left(\alpha, \frac{t}{R}, \frac{y}{a}\right) = B_0\left(\alpha, \frac{t}{R}\right) + B_1\left(\alpha, \frac{t}{R}\right)\frac{y}{a}. \qquad (2.22)$$
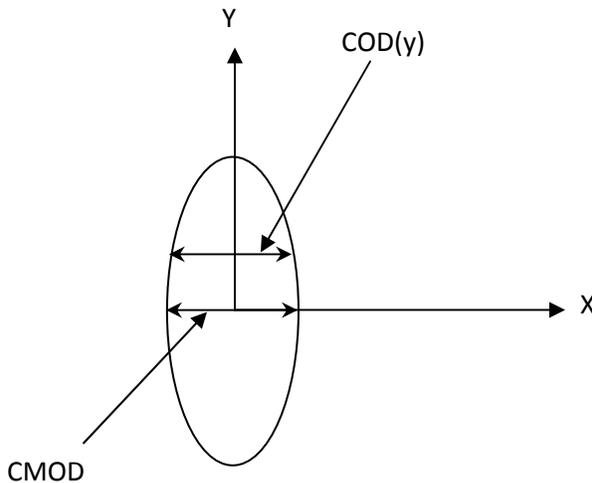
Figure 2.3 Shape of Crack Displacement.

The definition of y is shown in Figure 2.3, while the values of the coefficients B_0 and B_1 are shown in Table 2.5, and a is the half length of the crack. The values for B_0 and B_1 are given in Table 2.5. The $CTOD_c$ can thus be determined.

Table 2.5. Coefficients B_0 and B_1 (Tang, 1994).

a/R	Concentrated load		$t/R = 0.1$		$t/R = 0.2$		$t/R = 0.28$	
	B_0	B_1	B_0	B_1	B_0	B_1	B_0	B_1
0.1	1.0001	-0.00268	1.0003	-000480	1.0008	-0.0105	1.0011	-0.01892
0.2	1.0004	-0.00527	1.0008	-0.00994	1.0017	-0.02152	1.0047	-0.04227
0.3	1.0016	-0.02479	1.0027	-0.03504	1.0050	-0.06263	1.0081	-0.09781
0.4	1.0051	-0.06838	1.0072	-0.08679	1.0106	-0.13411	1.0155	-0.19477
0.5	1.0113	-0.14385	1.0143	-0.17163	1.0231	-0.25323	1.0322	-0.35121
0.6	1.0241	-0.24735	1.0323	-0.30083	1.0511	-0.43883	1.0687	-0.59244

2.1.3 Mix Designs Examined

Since there are several types of mixes currently being utilized for bridge decks in Texas, a number of them had to be tested in fracture to try and cover the types that are most commonly used. Limestone and siliceous aggregates are used, and cementitious materials such as fly ash (Class C, Class F), and GGBS are included in varying percentages. The TxDOT specifications in use at the time the research was carried out

allowed the content of slag or fly ash used in bridge deck concrete to be varied between none and 50%. The inclusion of such materials changes the characteristics of the concrete produced considerably. Admixtures (retarders, water reducers, and air entrainers) are used to impart specific properties to the concrete, and are used in various combinations and dosages.

After identifying mixes that are representative of the concrete being used in bridge deck construction in select TxDOT districts, such materials were obtained from concrete manufacturers in those regions and transported to Lubbock, Texas, where the specimens were manufactured and tested. As the water available in Lubbock has significantly high calcium content, adequate water was also obtained from each site to produce all the specimens that are needed for testing. As part of the research, test bridge decks were constructed in several regions in Texas, and some fracture specimens were manufactured, cured, and exposed to the environment in those regions. A summary of the mix designs examined are shown in Table 3.6. For the sake of brevity each mix design will simply be named by the district the materials were brought from.

Table 2.6 Mix Designs Used in Testing.

Constituent	El Paso	Fort Worth	San Antonio	Lubbock	Atlanta	Pharr
Cement Type	I/II	I/II	I/II	I/II	I	I
Pozzolan Type	Ggbs	Class F	Class C	Class F	Class F	-
Pozzolan Content (%)	50	25	20	35	22	0
Coarse Aggregate Type	LS	LS	LS	LS	Sil	Sil
Water/Cementitious ratio	0.42	0.43	0.44	0.40	0.46	0.41
Air Content (%)	5	5	6	6	6	5.5
Air Entrainer Dosage (oz/cu.yd)	4.5	4	6.1	4	3.5	2.5
Retarder Dosage (oz/cu.yd)	None	None	18.3	23*	None	25*
Water Reducer Dosage(oz/cu.yd)	61.1	22	18.3	23*	17.5	25*

Notes:
LS: Crushed limestone, Sil: Siliceous gravel   * Combined

The compressive strengths of the above concretes, as determined by testing cylinders of 6 in. diameter and 12 in. length, were obtained at 28 day-age for several curing durations by Garcia (2003). The data obtained from specimens cast in the lab under conditions described in this dissertation and cured in lime-baths are shown in Table 2.7. For

Lubbock mix, compressive strength specimens were cast in the field, with the average temperature over 14 days about 50 ^{0} F, and cured in lime-saturated baths. The compressive strengths obtained are shown in Table 2.8. Compressive strength data for Lubbock mix is available only for specimens cast in the field.

Table 2.7 Compressive Strengths of Mix Designs Except Lubbock.

Duration of Curing (days)	El Paso (psi)	Fort Worth (psi)	San Antonio (psi)	Atlanta (psi)	Pharr (psi)
4	6713	6575	6497	5739	5650
7	6230	6440	8061	6374	5250
14	6117	6460	8156	6315	5331

Table 2.8 Compressive Strengths of Lubbock

Duration of Curing (days)	Compressive Strength (psi)
2	6376
4	6407
8	6638
14	6569

2.1.4 Specimen Preparation

The coarse aggregate was air dried (Figure 2.4) and sieved (Figure 2.5) into individual size components, and then recombined in the correct proportions to make up the weight required to manufacture each batch of concrete. Most specimens were manufactured to compare the effects of varied moist-curing time at a certain test age; to narrow the effects of the slight differences between each batch of concrete; an equal number of specimens were manufactured for each curing age being examined. Once the fresh concrete was ready, it was deposited in the molds and rodded and finished according to the guidelines given in ASTM C 192 (ASTM 2000d). The notched cylinders were manufactured with the cylinder upright and steel notch of the required width held in place in the middle by a wooden assembly. After each cylinder had been finished, the exposed surfaces were covered with plastic sheets to prevent the loss of moisture until the de-molding is carried out the following day.

Figure 2.4 Coarse Aggregate being Air-Dried.

Figure 2.5 Coarse Aggregate being Sieved

2.1.5 Curing of Fracture and Fatigue Specimens

All fracture and fatigue specimens reported were kept moist for the specified period by using wet mats to simulate the manner that bridge decks are typically cured in Texas. A

mat was placed on the floor and wetted, on which the specimens being cured were placed, and then another wetted mat was placed above the specimens. Finally, a plastic sheet was placed above the mats after they had been wetted to minimize moisture loss from them. The mats were wetted periodically to maintain sufficient levels of free moisture on the specimen surfaces. After the specimens had been cured for the required period, they were kept indoors in a dry condition until the time of testing. The laboratory where the specimens were manufactured, cured, and kept until the time of testing, had a relative humidity of about 15%-25% and temperature typically 70-80 ^{0}F. Monitoring of the temperatures within the wet mats revealed that the temperature within them was usually 2-4 ^{0}F lower than the temperature of the air in the laboratory.

2.1.6 Testing of Specimens

2.1.6.1 Notched Cylinder Size-Effect Specimens

Testing was carried out on specimens at 7-day age that have been subjected to curing durations of 4 and 7 days, and on specimens at 16-day age that have been subjected to 2, 4, 8, and 14-day curing durations. The cylinders used for all sites had diameters of 5 in., 8 in., and 12 in., and radial notches $^{1}/_{6}$ of the diameter. The nominal lengths of the cylinders used in testing San Antonio, Forth Worth, Atlanta, El Paso, and Pharr were of 6 in. length, while the nominal lengths of the cylinders used in testing Lubbock was 6 in., 4 in., and 3.5 in. for the 5 in., 8 in., and 12 in. diameter cylinders respectively. After the specimens had reached the required test age, the specimens were tested in a machine that is typically used for testing of compression cylinders. A schematic diagram of the loading is shown in Figure 2.6. When carrying out the split-cylinder test, it is required that loading strips be placed between the loading platens and specimens, as otherwise specimens get crushed at the points where the loads are applied. Balsa wood of $^{3}/_{32}$ in. thickness was used in this test series for this purpose. For the testing of specimens made with materials obtained from four districts, i.e. San Antonio, Fort Worth, Atlanta, and Pharr districts, the strips inserted were of $1^{1}/_{8}$ in., $1^{1}/_{8}$ in., and $1^{3}/_{8}$ in. width for the small, medium and large sized cylinders, while for specimens made from El Paso and Lubbock mix designs, strips of $^{1}/_{12}$ and $^{1}/_{6}$ of the diameter of the cylinder being tested were used respectively.
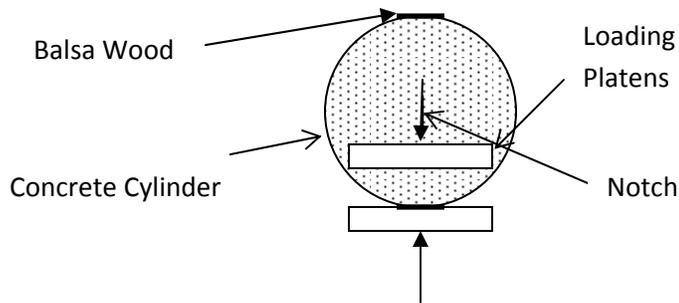
Figure 2.6 The Notched Cylinder Test.

As can be seen in the figure, the cylinders were placed in the loading machine with the notch vertical. The loading rates for the small, medium and large size cylinders were 6000, 9000, and 14000 lb/min, respectively, which meant that the rates at which the stresses developed within the cylinders were approximately constant, and that the cylinders failed in about three minutes. For cylinders of smaller length used in subsequent testing, the loading rates were changed appropriately. The failure load of each cylinder was recorded, and the measured length of each cylinder was used to correct for deviations from the nominal length. It should be pointed out that notched beams tested without crack mouth opening control in three-point bending failed explosively while these cylinders failed in a stable manner, though the loading was not servo-controlled. The machine used in testing these specimens is shown in Figure 2.7, and cylinders ready for testing are shown in Figure 2.8.

Figure 2.7 Machine Used in Testing Fracture Specimens.

Figure 2.8 Size-Effect Specimens Ready for Testing.

2.1.6.2 Young's Modulus Cylinders

For the fracture energy of concrete to be calculated, its modulus of elasticity is required, along with the failure loads of the cylinders. For each combination of testing age and moist-curing period, two standard compression cylinders (6 in diameter, 12 in. length) were cast and the modulus was determined by averaging the two values obtained from the two cylinders. The modulus was determined by loading the cylinders to a fraction of its compressive strength while measuring the shortening, using the apparatus shown in Figure 2.9. The compression between two surfaces 8 inches apart along the length of the cylinder is found upon loading. ASTM C 469-94 was used in determining the test procedure (ASTM, 2000f).

Figure 2.9 Apparatus Used to Determine Young's Modulus.

2.1.6.3 Notched Cylinder Fatigue Specimens

Cylinders similar in geometry and size to the smallest cylinders that were used in the size-effect tests were used in these tests on specimens aged 10 and 28 days, except for Lubbock mix, where cylinders of 8 in., and 4 in. diameter and 4 in. length were used. The loading was accomplished using an MTS hydraulic testing machine and software generated loading patterns. The cylinders were placed with the notch vertical, and balsa wood loading strips $^1/_6$ of the diameter were used between the loading platens and the load bearing lines along the cylinders. The data collected consisted of either the number of cycles to failure, or if the specimen did not fail, the widening of the notch at the end of the specified number of cycles, as measured by a clip-on gauge.

Several problems had to be overcome in the use of the clip-on gauge. The knife edge set that is provided for the mounting of the gauge on the specimen had holes in them for them to be screwed on to metallic surfaces. It was impossible to screw knife edges on to concrete specimens, and therefore, a glue such as epoxy has to be used. A convenient solution was to epoxy small rectangular steel plates with threaded holes on to the concrete and then screw the knife edges on to the steel plate. It was found to be critical to thoroughly clean the concrete surface before epoxying the steel plates on to them, as otherwise they sometimes came off during the test. A specimen was considered "failed" when the clip-on gauge showed a crack opening of 0.006 in.

All fatigue tests were conducted at 10 Hz using ramp type loading, for a maximum duration of 54,000 cycles. A delicate balance had to be achieved between testing at a load range that is too low, when most of the specimens would not fail, and a load range that is too high, when most of the specimens would fail in fracture rather than fatigue. It was found to be preferable to set a load range that would fail as many specimens as possible, as the fatigue damage assessment from the clip-on gauge did not show a strong trend with changing specimen moist curing periods, whereas the cycles to failure did. However, the clip-on gauge provided a valuable aid in detecting failed specimens early, and shutting off the loading; specimens tested without an automatic shut-off triggered by the clip-on gauge fail explosively, possibly causing damage to the testing machine. Figure 2.10 shows a specimen being tested in fatigue.
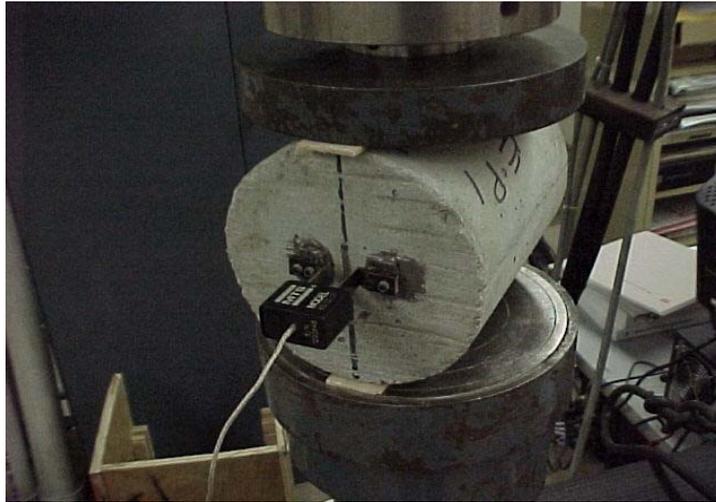
Figure 2.10 Specimen Being Tested in Fatigue

2.1.6.4 Absorption-Desorption Tests

Young's modulus testing confirmed that concrete stiffness increased with curing duration up to 14 days of curing, which was the longest duration used. This is an indication that concrete that cured for longer periods of time has hydrated better, as hydrated cementitious materials are stiffer than their un-hydrated forms. Another indicator of hydration is absorption/desorption; it is well known that increased degrees of hydration lead to lower rates of both. In an attempt to compare the degrees of hydration within specimens taken out of the wet mats at different ages, their moisture losses were tracked up to an age of 28 days. Specimens manufactured with concrete from Pharr and Fort Worth were used in this analysis. The former of the two mixes has no fly ash or GGBS and the only cementitious material in it is Type I cement, while the latter has Type I/II cement and Class F fly ash. As such, it can be expected that the specimens made from concrete from Pharr, relative to the specimens made from concrete from Fort Worth will, (1) lose more moisture (2) have moisture losses or gains that are rather close to each other at the higher curing ages, as concrete containing fly ash takes a significantly longer time to complete hydration. During the time these measurements were taken, they were kept indoors in a room with a temperature of about 65° F, and approximately 30% relative humidity.

Further experiments were carried out when the specimens reached 28-day age where the specimens were kept in a water bath for 24 hours and the weight of water absorbed was measured. However, the specimens taken out of the wet mat at two days age are "drier" than the others, and can be expected to absorb more water, independent of the level of hydration in them. The final step, where the specimens, after being saturated for 24

hours, were air-dried for 24 hours was expected to give the best indicator of the levels of hydration within the specimens.

2.1.6.5 Tests to Determine Effects of Varying Thickness of Size-Effect Specimens

It is clear that size-effect specimens cure and dry differently according to their size; the pore relative humidity within the interior of larger specimens drops slower than the relative humidity in smaller ones. An experimental program was carried out to determine whether it is possible to make large specimens progressively shorter to address this issue. Notched cylinders of the dimensions shown in Table 2.9 were used in the study.

Table 2.9 Dimensions of Cylinders Used in Study of Differential Drying

Series	Diameter (in)	Length (in)
Uniform Length	4	4
	8	4
	16	4
Varying Length	4	4
	8	2.5
	16	2.25

Three specimens with notches $^1/_6$ of the diameter were manufactured for each size, while the 4 in. diameter cylinders were common to both series. The cementitious materials and admixtures from Fort Worth were used with aggregate from Lubbock, while limiting the maximum size of the coarse aggregate to ¾ inches. Two curing ages were examined; 15-day curing in wet mats and 4-day curing in lime saturated curing baths. The cylinders were fractured under crack opening displacement (COD) control at the rates shown in Table 2.10.

Table 2.10 COD Control Rates Used in Testing.

Duration of Curing (days)	Diameter (in)	COD rate
15	4	0.006 inches in 20 minutes
	8	0.009 inches in 15 minutes
	16	0.009 inches in 15 minutes
4	4	0.004 inches in 40 minutes
	8	0.006 inches in 40 minutes
	16	0.009 inches in 60 minutes

The RILEM specifications for the two-parameter model state that the peak load should be reached in about 5 minutes. However, upon testing the specimens cured for 15 days, it was found that if the loading rates were set accordingly, it was difficult to obtain the post-peak behavior. Therefore, the COD rates were reduced to levels where the peak loads of the specimens were reached later than 10 minutes from the initiation of loading when testing the 4 day specimens.

2.1.6.6 Tests to Determine the Equivalence of the Size-Effect Law and the Two-Parameter Model

The tests described in section 2.1.6 were performed in such a manner that K_{Ic} and c_f of the concrete could be obtained as well as $CTOD_c$ of the concrete. Using these values and Equation 2.19, the consistency of the results obtained by the two models can be found.

2.2 FLEXURE

2.2.1 Curing of Flexural Strength Specimens

The specimens that were cast in the field, i.e., San Antonio, El Paso, and Fort Worth, were cast when constructing test bridge decks in the respective districts. The specimens were cured in a lime saturated bath for the designated curing durations of 2,4, and 7 days, and were subsequently exposed alongside the bridge decks. They were transported to Texas Tech University at seven days of age and tested. Three specimens were manufactured for each curing duration, and three specimens were not cured at all, and were exposed immediately after demolding.

The lab-cast specimens were manufactured, cured and kept indoors until the time of testing. The curing was accomplished in lime-baths.

2.2.2 Testing of Flexural Strength Specimens

Flexural strength tests were carried out on 6 in. x 6 in. x 20 in. specimens at 7-day age in four point bending. The testing was accomplished by using a compressive strength testing machine with additional apparatus specially designed to apply the loads. The horizontal distance between the rollers used as supports was 18 in., while the load was applied from the top using two rollers 6 in. apart at the center of the specimen. The ASTM standard C-78 "Standard Test Method for Flexural Strength of Concrete (Using Simple Beam with Third Point Loading)" was used in determining the test procedure (ASTM, 2000e).

2.3 SHRINKAGE

2.3.1 Free Linear Shrinkage Tests

2.3.1.1 Introductory Background

The free linear shrinkage test was used to compare the effect of different curing durations on free shrinkage and to estimate the shrinkage stresses developed under 100% restraint. The amount of free shrinkage depends on many factors including the properties of the material, temperature and relative humidity of the environment and the age of concrete. Here different bridge deck concrete mixes have been exposed to different curing durations to help understand the effect of curing and to estimate the minimum curing period necessary for concrete bridge decks.

Rogalla (1995) suggested that extending the wet curing time decreases the rate and extent of shrinkage and suggested that to minimize transverse cracking moist curing should normally last at least seven days based on the field study of bridge decks, preferably longer [Rogalla et al. 1995]. However, it has been reported by latest research studies that well-cured concrete shrinks rapidly and therefore the relief of shrinkage stresses by creep is smaller. Thus, increased curing is not expected to decrease shrinkage cracking despite increase in tensile strength with increased curing [Neville 1996].

An analysis made at the University of Minnesota showed that the ultimate shrinkage did not have a significant effect on the tensile stresses in the deck because creep mitigates these stresses [French et al. 1999]. Thus, study of initial shrinkage is considered to be of paramount importance for the development of tensile stresses in bridge decks. Thus, a decrease in the rate of initial shrinkage can significantly effect the reduction of crack density in concrete bridge decks. Therefore, in this investigation, to conclude that a particular curing period is good for concrete from shrinkage perspective, it should result in a low initial rate of shrinkage or low initial free shrinkage strains.

As discussed earlier, delaying the age of first crack has a significant impact on the crack widths, as crack development at an early age results in larger crack openings leading to greater deck deterioration [Weiss 1998]. Thus, suggesting that for a reduction in crack density, concrete mix and/or curing conditions should result in the delay of the age of first shrinkage-induced crack.

To compare the effect of different curing durations free shrinkage strain values are used with modulus of elasticity values to estimate the shrinkage stresses developed. Splitting tensile strength values are used to estimate the age of first crack, which occurs when tensile shrinkage stresses exceed the splitting tensile strength. However, different

methods to estimate the day of first crack have been used recently such as, use of restrained specimens in a Tensile Stress Testing Machine (TSTM) [Koenders 1997; Sule 2003] and use of ring specimens to assess the susceptibility of concrete to early-age cracking [Weiss 1999; Weiss et al. 2000]. Altoubat also used a uniaxial restrained shrinkage test setup to estimate the failure stresses and the day of first crack [Altoubat et al. 2001].

The TSTM machine showed in Figure 2.11 was used to measure autogenous shrinkage stresses from the time of casting. The ring specimens used by Weiss W. J. use axi-symmetry to simulate an infinitely long slab, that is easy to conduct in the lab due to the removal of difficulties encountered with the end conditions when testing tensile specimens as in the TSTM.

However, both TSTM and ring specimens are never cured, TSTM specimens are sealed to assess autogenous shrinkage stresses and ring specimens are allowed to dry immediately after demolding as they use a wooden base and a solid steel ring to apply the restraint as shown in Figure 2.12. Therefore, these tests are not suitable for curing the specimens thus they cannot be used to understand the effect of curing on concrete, however, these tests are effective in comparing two different concrete mixes. Thus, this leaves ultimate tensile strength approach as the only possible approach for the study of the effect of curing on bridge deck concrete.

Figure 2.11 Temperature Stress Testing Machine at Delft University of Technology
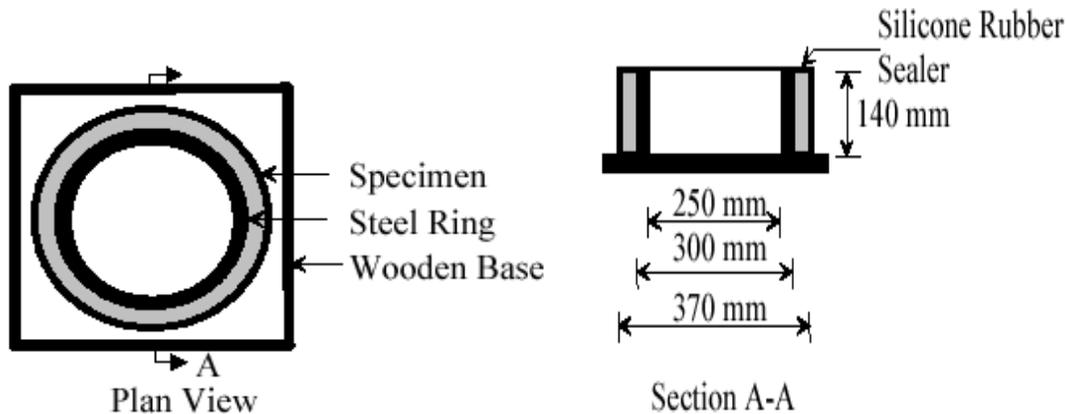
Figure 2.12 Restrained shrinkage ring specimen used by Weiss W. J.

This chapter discusses the test method to measure free shrinkage values that lead to the estimation of shrinkage stress development under 100% restraint. However, this method has also been used to compare different mixes for free shrinkage based on the development of shrinkage strain based on the internal moisture content. Internal moisture content was tracked taking weight measurements and by oven drying the specimens to obtain a 0% relative humidity weight. However, it is explained in detail, later in the chapter.

It has been observed by Shah et al. (1997) that for an equal amount of water loss in different free shrinkage specimens with and without shrinkage reducing admixtures (SRAs), the shrinkage values observed in specimens with SRAs showed less free shrinkage. This approach to compare different concrete mixes using the water loss measurements will be used to compare different bridge deck concrete mixes in the investigation of this thesis.

2.3.1.2 Test Procedure

The free linear shrinkage measurements have been obtained using *modified ASTM 157 – 93* method for length change of concrete specimens. The apparatus used for the determination of length change were in accordance with *ASTM 490 – 96* except some modifications in specimen geometry.

2.3.1.3 Apparatus

The apparatus used for free shrinkage test have been discussed in this subsection.

• The molds used for casting prismatic specimens for linear shrinkage measurements are in accordance with *ASTM C 490 – 96*. The mold used, provided for 3-in square cross-section according to *ASTM C 157 – 93*, as all the aggregate passed 1-in sieve. The length provided by the mold was 11 ¼-in with a gage length of 10-in. The gage length is considered as the nominal length between the innermost ends of the gage studs. The picture of the mold used, is shown in Figure 2.13.

Figure 2.13 Mold to cast 3 X 3 X 11.25 in prismatic shrinkage specimen

- The length comparator shown in Figure 2.14 was used to determine the length change of specimens, which is in accordance with *ASTM C 490 – 96*. The length comparator used, that is shown in figure 2.14 uses a digital indicator to read in 0.0001-in units, accurate within 0.0001-in.
- The gage studs shown in Figure 3.5 that are made of Type 316 stainless steel have been used in accordance with *ASTM C 490 – 96*.

Figure 2.14 Length Comparator

Figure 2.15 Gage Stud

2.3.1.4 Concrete Materials and Proportioning

The cement, aggregate and admixtures were from the source of the bridge deck mix, designated by the contractor in respective districts. Materials and resulting mix designs confirm to the standard provisions of the standard specifications. The mix designs used for a cubic yard of mix in the bridge decks, which are being tested under this program, are listed in Table 2.11.

Table 2.11 Mix Designs Used in Bridge Decks in Different Districts of Texas

Parameter	Districts						
	San Antonio	El Paso	Pharr	Fort Worth	Lubbock	Atlanta	Houston
Cement Type	I/II	I/II	I	I/II	I/II	I	I/II
Mineral Admixture	Flyash C 20%	Slag 50%	None	Flyash F 22%	Flyash F 31%	Fly ash F 21%	Flyash C 27%
Coarse Aggregate	LS	LS	Sil	LS	LS	Sil	LS
W/C	0.43	0.42	0.41	0.43	0.45	0.46	0.46
Air	6%	5%	6%	6%	6%	6%	5%

LS = Lime Stone
Sil = Siliceous gravel

As shrinkage tests should be conducted in a controlled environment, no specimens have been cast in the field. The cement, aggregate and admixtures have been brought to Lubbock and mixed and cast in a controlled environment of the lab.

The molding of shrinkage specimens was conducted in accordance to *ASTM C 157 – 93*. Figure 2.16 shows the shrinkage specimens in the molds immediately after finishing.

Figure 2.16 Shrinkage specimens in molds immediately after finishing

2.3.1.5 Curing and Drying Specimens

The process of curing and drying of specimens and taking different measurements has been discussed in this subsection.

- The specimens are cured in the molds for approximately 24 h covered with plastic sheets. Except for Houston-mix were it was found necessary to allow specimens to remain in the molds for more than 24 h in order to avoid damage during removal from the molds.

- Three prismatic specimens were used for each curing period to ensure repeatability. The curing durations used for Pharr, Atlanta and Houston mix designs are 0, 2, 4, 7, 10 and 14 days, for San Antonio and El Paso mix designs its 0, 4, 7 and 14 days, and for Fort Worth and Lubbock its 0, 4, 7 and 10 days.

- Initial length comparator reading is taken immediately after removing the specimens from the molds, instead of leaving them in the lime-saturated water bath for 30 min before taking an initial reading as suggested by *ASTM C 157 – 93*. Length comparator readings are taken in accordance with *ASTM C 490 – 96*.

- Weight and surface temperature measurements also taken to track the internal relative humidity of the concrete and to avoid the error in the readings caused due to variation in temperature for Pharr, Fort Worth and Lubbock mix-designs immediately after removing specimens from the molds.

- After taking initial comparator reading, the specimens are stored in lime-saturated water in the controlled environment (except the 0-day cured specimens) until they have reached the required curing period.

- Once specimens are taken out of the water bath, another reading of length comparator is taken for all the mix designs; weight and surface temperature readings

are taken for Pharr, Fort Worth and Lubbock. These readings were taken at points of interest until day-28. Figure 2.17 shows the picture the shrinkage specimens being dried in a controlled environment.

- After day-28 readings were taken, Pharr, Fort Worth and Lubbock specimens were oven-dried at 110^0 C for 24 h and weight measurements of the oven-dried specimens were recorded immediately after they were taken out of the oven.

Figure 2.17 Shrinkage specimens being dried in a controlled environment

2.3.1.6 Calculating Length Change

Calculating length changes and shrinkage strains is described in this subsection.

- To measure the length of the specimen with respect to the length of the reference bar, first place the reference bar in the comparator and set the digital indicator reading to zero as shown in Figure 2.18 then place the shrinkage specimen in the comparator and read the digital indicator. The specimens were rotated gently in the measuring instrument while the comparator reading is being taken in accordance with *ASTM C 490 – 96* as shown in Figure 2.19.

- The length change at any age after initial comparator reading, is calculated using

$$L = L_x - L_i \qquad \text{Eq. 2.23}$$

L = change in length on day x after taking the initial reading in inches,
L_i = initial comparator reading taken immediately after demolding in inches,

L_x = comparator reading taken on *day x* in inches.

• Shrinkage of the specimen with respect to the day-1 (immediately after removing from the molds) reading is being used to estimate the tensile stresses developed due to shrinkage of concrete under 100 % restraint conditions using:

$$L_{24h} = L_i - L_x$$ Eq. 2.24

L_{24h} = shrinkage after 24 h, on day x in inches.

• Shrinkage of the specimen from the day it is taken out of the water bath is also calculated; it will be referred to as the drying shrinkage of the specimen hereafter. This is not used to estimate the developed restrained stresses; however, this will help compare different mix designs based on the internal relative humidity that is discussed later.

$$L_d = L_y - L_x$$ Eq. 2.25

L_d = shrinkage after the specimen is taken out of the water bath, on day x in inches,
y = day when the specimen was taken out of the bath for drying.
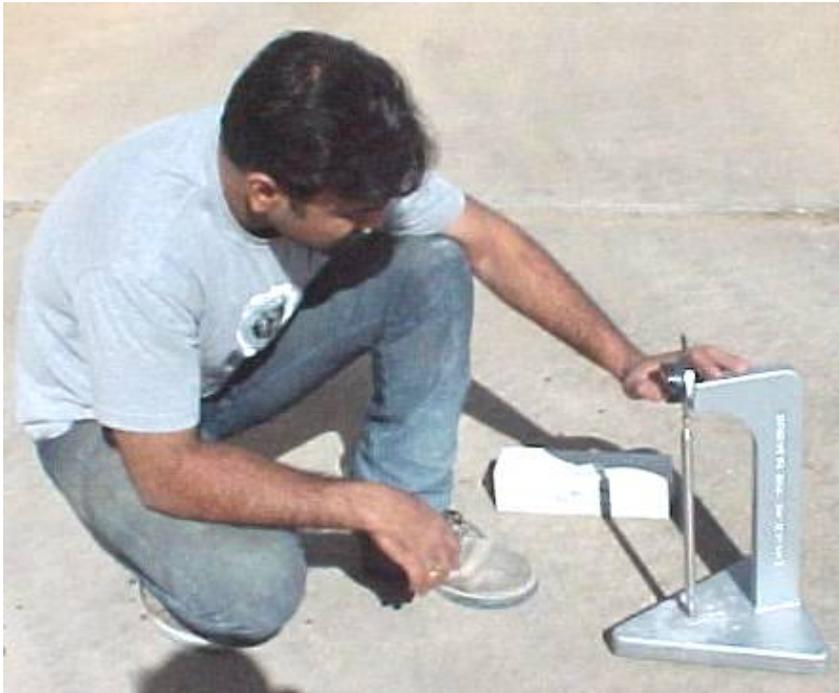
Figure 2.18 Setting Length Comparator Reading to zero for the reference bar

Figure 2.19 Taking Length Comparator Reading of the specimen

- Shrinkage strain is calculated using the 10 in. gage length of the specimen which is the nominal length between the innermost ends of the gage studs. It is calculated as follows:

$$\delta_{d/24h} = \frac{L_{d/24h}}{G} \times 10^6$$ Eq. 2.26

$\delta_{d/24h}$ = shrinkage strain in $\mu\varepsilon$; either after 24 h or drying shrinkage strain
$L_{d/24h} = L_{24h}$ or L_d in inches.
G = gage length in inches, 10 in.

2.3.1.7 Temperature Correction

The description of temperature corrections introduced in the calculation of shrinkage strains is given in this subsection.

- The ambient temperature in the controlled environment of the storage room was always $\pm 5^0 F$ of the average temperature. Based on the testing conducted on the shrinkage specimens of different district mixes, average coefficient of thermal expansion of concrete was found to be approximately $6 \mu\varepsilon /^0 F$. Thus leading to a possible variation of $\pm 30 \mu\varepsilon$ where as the least count of the 10 in. gage length comparator is $10 \mu\varepsilon$, therefore surface temperature of the specimens has been recorded along with the comparator reading for Pharr, Fort Worth and Lubbock mixes.

- Using surface temperature readings and the approximate coefficient of thermal expansion of the concrete, all comparator readings have been brought to a reference temperature of $70^0 F$ as shown below:

$$L_{70} = L_t + (70^0 F - t) \times \alpha_c \times G \qquad \text{Eq. 2.27}$$

t = surface temperature in $^0 F$ of the specimen while the reading is taken
L_t = Length comparator reading in in. at a specimen surface-temperature of t
$_c$ = Coefficient of thermal expansion of concrete
G = gage length of the specimen

2.3.1.8 Internal Relative Humidity Calculations

Using the weight of the specimens taken for Pharr, Fort Worth and Lubbock mixes at different ages (Figure 2.20 shows the picture of the weight measurements) the moisture loss of the specimens was tracked. As discussed earlier the specimens were oven-dried at 110^0 C after the 28-day reading; specimens were placed in the oven for 24 h (Figure 2.21) and the weight measurements are taken immediately after they were taken out. The difference of the weight of the specimen at a given time to the oven-dried weight, gives the amount of internal water content of the concrete at that point of time.

- The internal relative humidity relative to the humidity on day-1 is given as:

$$R.H._{.24h} = \frac{w_x - w_o}{w_1 - w_o} \times 100 \qquad \text{Eq. 2.28}$$

R.H.$_{24h}$ = Internal relative humidity (%) relative to day-1 humidity.
w_x = weight of the specimen in grams on day x.
w_o = weight of the oven-dried specimen in grams.

Figure 2.20 Measuring Weight of Shrinkage Specimen

Figure 2.21 Specimens placed in the oven for drying at 110^0 C

2.3.2 Modulus of Elasticity Tests

2.3.2.1 Introductory Background

As discussed earlier, stiffer concrete leads to increased tensile stresses for a particular strain induced due to shrinkage. It has been well established from recent research that greater modulus of elasticity results in an increase in cracking [French et al. 1999]. However, it should be noted that a reduction in the modulus of elasticity of deck concrete will reduce the concrete tensile strength. Also, in restrained shrinkage tests conducted by Altoubat (2001) it was observed that decrease in plastic shrinkage resulted in an increase in the modulus of elasticity of concrete. This in turn resulted in greater restrained shrinkage stresses. Thus, it can be said that, development of concrete microstructure plays an important role in the development of the stiffness of concrete.

The strains in concrete developed due to shrinkage of concrete result in tensile stresses. Therefore, the modulus of elasticity of concrete in tension should be determined. However, due to the problems associated with conducting tensile modulus of elasticity test, standard specifications allow the use of *ASTM C 469 – 94*, which is a modulus of elasticity test in compression. The modulus of elasticity values obtained from this test for different curing durations will be used to understand the effect of curing on the stiffness of concrete.

Apart from comparing the modulus of elasticity values for different curing durations, these values will be used to estimate shrinkage tensile stresses. Thus, the age of first shrinkage-induced crack is estimated for different curing durations.. The mixes tested for modulus of elasticity are El Paso, San Antonio, Fort Worth and Lubbock. All specimens were stored at around 50% ambient relative humidity.

2.3.2.2 Test Procedure

The standard test method used to estimate the modulus of elasticity was *ASTM C 469 – 94*. Figure 2.22 shows the specimens cast for El Paso district mix and Figure 2.23 shows the specimens just before testing. For all the district mixes tested for modulus, three 12-in tall and 6-in diameter cylinders were used for each curing period and each day of testing. However, for San Antonio district mix only two specimens each were used, as not enough material was available.. The curing durations used for San Antonio and El Paso was 0, 4, 7, and 14 days; and for Fort Worth and Lubbock it was 0, 4, 7, and 10 days.

Fig. 2.22 Finishing Specimens Cast for El Paso District Mix

For El Paso and San Antonio district mixes, 0 and 4 day cured specimens were tested on day 4, day 7 and day 16; 7-day cured specimens were tested on day 7 and day 16; and 14-day cured specimens were tested on 16 day. For Fort Worth and Lubbock district mixes, 0-day cured specimens were tested on day 1, 4, 7, 12, and day 21; 4-

day cured specimens were tested on day 4, 6, 9, 12, and day 21; 7-day cured specimens were tested on day 7, 9, 12, and day 21; and 10 day cured specimens were tested on day 10, 12 and day 21. The modifications made to the standard specification *ASTM C 469 -94* and calculation of the modulus of elasticity of the concrete are discussed in sub-sections 2.3.2.4 and 2.3.2.5, respectively.
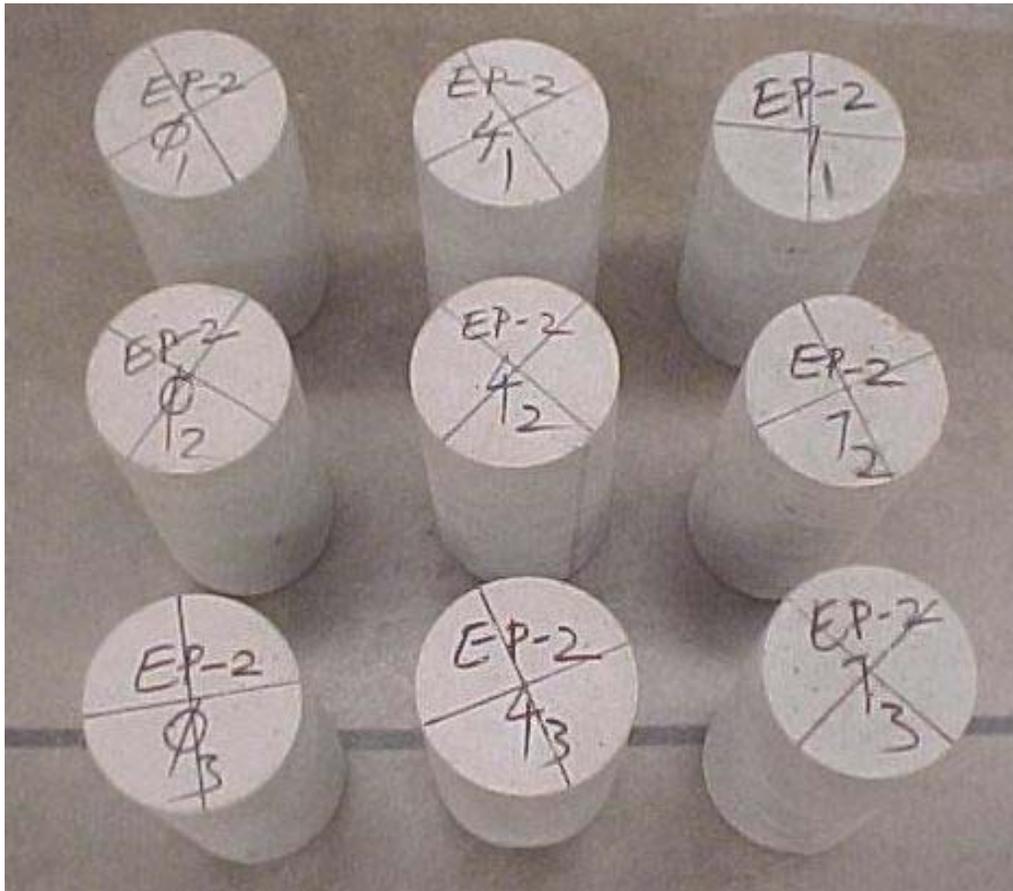
Fig. 2.23 El Paso district mix cylinders before the test

2.3.2.3 Apparatus

The apparatus used to measure the deformation was, H-2911 Humboldt manufactured compressometer. The compressometer used, is illustrated in Figure 2.24, which shows the test setup. A nominal gage length of 8-in between top and bottom rings was maintained by the fixed rod shown in Figure 2.24. The bottom ring was fixed to the cylinder through three screws while the top ring was free to pivot, attached with two contact points at point (b) shown in the Figure 2.24. The other end shown by point (c) in Figure 4.3 has a dial gage that measures length changes.
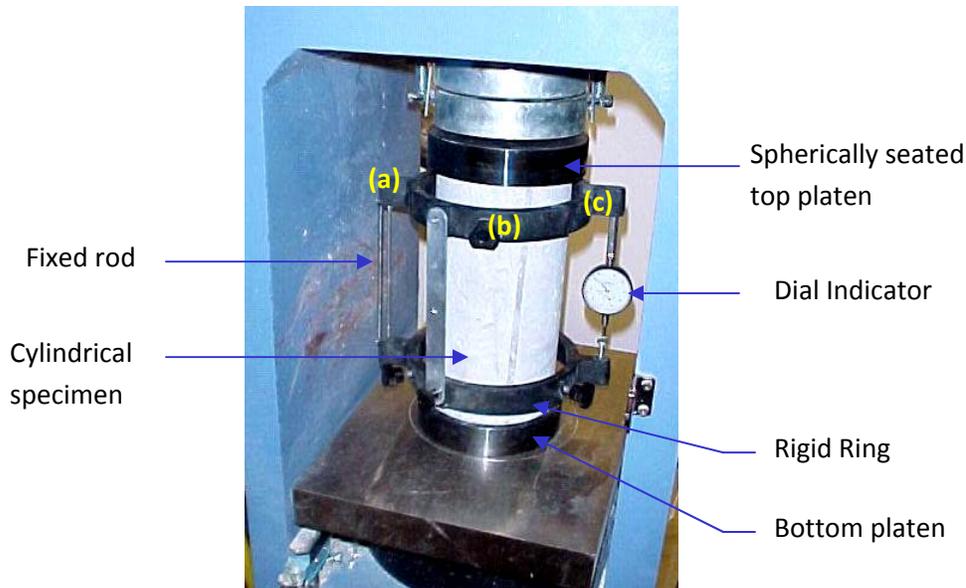
Fig. 2.24 Modulus of Elasticity test set-up in the loading machine

This dial gage can measure the length changes with a least count of 0.0001 inches. Dividing this by 2 to account for the lever ratio gives a deformation of 0.00005 inches. Figure 4.4 is used to explain the geometric relation between the deformation of the concrete cylinder at the center with respect to the dial gage reading. A detailed explanation of this can be obtained from *ASTM C 469 – 94*.
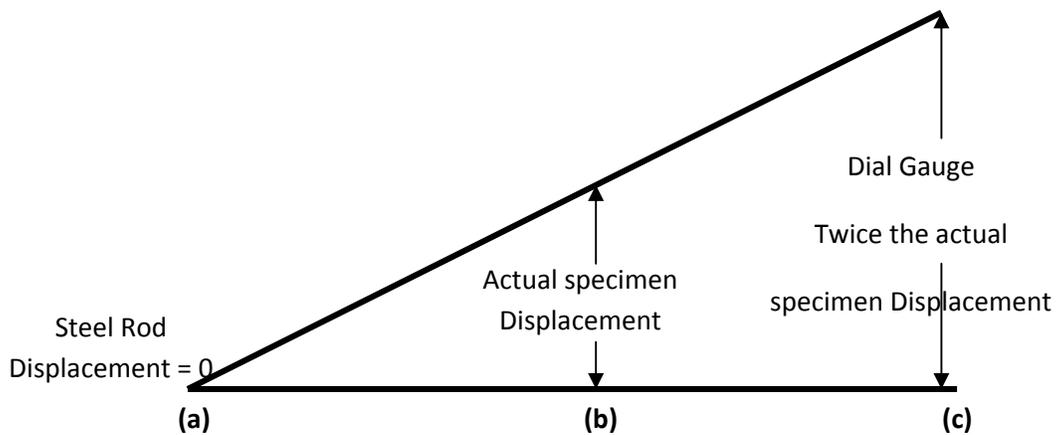
Fig. 2.25 Geometric Relation to explain the lever ratio

2.3.2.4 Modifications

The modifications made to *ASTM C 469–94* are discussed in this subsection.

- The working stress range according to the *ASTM C 469 – 94* is 0 to 40% of ultimate concrete strength. An estimate was made to approximate the 40% ultimate concrete strength based on the compressive strength results of the tests conducted on these mix designs by Garcia (2003). However, the load range was restricted to a maximum of 45,000 lb.
- Each specimen was loaded twice. The data of the first loading is not used. The calculations are based on the second loading.

2.3.2.5 Calculation of modulus of elasticity

Modulus of elasticity calculation is made to the nearest 50 ksi using Eq. 2.29. The stress corresponding to a longitudinal strain of 50 millionths is recorded as S_1 in psi. and ε_2, i.e., the strain corresponding to 40% ultimate load is calculated using the deformation recorded at this load.

$$E = \frac{(S_2 - S_1)}{(\varepsilon_2 - 0.000050)} \qquad \text{Eq. 2.29}$$

where:

E = modulus of elasticity, psi.

S_2 = stress corresponding to 40% of ultimate load, psi.

S_1 = stress corresponding to a longitudinal strain of 50 millionths, psi.

ε_2 = longitudinal strain produced by stress S_2.

2.3.3 Split Tensile Strength Tests

2.3.3.1. Introductory Background

Split tensile strength values have been used to estimate the strength of concrete to sustain the tensile stresses induced due to restrained shrinkage strains. As the split tensile strength and free shrinkage tests are conducted on different specimens. It is however, important to ascertain the accuracy of predicting the age of first shrinkage-induced crack using tests conducted on two different specimens. The specimens tested for modulus of elasticity are used in the split cylinder test, immediately after they were tested for modulus of elasticity. However, this is not expected to affect the split cylinder strength results, as the loading in the modulus of elasticity test are in the elastic stress range.

Tests conducted at Delft university of Technology on the Temperature Stress Testing Machine (TSTM) by Koenders (1997) for restrained shrinkage revealed that specimens cracked at a tensile stress, which was 0.69 times of the mean split tensile strength. A similar observation was made by Altoubat (2001), which indicate that the ratio of the stress to the splitting tensile strength at failure was approximately 0.60 to 0.64. The lower strength compared to split tensile strength can be attributed to static fatigue that leads to slow crack growth under sustained load that eventually leads to failure. Thus, a strength reduction factor for predicting the time of first crack due to sustained load such as restrained drying shrinkage should be used [Koenders 1997]. However, in this work no strength reduction factor is being used, assuming that it is compensated by a conservative assumption of 100% restrain.

As this work is only concentrating on the *relative* understanding of concrete mixtures to different curing durations creep relaxation was not tested. However, to understand the effect of creep, creep correction based on Altoubat (2001) was used to estimate age of first shrinkage-induced crack.

2.3.3.2 Test Procedure

Split cylinder test was conducted in accordance with *ASTM C 496 – 96* without any modifications. Figure 2.26 shows the test setup. Split tensile strength of the specimens is calculated using the following equation.

$$T = \frac{2 \times P}{\pi l d}$$
Eq. 2.30

T = splitting tensile strength, psi.

P = maximum applied load indicated by the testing machine, lbf.

l = length of cylinder = 12in, d = diameter = 6in.

Fig. 2.26 Split cylinder test set-up

CHAPTER III

RESULTS AND DISCUSSIONS

3.1 FRACTURE

3.1.1 Field-Cast Notched Cylinders

The field-cast notched cylinders were of 6 in. diameter and 12 in. length, and had notches of length equal to $\frac{1}{6}$ of the cylinder diameter. They were tested at 28-day age in a similar manner to the lab-cast cylinders, and the average failure loads are presented in Table 3.1 and plotted in Figure 3.1.   In contrast to the data from the field-cast flexural strength tests, the field-cast notched cylinders showed much clearer trends in fracture strength data obtained. The relative strengths of the different mixes found in the field-cast specimens also match what is found in the lab-cast specimens, giving confidence to the extent the lab work simulate field conditions. As found in data from the flexural strength tests, it is apparent that San Antonio mix seems to be relatively strong in tensile strength, while El Paso mix is rather weak. From examining the data, it would seem logical to conclude that the fracture strength of concrete increases significantly with duration of curing up to about 4 days, but this finding could possibly be influenced by size-effects, as will be discussed later.

To quantitatively compare the levels of scatter found from flexural strength tests and field-cast notched cylinder tests, the following calculations were carried out. The standard deviation of the flexural strengths obtained from the three replicates used in the tests were found for every type of concrete and duration of curing. The standard deviation obtained was divided by the average flexural strength for that particular concrete and curing duration. The average of the % standard deviation values obtained for all concretes and curing durations was 8.7 % for flexural strength beams, while for notched cylinders the average obtained was 8.4 %. Thus it appears that, though the scatter is about the same, the *trends* found from testing notched cylinders were cleaner.

Table 3.1 Average Failure Loads of Field-Cast Notched Cylinders.

Duration of Curing (Days)	El Paso (kips)	Fort Worth (kips)	Lubbock (kips)	San Antonio (kips)
0	22.0	27.1	27.4	38.6
2	25.9	33.8	32.6	43.8
4	30.2	35.6	39.1	41.6
8	30.6	38.4	38.8	45.4
10	26.2	37.4	43.7	42.5
14	32.8	37.4	40.3	44.4
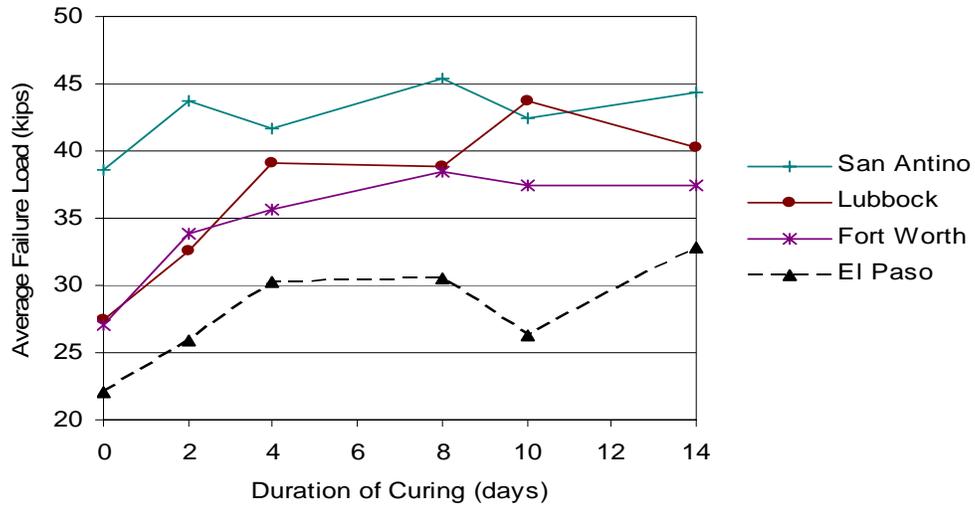
Fig. 3.1 Average Failure Loads of Field-Cast Notched Cylinders

3.1.2 Size-Effect Tests

3.1.2.1 Tests Carried Out at 16-Day Age

The observations from each size of specimen are discussed first, followed by a discussion of the fracture properties gleaned by combining data from all sizes. The average failure loads of 5 in. diameter specimens for each mix and curing age are shown in Table 3.2 and Figure 3.2. In order to facilitate comparison between mix designs, all the failure loads presented in Section 3.1.2 have been normalized to cylinders of 6 in. length, the average nominal lengths of most specimens tested. It should be remembered that small specimens dry out very fast upon curtailing of curing, and as such, the trends can be expected to be very sharp. A cursory inspection of the data reveals that there is a distinct upward trend of failure loads with curing except for Pharr and Lubbock mixes. The fact that Pharr is an outlier to the general trend can be attributed to Pharr not containing any fly ash or slag. In general, San Antonio mix and Atlanta mix had the higher fracture strengths than the other mixes, a trend which is evident in the fracture data from all sizes. El Paso mix contained 50% slag, and it is probable that such a high percentage of the material in a concrete adversely affects its fracture strength. There is a fairly good match in the trends found from testing field-cast notched cylinders to what was found from testing 5 in. diameter notched cylinders in the lab, the lab-cast cylinders which are closest in size to the field-cast cylinders.

Table 3.2 Average Failure Loads at 16-Day Age for 5 in. Diameter Specimens.

Duration of Curing (days)	San Antonio (kips)	Pharr (kips)	Atlanta (kips)	Fort Worth (kips)	El Paso (kips)	Lubbock (kips)
2	17.0	19.3	18.8	16.5	15.1	15.5
4	18.3	18.3	19.1	17.3	14.9	15.0
8	18.5	18.8	20.7	17.5	16.2	14.7
14	19.3	18.1	20.6	17.8	16.7	15.2
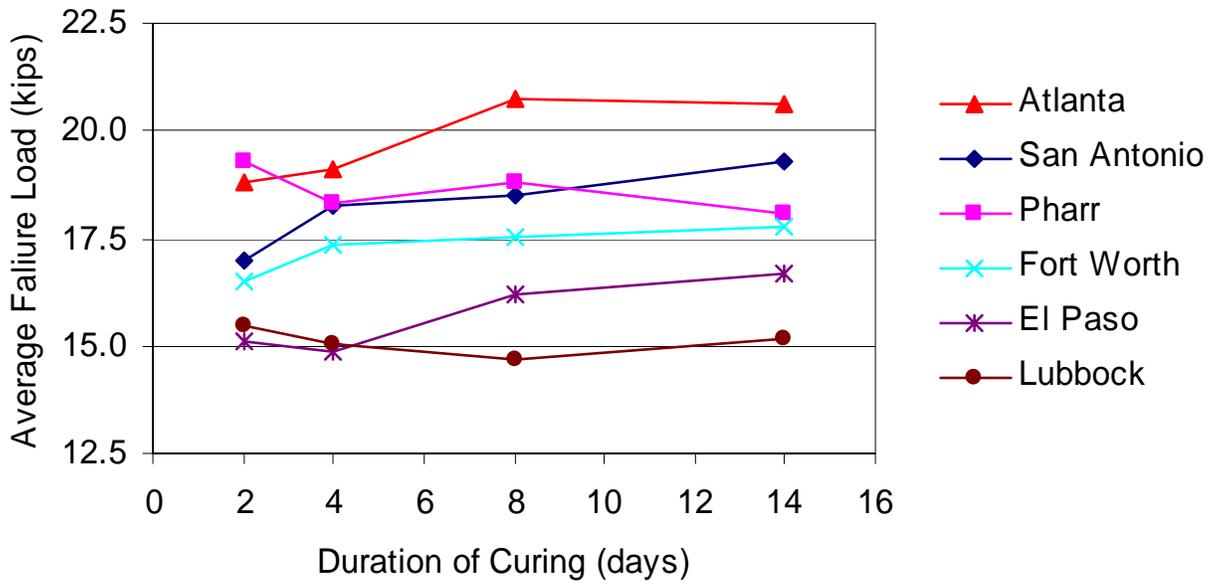
Figure 3.2 Average Failure Loads at 16-Day Age for 5 in. Diameter Specimens

The average failure loads of 8 in. diameter specimens are shown in Table 3.3 and Figure 3.3. It is apparent that the general trend of increasing fracture loads with increasing curing time found in the smaller specimens is not present in 8 in. diameter specimens. It is quite significant that, unlike in the case of 5 in. diameter cylinders, there are no mixes for which the fracture strength seems to increase with increased curing time for medium sized specimens, perhaps except El Paso mix. As before, San Antonio mix and Atlanta mix display the highest failure loads, and El Paso mix displays one of the lower failure loads.

Table 3.3 Average Failure Loads at 16-Day Age for 8 in. Diameter Specimens.

Duration of Curing (days)	San Antonio (kips)	Pharr (kips)	Atlanta (kips)	Fort Worth (kips)	El Paso (kips)	Lubbock (kips)
2	26.3	26.2	28.9	24.8	21.1	23.7
4	26.7	27.1	25.8	23.9	24.9	21.0
8	26.7	25.8	28.7	24.6	23.9	25.4
14	26.0	25.4	28.2	23.6	24.1	22.6
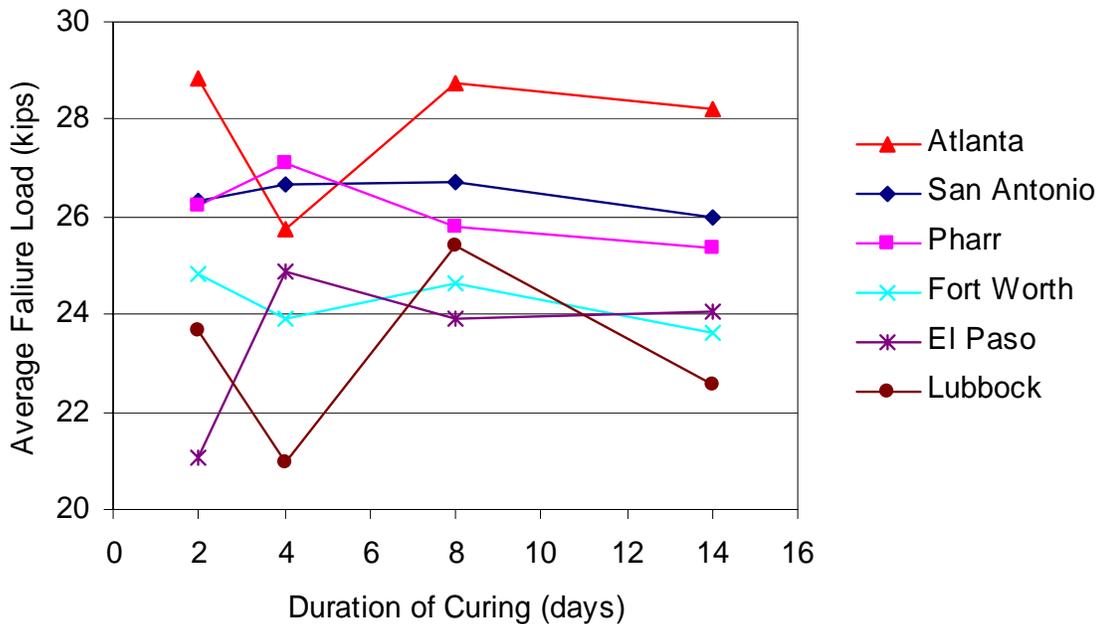
Fig. 3.3 Average Failure Loads at 16-Day Age for 8 in. Diameter Specimens.

The average failure loads for 12 in. diameter specimens are shown in Table 3.4 and Figure 3.4. An inspection of the data reveals a very significant finding. Mixes that are relatively weak in fracture have gained strength with increased duration of curing, while mixes with a relatively high fracture resistance have lost strength with increased duration of curing except Fort Worth. This phenomenon can be explained by concrete with higher fracture toughness getting more brittle with increased curing.   Another significant fact that comes to light from comparing the trends in the small, medium and large sizes is that it could be quite erroneous to base findings of fracture resistance on a single size of specimen. The size of the fracture process zone affects specimens of different sizes in a dissimilar manner, leading to varying trends in fracture resistance, as will be discussed later. Furthermore, the conclusions from the study of the failure loads of small specimens would be that the concrete gains strength with increased curing, while the conclusion from examining the data from the medium sized specimens would be that the strength does not vary significantly with curing duration.   The importance of considering a range of sizes in testing of concrete in fracture is thus exposed.

Table 3.4 Average Failure Loads at 16-Day Age for 12 in. Diameter Specimens.

Duration of Curing (days)	San Antonio (kips)	Pharr (kips)	Atlanta (kips)	Fort Worth (kips)	El Paso (kips)	Lubbock (kips)
2	41.8	33.8	43.1	36.2	33.7	30.2
4	37.7	37.1	42.9	33.7	33.2	40.3
8	38.1	35.1	42.8	34.6	36.7	38.0
14	37.8	36.2	41.9	35.9	40.1	36.7
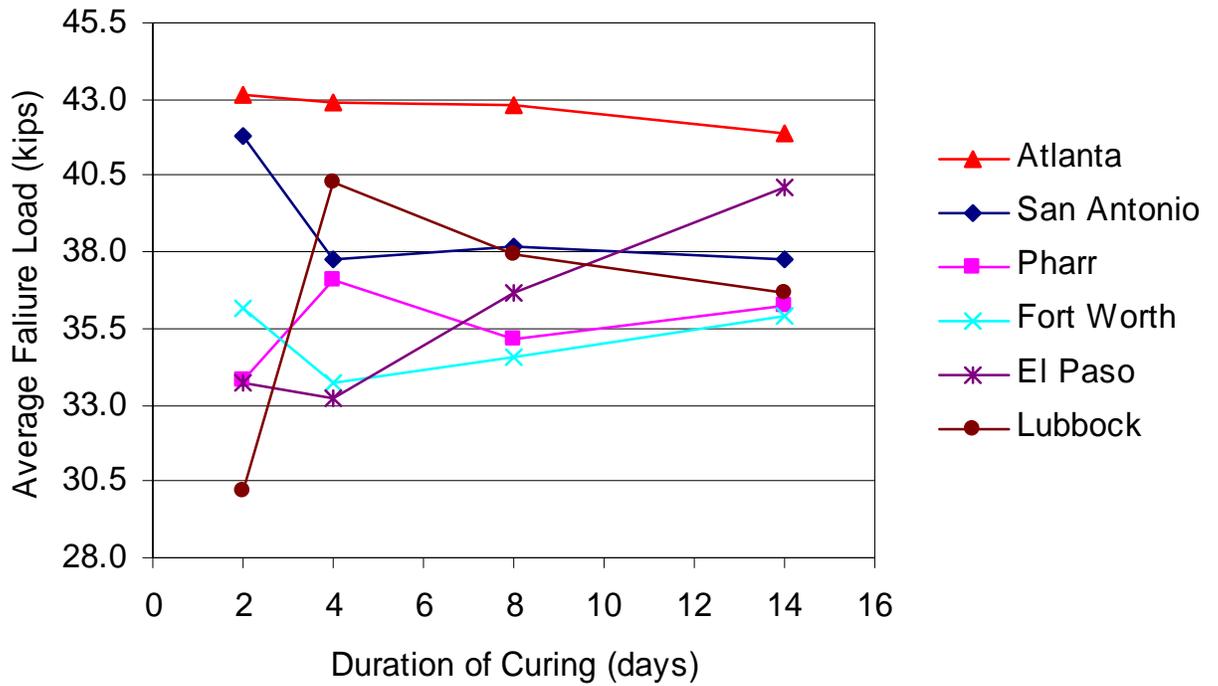
Figure 3.4 Average Failure Loads at 16-Day Age for 12 in. Diameter Specimens.

The Young's modulus data for 16-day age obtained from testing cylinders of 6 in. diameter and 12 in. length are presented in Table 3.5 and Figure 3.5. There is a clear trend of increasing modulus with increasing duration of curing, establishing that concrete kept in the wet mats for longer durations have hydrated better. However, it should be borne in mind that concrete with relatively high stiffness develop high stresses due to shrinkage, an undesirable phenomenon which is coupled with decreased creep capability. It should be noted that El Paso mix has significantly lower modulus values than the other sites, underlining the differences in concretes with high percentages of slag compared to those with limited amounts of fly ash or no pozzolanic materials.

Table 3.5. Young's Modulus at 16-Day Age.

Duration of Curing (days)	San Antonio (10^6 psi)	Pharr (10^6 psi)	Atlanta (10^6 psi)	Fort Worth (10^6 psi)	El Paso (10^6 psi)	Lubbock (10^6 psi)
2	4.97	5.07	5.19	5.15	3.27	4.83
4	5.32	5.13	5.66	5.51	3.90	5.10
8	5.52	5.66	5.45	5.52	4.13	5.50
14	5.62	5.76	5.39	5.60	4.25	5.46
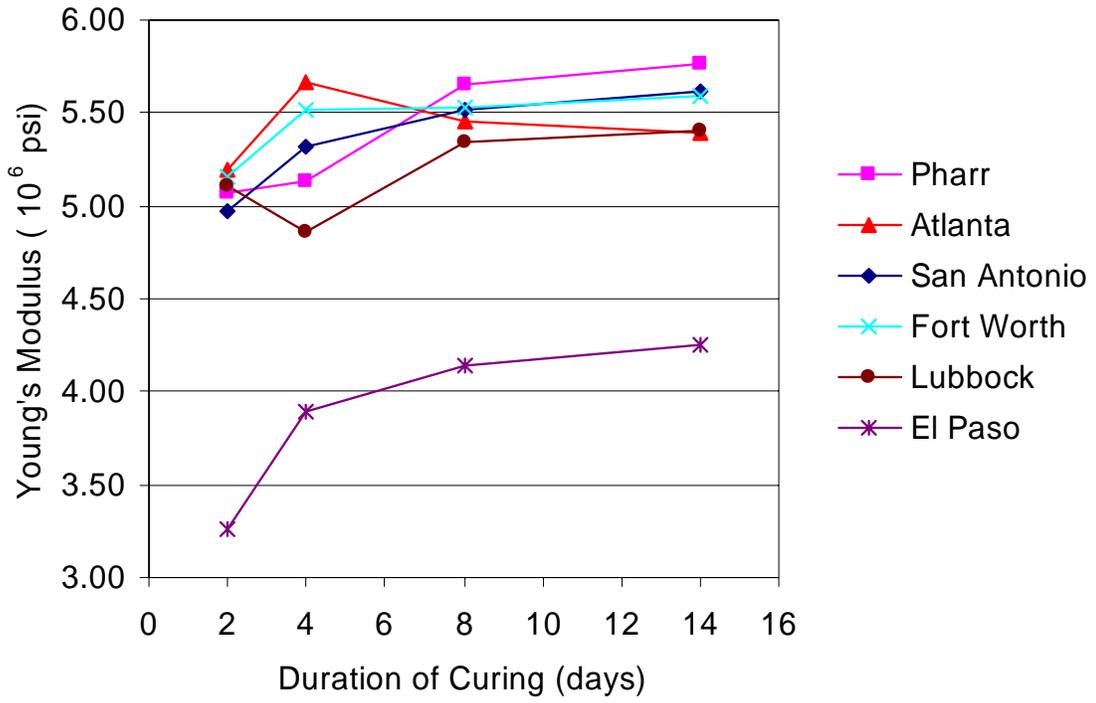
Figure 3.5. Young's Modulus of Concretes at 16-Day Age.

The values of the fracture toughness obtained from combining data from all specimen sizes for the concretes at 16-day age are shown in Table 3.6 and Figure 3.6. In order to add clarity to the figure, only the results for San Antonio mix and El Paso mix are shown. It should be noted that strong reversals in the size-effect trend were observed for some concretes at certain combinations of curing duration and testing age, and these instances have been reported as "reversal." One explanation why the reversal occurs is that in some cases for larger cylinders, the failure mode changes, and the specimens fail by the formation of plastic wedges at the loading platens (Bazant and Planas, 1998). Reversal seriously affects data from concretes with relatively large fracture toughness and large fracture process zone, as the former causes the larger cylinders to fail at relatively high loads, and the latter causes smaller cylinders to fail at relatively low loads. Therefore, for such concretes, even a mild reversal of the size-effect at large sizes is exacerbated. The trends are quite clear except for Fort Worth mix; the mixes with the higher failure loads have all lost fracture toughness with increased duration of curing, while the mixes with lower fracture strengths have gained strength with increased curing time and the mixes with intermediate fracture strength have not gained or lost strength consistently due to increased curing time.

Table 3.6 Fracture Toughness at 16-Day age.

Duration of Curing (days)	Fort Worth (psi.in$^{1/2}$)	El Paso (psi.in$^{1/2}$)	San Antonio (psi.in$^{1/2}$)	Pharr (psi.in$^{1/2}$)	Atlanta (psi.in$^{1/2}$)	Lubbock (psi.in$^{1/2}$)
2	1527	1120	Reversal	619	Reversal	611
4	836	1084	1126	1207	Reversal	Reversal
8	906	1486	1068	770	1343	Reversal
14	1044	Reversal	978	941	1222	Reversal
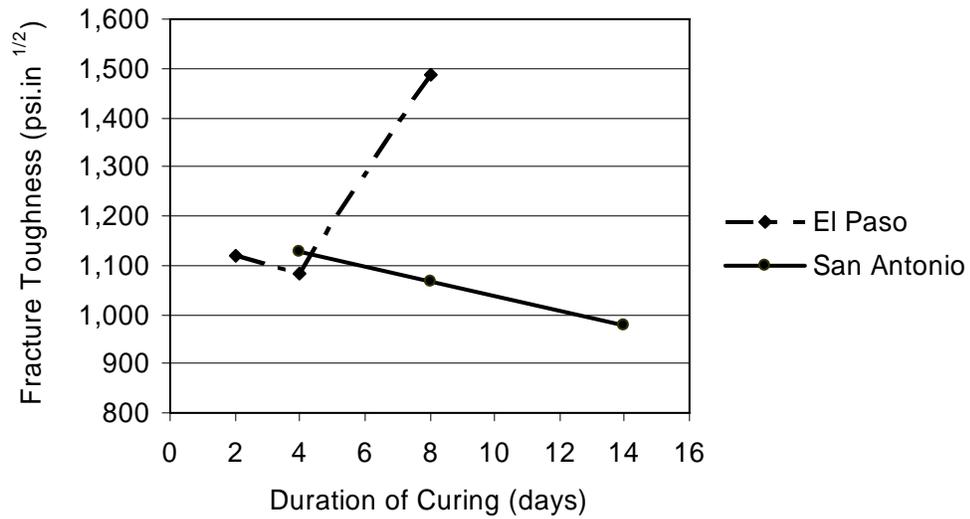
Figure 3.6 Fracture Toughness of El Paso and San Antonio Mix at 16-Day Age.

Fracture energy can be calculated from the fracture toughness and the Young's modulus of a concrete mix using equation 3.13, and is shown in Table 4.7 and Figure 4.8. It can be seen that the fracture energy exhibits similar trends to fracture toughness, but its variation is more exaggerated.

Table 3.7 Fracture Energy at 16-Day Age.

Duration of Curing (days)	Fort Worth (psi.in)	El Paso (psi.in)	San Antonio (psi.in)	Pharr (psi.in)	Atlanta (psi.in)	Lubbock (psi.in)
2	0.452	0.384	Reversal	0.076	Reversal	0.072
4	0.127	0.302	0.238	0.284	Reversal	Reversal
8	0.149	0.534	0.207	0.105	0.331	Reversal
14	0.195	Reversal	0.170	0.154	0.277	Reversal
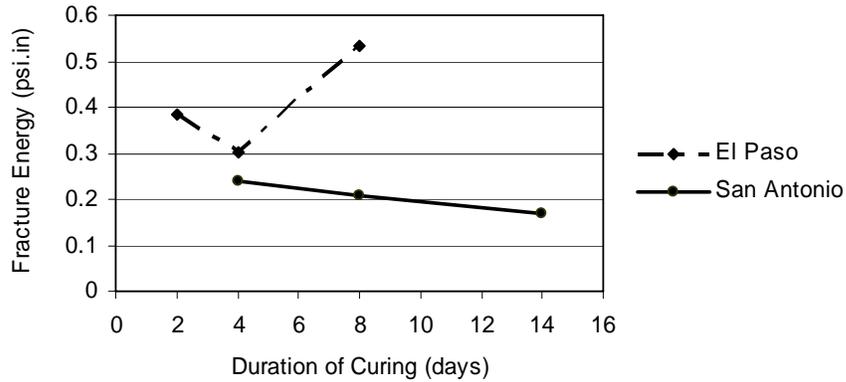
Figure 3.7 Fracture Energy of El Paso mix and San Antonio mix at 16-Day Age.

The sizes of fracture process zones for the concretes are shown in Table 3.8 and Figure 3.8. The values are much higher than many reported in literature, and perhaps only reflect the variations in their magnitudes qualitatively. For example, Bazant and Planas (1998) report of a concrete containing aggregate with maximum size ½ in. with c_f of 0.5 in., while Bazant and Schell (1993) found c_f to be 0.3 in. of a concrete with maximum aggregate size $^3/_8$ inch. Gettu et al. (1990) tested on a high-strength concrete with maximum aggregate size $^3/_8$ in. and found c_f to be 0.10 inches. In general, the mixes that have high fracture loads, i.e., San Antonio mix and Atlanta mix, have smaller fracture process zones at increased curing durations, while the reverse is true of El Paso mix. The critical crack-tip opening displacements of the mixes have very similar trends to the sizes of fracture process zones, and are shown in Table 3.9 and Figure 3.9.

Table 3.8 Sizes of Fracture Process Zone at 16-Day Age.

Duration of Curing (days)	Fort Worth (in)	El Paso (in)	San Antonio (in)	Pharr (in)	Atlanta (in)
2	10.951	6.440	Reversal	0.664	Reversal
4	2.556	5.280	4.442	5.359	Reversal
8	3.018	10.077	3.852	1.567	5.176
14	4.334	Reversal	3.040	3.045	4.242
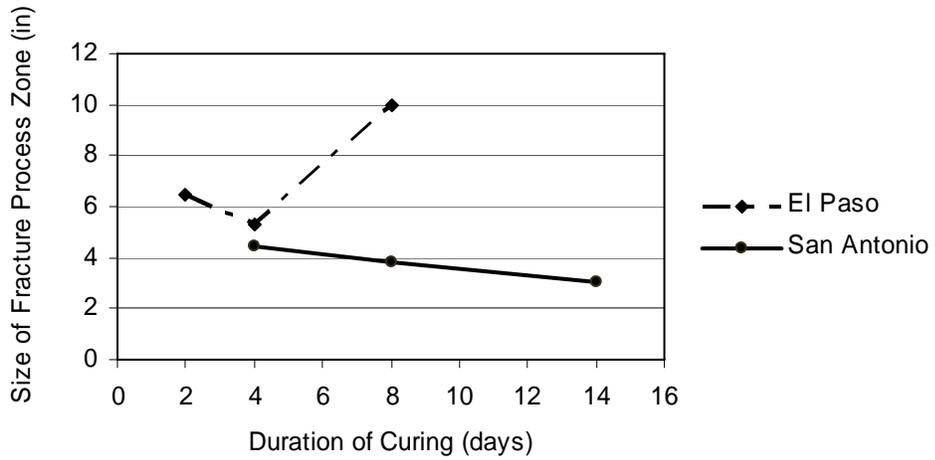
Figure 3.8. Sizes of Fracture Process Zone for El Paso mix and San Antonio mix at 16-Day Age.

Table 3.9. Critical Crack-Tip Opening Displacement at 16-Day Age.

Duration of Curing (days)	Fort Worth (in)	El Paso (in)	San Antonio (in)	Pharr (in)	Atlanta (in)
2	0.00313	0.00278	Reversal	0.00032	Reversal
4	0.00077	0.00204	0.00142	0.00174	Reversal
8	0.00091	0.00363	0.00121	0.00054	0.00179
14	0.00124	Reversal	0.00097	0.00091	0.00149
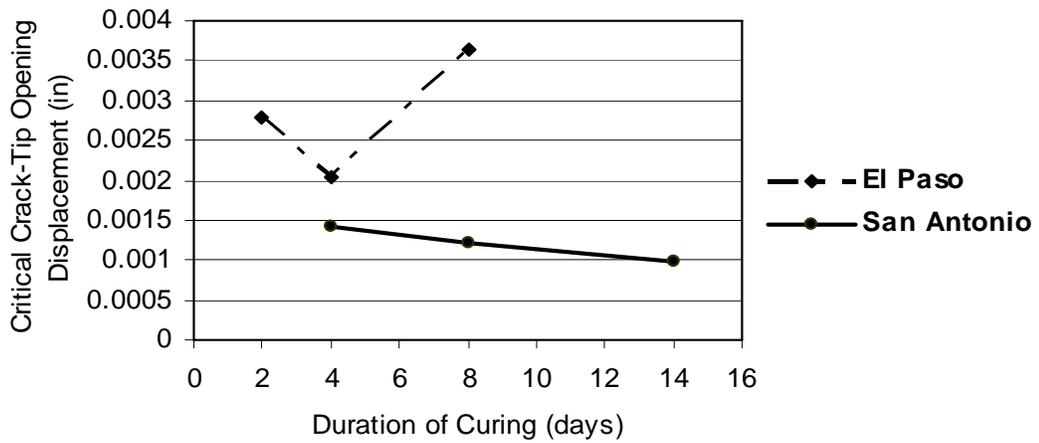
Figure 3.9. Critical Crack-Tip Opening Displacement of El Paso mix and San Antonio mix at 16-Day Age.

3.1.2.2 Tests Carried Out at 7-Day Age

The average failure loads of the 5 in. diameter specimens are shown in Table 3.10 and Figure 3.12. It becomes immediately apparent that for most mixes, the average failure loads of specimens cured for 7 days are lower than the average failure loads of specimens cured for 4 days. This is quite contrary to what was found in the specimens aged 16 days. To ascertain whether the lowering of failure loads with extended curing is caused by moisture gradients, El Paso mix concrete specimens of the above diameter were re-cast, but now the 7-day cure specimens were tested in a saturated condition. The average failure loads obtained at 4-day curing and 7-day curing were 15,793 lbs and 14,293 lbs. The failure loads are higher than reported before, possibly due to the fact the wider load distributing strips were used or aggregate from Lubbock mix were substituted in the manufacturing of specimens, but the trend is still the same. It was thus concluded that the above trends are systematic, and not caused by random errors or moisture gradients. However, the specimens cured for 7 days are admittedly in a more moist condition at the time of testing.

Table 3.10. Average Failure Load at 7-Day Age for 5 in. Diameter Specimens.

Duration of Curing (days)	San Antonio (kips)	Pharr (kips)	Atlanta (kips)	Fort Worth (kips)	El Paso (kips)
4	17.2	16.6	18.3	18.2	14.0
7	17.3	15.4	16.5	16.8	10.7
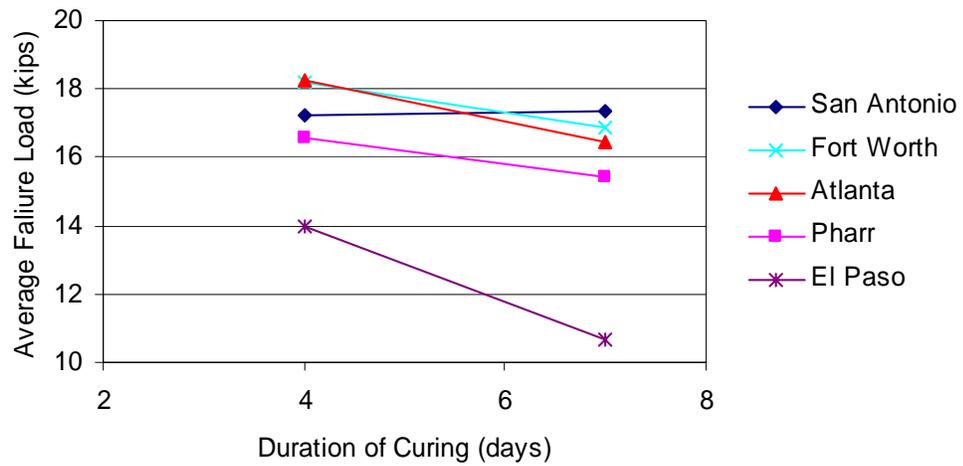
Figure 3.10. Average Failure Load at 7-Day Age for 5 in. Diameter Specimens

The average failure loads of 8 in. diameter specimens are shown in Table 3.11 and Figure 3.11. With the exception of Atlanta mix, specimens of all other mixes have lower failure loads at 7-day age for specimens of this size.

Table 3.11. Average Failure Load at 7-Day Age for 8 in. Diameter Specimens.

Duration of Curing (days)	San Antonio (kips)	Pharr (kips)	Atlanta (kips)	Fort Worth (kips)	El Paso (kips)
4	27.1	21.6	23.2	25.2	19.6
7	26.7	21.3	25.6	23.6	17.8
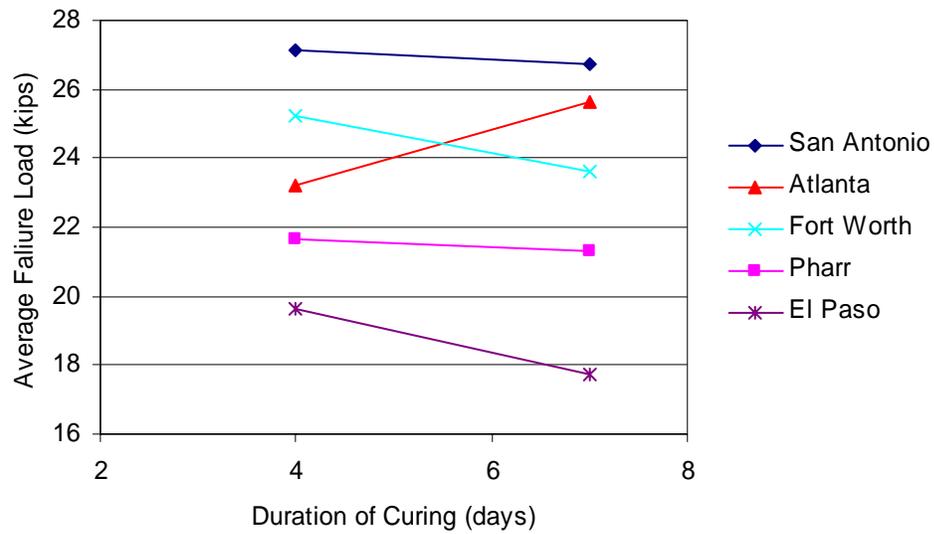
Figure 3.11. Average Failure Load at 7-Day Age for 8 in. Diameter Specimens

The average failure load of 12 in. diameter specimens are shown in Table 3.12 and Figure 3.12. There are no clear-cut trends in the variation of the failure loads with curing time when all mixes are considered, though individually, some mixes have gained strength and some have lost strength.

Table 3.12. Average Failure Load at 7-Day Age for 12 in. Diameter Specimens.

Duration of Curing (days)	San Antonio (kips)	Pharr (kips)	Atlanta (kips)	Fort Worth (kips)	El Paso (kips)
4	35.3	31.8	36.2	34.8	30.9
7	36.6	31.0	36.1	35.8	31.0
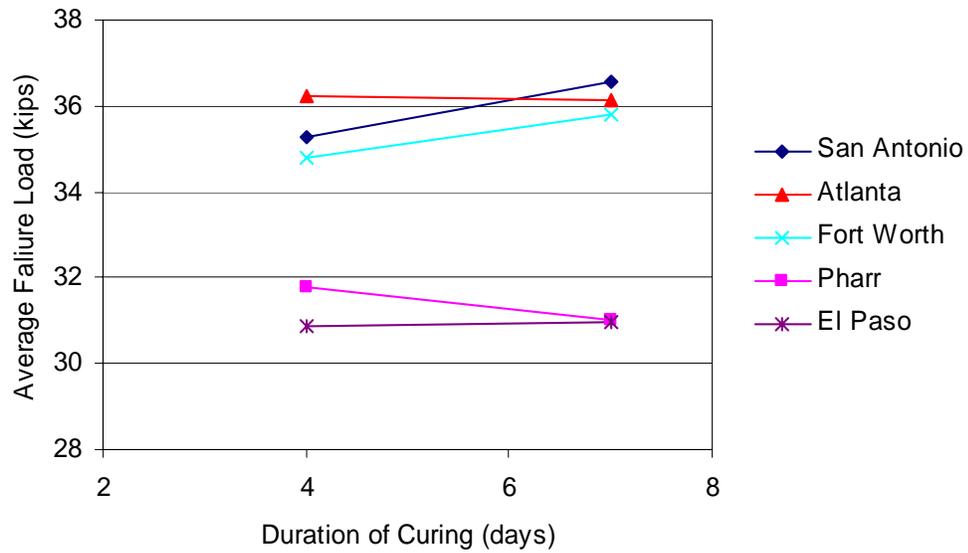
Figure 3.12. Average Failure Load at 7-Day Age for12 in. Diameter Specimens.

The Young's Modulus of the concretes are shown in Table 3.13 and Figure 3.13. Most concretes are considerably stiffer after being cured for 7 days as compared to concretes cured only for 4 days, with the exception of San Antonio mix.

Table 3.13. Young's Modulus at 7-Day Age.

Duration of Curing (days)	San Antonio (10^6 psi)	Pharr (10^6 psi)	Atlanta (10^6 psi)	Fort Worth (10^6 psi)	El Paso (10^6 psi)
4	5.38	4.72	4.59	5.15	4.20
7	5.44	5.17	4.82	5.78	4.51
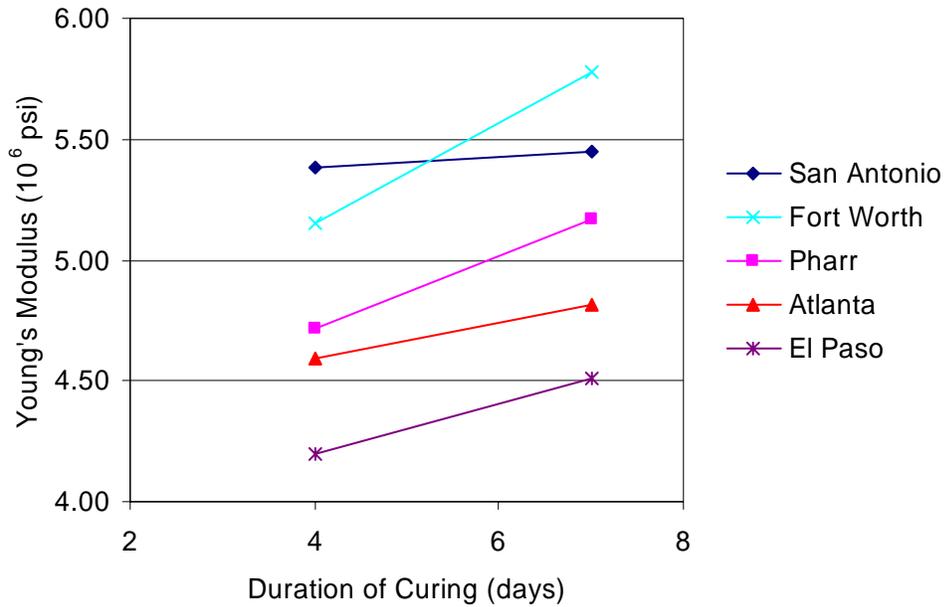
Figure 3.13. Young's Modulus at 7-Day Age.

The fracture toughness of the concretes are shown in Table 3.14. and Figure 3.14. Though the fracture toughness of San Antonio mix at 7-day age seems unnaturally high, it is apparent that, without exception, the concretes have gained fracture toughness with increased curing at the age of 7 days.

Table 3.14. Fracture Toughness at 7-Day Age.

Duration of Curing (days)	Fort Worth (psi.in$^{1/2}$)	El Paso (psi.in$^{1/2}$)	Pharr (psi.in$^{1/2}$)	San Antonio (psi.in$^{1/2}$)	Atlanta (psi.in$^{1/2}$)
4	722	889	674	1079	789
7	1446	Reversal	896	5868	874
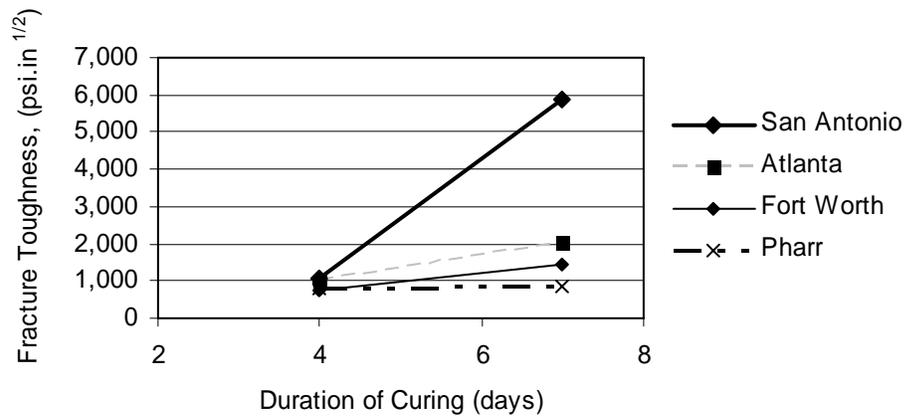
Figure 3.14 Fracture Toughness at 7-Day Age.

The fracture energy of the concretes at 7-day age is shown in Table 3.15 and Figure 3.15. The trends are very similar to what was found for fracture toughness.

Table 3.15. Fracture Energy at 7-Day Age.

Duration of Curing (days)	Fort Worth (psi.in)	El Paso (psi.in)	Pharr (psi.in)	San Antonio (psi.in)	Atlanta (psi.in)
4	0.113	0.188	0.096	0.217	0.132
7	0.434	Reversal	0.141	6.324	0.148
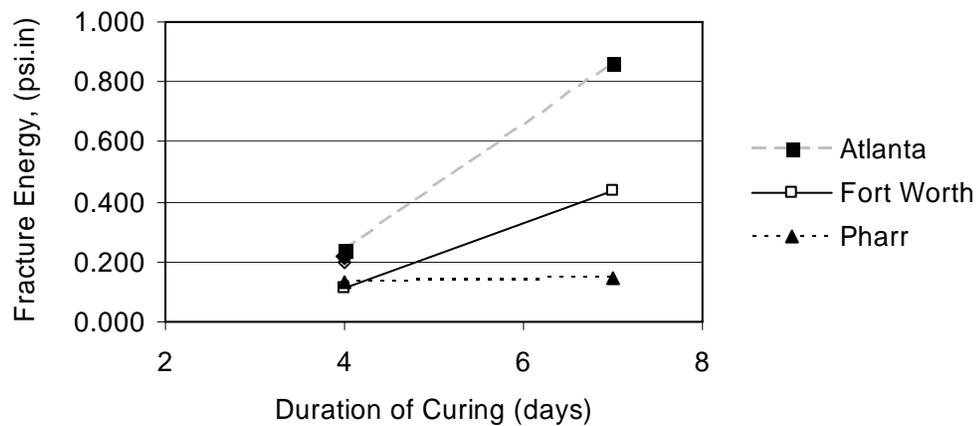
Figure 3.15 Fracture Energy at 7-Day Age.

The sizes of the fracture process zones are shown in Table 3.16 and Figure 3.16. It is immediately apparent that without exception, the sizes of the fracture process zones have increased with duration of curing, though some of the values are unreasonably high. Perhaps in this case, the evaluation has to be limited to a qualitative rather than quantitative one.

Table 3.16. Size of Fracture Process Zone at 7-Day Age.

Duration of Curing (days)	Fort Worth (in)	El Paso (in)	San Antonio (in)	Pharr (in)	Atlanta (in)
4	1.40	4.62	4.38	2.61	2.08
7	9.74	Reversal	154.61	3.83	4.51
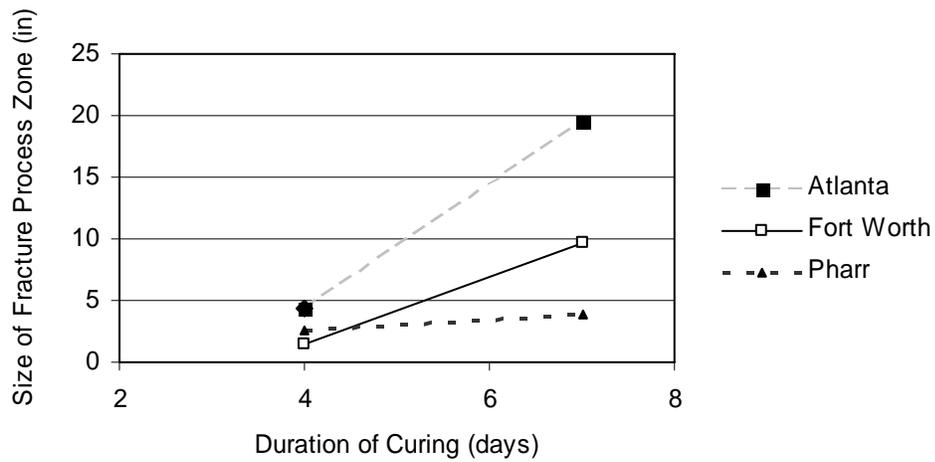
Figure 3.16 Size of Fracture Process Zone at 7-Day Age.

The critical crack-tip opening displacements are shown in Table 4.18 and Figure 4.19. The trends are very similar to what was found for the size of fracture process zone.

Table 3.17 Critical Crack-Tip Opening Displacement at 7-Day Age.

Duration of Curing (days)	Fort Worth (in)	El Paso (in)	San Antonio (in)	Pharr (in)	Atlanta (in)
4	0.00059	0.00145	0.00134	0.00086	0.00150
7	0.00299	Reversal	0.04277	0.00106	0.00596
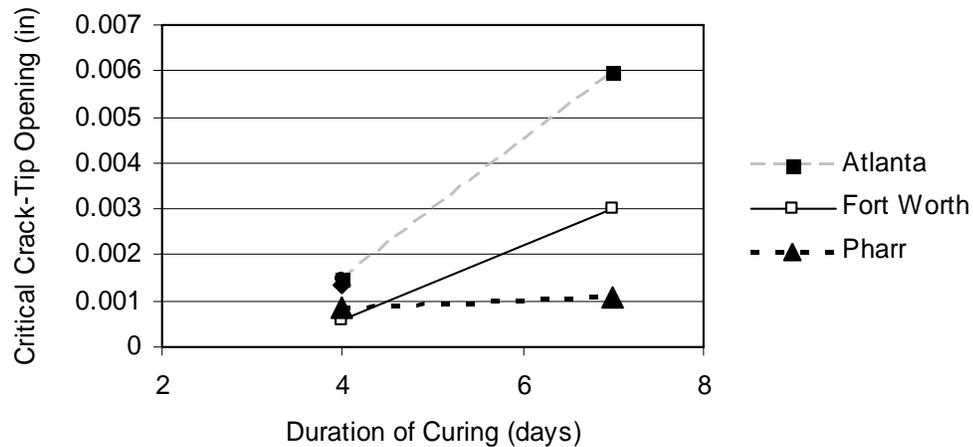
Figure 3.17 Critical Crack-Tip Opening Displacement at 7-Day Age.

3.1.2.3 Significance of Results Obtained in the Size-Effect Testing

On comparing the results obtained at 7-day age and 16-day age, several important trends can be found. In general, at 7-day age, the concretes were getting less brittle and increasing in fracture toughness with increased curing. On the other hand, it was found at 16-day age that some concretes grow more brittle with increased curing. Therefore, it would seem that some concretes initially grow less brittle with increased curing, and as hydration continues with age, the trends are reversed.

Further analysis can be carried out to determine the differences between concrete made with Type I cement and concrete made with Type I/II cement and fly ash or slag. It can be observed that when the failure loads of small-sized specimens are examined, Pharr is relatively strong, whereas in the case of medium and large cylinders Pharr is becoming less strong in relation with other mixes. This phenomenon is consistent with Pharr having a relatively smaller fracture process zone and fracture toughness compared with other mixes.

The above findings bring up some interesting issues. It appears that whenever a concrete mix gains fracture toughness due to a change in curing duration, there is a concomitant increase in the size of the fracture process zone, a fact that has been confirmed by limited testing on notched beams. Now, if one type of concrete had higher fracture toughness and a smaller fracture process zone than another type of concrete, it would mean that the nominal stress at failure of specimens of *any* size would be higher in the first concrete.

But take, for instance, the San Antonio mix concrete with fracture toughness and size of fracture process zone 1126 psi.in$^{1/2}$ and 4.4 in. at 4-day of curing and 928 psi.in$^{1/2}$ and 3.0 in. at 14-day curing. It can immediately be seen that according to which size of specimen is being tested, the type of concrete that is found to be "stronger" might be different. For instance, the split tensile strengths of Lubbock mix concrete after 2 and 14 days of curing and at 16-day age were obtained using 5 in.- diameter and 12 in.-diameter cylinders. The tensile strengths obtained for the 2 and 14 days of curing from the smaller cylinders were 453 psi and 445 psi, while that for larger cylinders were 466 psi and 529 psi, respectively. These results closely match the results obtained from the testing of notched cylinders, and the reproducibility of the trends obtained in this dissertation is somewhat confirmed. Thus the importance of taking the size-effect into account is clear in any comparison of fracture or fatigue fracture of concrete, and possibly many studies where only one size of specimen was tested, for example, the studies carried out by Issa and Shafiq (1999) and Raithby and Galloway (1974) could be improved upon . There is no published data where the more than one size of specimen was tested in fatigue for the purpose of comparison of different types of concrete; the only related investigations have been made on the size-effects in fatigue of a particular concrete (Bazant and Scell, 1993; Bazant and Xu, 1991). However, one size of specimen can be used if a second measurement such as the crack mouth opening displacement is concurrently taken to capture the size-effects, as done in the studies carried out by Navalurkar et.al. (1999) and Li and Ansari (2000). The energy of fracture of concrete is derived sometimes by experimentally computing the work done to create the fractured surface (Darwin et.al., 2001); again a comparison between concretes based on a single size of specimen might be inaccurate. For instance, a researcher testing only one size of specimen reported in this study would have come to entirely different conclusions depending on which size is being tested. Furthermore, the importance of structural dimension comes to light; for small structures the size of the fracture process zone could dominate, while for large structures, the fracture toughness could dominate.

The reasoning can be extended to bridge decks and pavements, where tensile stresses may be generated due to shrinkage or due to live or dead loads. The issue of the size and shape of starter flaws have been elucidated by some authors (Broek, 1986), and a finite element analysis could possibly be carried out to determine even approximately the values of $g(\ )$, $g'(\ )$, and the characteristic size d of these structures. It would then be possible to determine the relative effects of the fracture process zone and fracture toughness on the structure; such an approach would be key to determining a better concrete. Bazant and Planas (1998) have reported a limited number of analyses on applying the size-effect law to structures, but they are by no means complete.

The above findings bring up some critical issues regarding how representative the current philosophy of obtaining the fracture toughness of a type of concrete. Traditionally, the concrete is continuously moist-cured until the time of test, commonly 28 days, and fractured within about 4 hours of being taken out of the curing environment. If the specimens are not sealed to prevent loss of moisture, moisture gradients could influence

the failure loads. Furthermore, the fracture toughness and the size of process zone changes appreciably with curing duration, and not necessarily in a similar manner for all types of concrete, leading to the concrete in the tested specimens to be possibly very different from the concrete in structures. A possible improvement on the current test methods may be to curtail curing at a point in time to ensure that the levels of hydration in the concrete specimens are the same as in a structure.

3.1.3 Fatigue Tests

The number of cycles to failure, or if the specimen did not fail, the crack-mouth opening displacement (in inches) as measured by the clip-on-gauge is shown in Table 3.18 and Table 3.19 for testing carried out at 28-day age and 10-day age, respectively. Figure 3.18 and Figure 3.19 are plots with all the data points included. It would appear at first sight that, for most mix designs, the fatigue resistance at 28-day age has improved with duration of curing up to a curing time of 14 days. Similarly, the fatigue resistance of concretes at 10-day age could be said to have improved upon 7 days of curing when compared to 4 days of curing. However, the number of cycles to failure of a specimen subjected to fatigue loading is strongly correlated to its static strength. Therefore, from the work presented in section 3.1.2, testing of a different size of specimen could have led to totally different conclusions. It would appear that the great effort required to test many sizes of specimens in fatigue precludes comparisons of the fatigue resistances of a number of concretes.

Table 3.18 Results from Fatigue Testing at 28-Day Age for 5 in. Diameter Specimens.

Duration of Curing (days)	San Antonio		Pharr		Atlanta		Fort Worth		El Paso	
	spec 1	spec 2	spec 1	spec 2	spec 1	spec 2	spec 1	spec 2	spec 1	spec 2
	Number of Cycles to Failure or Crack-Mouth Opening Displacement (in)									
2	Failed Test	3127	7530	1076	6465	0.000035	67	57	27	37
4	2359	25866	0.000601	-0.000001	0.000074	0.000057	0.000237	21285	37	178
8	3485	11245	-0.000060	0.000053	0.000287	0.000036	890	0.000160	98	63
14	0.000572	0.000398	0.000044	0.000171	0.000023	0.000144	0.000115	7994	1312	2272
Set Point (lbs)	13500	13500	13500	13500	13500	13500	14000	14000	14000	14000
Amplitude (lbs)	3500	3500	3500	3500	3500	3500	3500	3500	3500	3500

Table 3.19 Results from Fatigue Testing at 10-Day Age for 5 in. Diameter Specimens.

Duration of Curing (days)	San Antonio		Pharr		Atlanta		Fort Worth		El Paso	
	spec 1	spec 2	spec 1	spec 2	spec 1	spec 2	spec 1	spec 2	spec 1	spec 2
	Number of Cycles to Failure or Crack-Mouth Opening Displacement (in)									
4	3090	Failed test	415	890	0.000044	0.000177	0.000027	1405	Failed Test	509
7	1749	30067	1362	13157	0.000479	4164	0.000654	0.000095	2065	209
Set Point (lbs)	13500	13500	13500	13500	13500	13500	13500	13500	13000	13000
Amplitude (lbs)	3500	3500	3500	3500	3500	3500	3500	3500	3500	3500
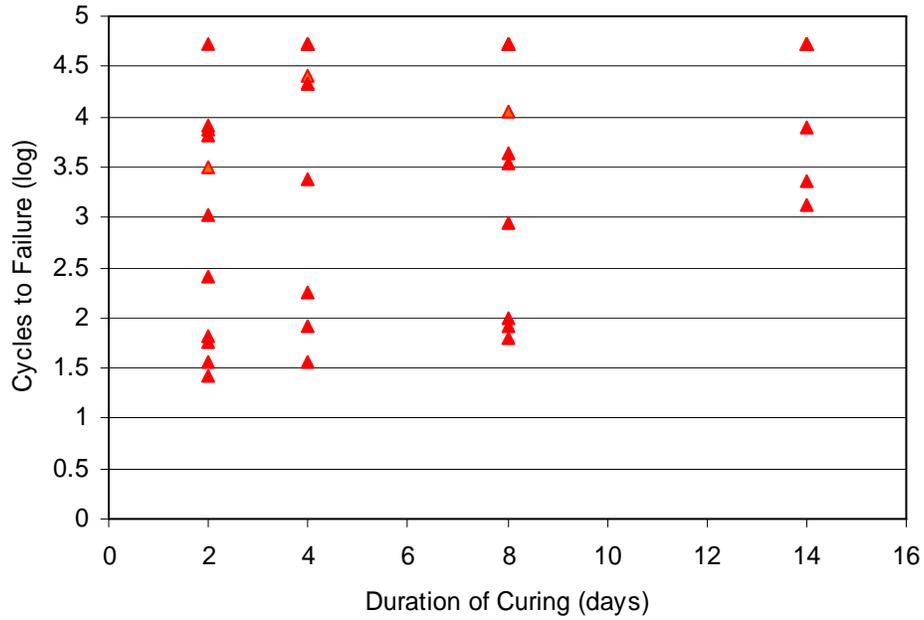
Figure 3.18. Fatigue Data at 28-Day Age for 5 in. Diameter Specimens.
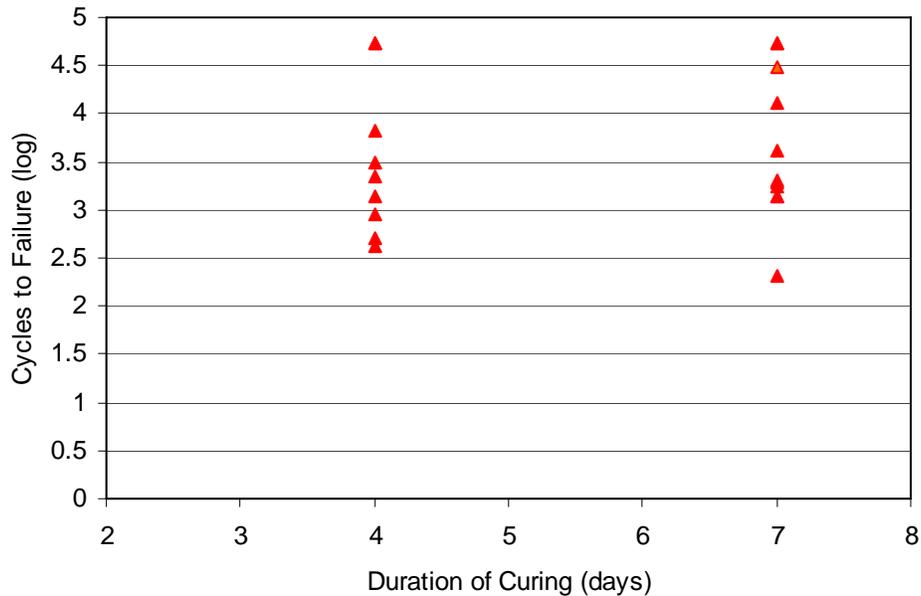
Figure 3.19 Fatigue Data at 10-Day Age for 5 in. Diameter Specimens.

All the above data were obtained by testing notched cylinders 5 inches in diameter and 6 inches in length. The fatigue testing of Lubbock was carried out on two sizes of cylinders to determine whether a size-effect could be captured. Cylinders of 8 in. diameter were tested at 28-day age, and cylinders of 4 in. diameter were tested at 19-day age. The cyclic loading was carried out at 10 Hz, and the data is presented in Table 4.21. All specimens were 4 inches long. When testing

the 4 in. diameter specimens, it was stipulated that if the specimens did not fail after 12,000 cycles, the set-point would be increased by 250 lbs for the next 12,000 cycles and so on; however, the increasing of the set-point had to be done only in the case of one specimen, as all the others failed within the initial 12,000 cycles. Unfortunately, the data presented do not seem to pinpoint the size-effect in fatigue, as was expected.

Table 3.20 Fatigue Data for Lubbock Mix.

Duration of Curing (days)	8 in. diameter		4 in. diameter	
	spec 1	spec 2	spec 1	spec 2
	Number of Cycles to Failure or Crack-Mouth Opening Displacement (in)			
2	0.000320	113	17	399
4	11612	0.000240	165	101
8	4567	0.000190	No test	No test
14	0.000240	0.000290	1220	14505
Set-Point (lbs)	11500	11500	6000	6000
Amplitude (lbs)	3500	3500	3500	3500

3.1.4 Absorption-Desorption Tests

Figure 3.20 and Figure 3.21 show for Pharr and Fort Worth mix, respectively, the average moisture losses from cylinders of 5 in. diameter and 6 in. length, tracked up to 14 days from the time they were taken out of the wet curing mat. The average weight losses of three cylinders were used to obtain the data shown in Figure 3.20., while the weight loss of two cylinders was tracked to generate Figure 3.21. During the time these measurements were taken, they were kept indoors in a room with a temperature of about 65° F, and a relative humidity of approximately 30%.
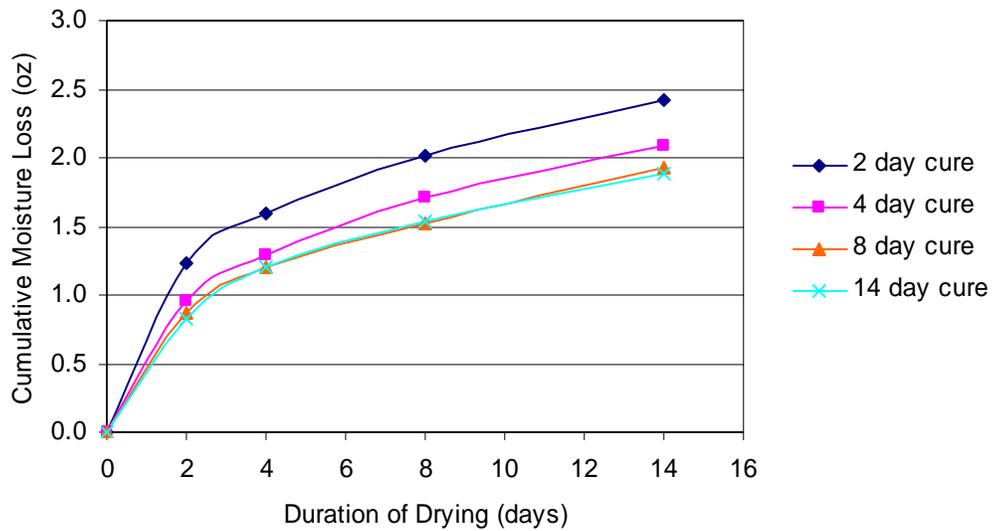
Figure 3.20. Moisture Loss from Pharr Specimens for 5 in. Diameter
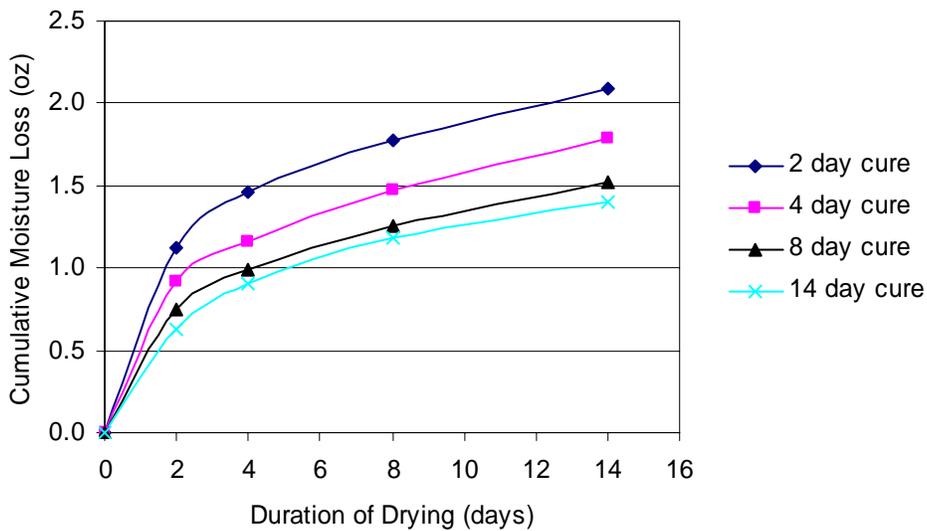
Figure 3.21. Moisture loss from Fort Worth Specimens for 5 in. Diameter.

Examining the two figures, several interesting conclusions can be made. First, in general, Pharr specimens lost more moisture, as expected. This is presumably because the fly ash included in

the Fort Worth specimens reduces permeability. Furthermore, there is a clear difference between the moisture lost by the specimens cured 8 and 14 days in the case of the Fort Worth specimens, whereas there is no such difference in the case of Pharr specimens. Thus, it seems that further hydration took place when concrete containing fly ash was cured more than 8 days, while in concrete without fly ash, this was not the case. Again, Pharr specimens display smaller gain in hydration from being cured eight days in comparison with 4 days, if the assumption that better hydration is revealed by lower moisture loss rates is valid.

Though the above trends are very clear-cut, it has to be taken into account that specimens taken out of the wet mats at 2-day age should lose more moisture than the specimens taken out of the wet mat at say, 14 days, purely because the concrete is more aged at 14 days. The effects of age add to the effects of curing, and should be accounted for in the analyses. Therefore, further experiments were carried out when the specimens reached 28-days age where the specimens were kept in a water bath for 24 hours and the weight of water absorbed measured. Again, the specimens taken out of the wet mat at 2-days age are "drier" than the others, and can be expected to absorb more water, independent of the level of hydration in them. The final step, where the specimens, after being saturated for 24 hours, were air-dried for 24 hours gave the best indicator of the levels of hydration within the specimens. The weights of water absorbed and desorbed in these periods are plotted in Figure 3.22 and Figure 3.23.
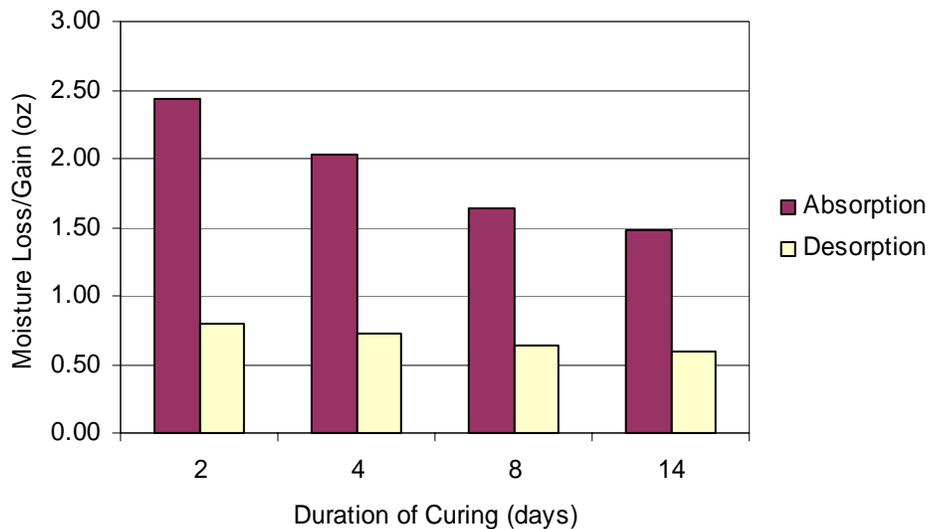
Figure 3.22. Absorption and Desorption of Pharr for 5 in. Diameter Specimens.
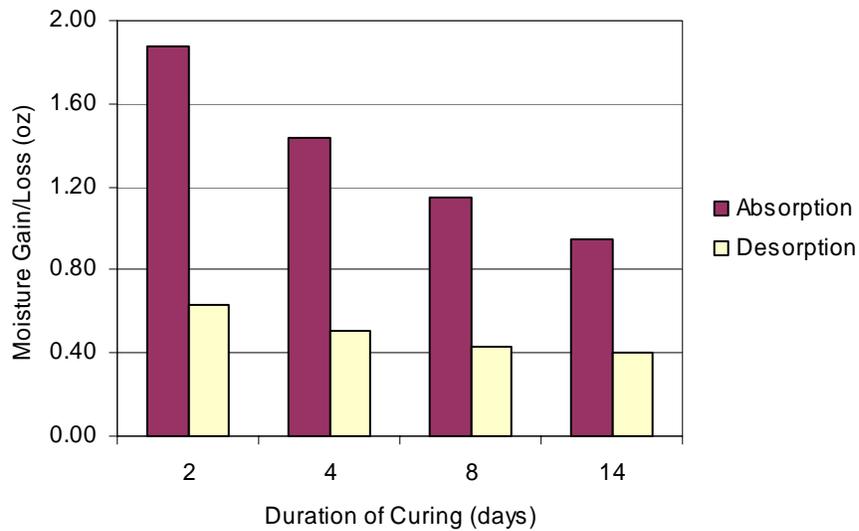
Figure 3.23 Absorption and Desorption of Fort Worth for 5 in. Diameter Specimens

The darker, taller columns in the above figures show the amounts of moisture absorbed in a 24 hour period, while the shorter columns show the moisture lost during the next 24 hours, while the specimens were been air dried. The trends are very clear-cut. The moisture gains decrease rapidly with increased curing time, though in the case of Pharr specimens, the difference in the moisture gain between 8-day cured specimens and 14-day cured specimens seem to be less striking than in the case of the Fort Worth Specimens. In both cases, the subsequent loss in moisture, which is the clearest indication of the level of hydration from all the above data, seems to be almost the same for specimens cured 8 days and 14 days.

To ascertain whether the above trends are reproducible using larger size cylinders, further tests were carried out on Fort Worth concrete using four cylinders of 8 in. diameter and 6 in. height. Again, weight loss was tracked after every specimen was taken out of the wet mat, and at 28-day age, they were submerged in a water-bath for 24 hours and then air dried for 24 hours. The weight gained by the cylinders and then lost during air-drying was recorded. The numbers obtained from these tests are shown in Figure 3.24 and Figure 3.25.
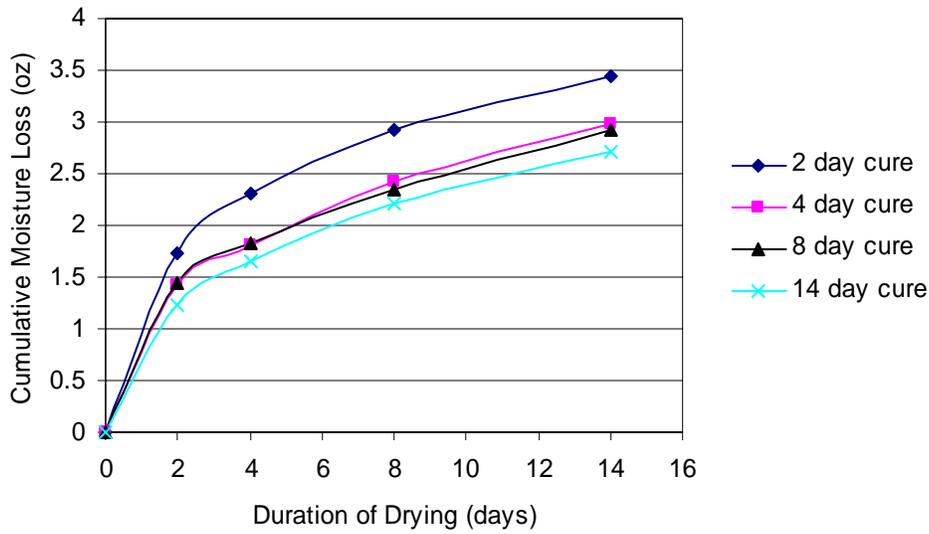
Figure 3.24. Moisture Loss from Fort Worth of 8 in. Diameter.
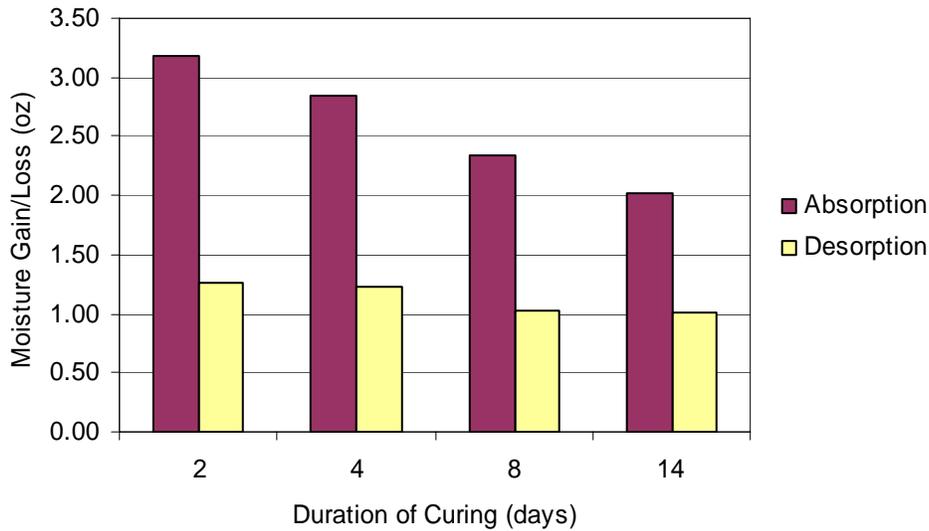
Figure 3.25 Absorption and Desorption of Fort Worth for 8 in. Diameter Specimens.

Assessing the trends presented in Figure 3.24, it is obvious that there are limited differences in the moisture loss profiles of the specimens cured four, eight, and fourteen days, while the specimen cured for 2 days showed substantially more moisture loss. This is in contrast to results obtained using 5 in. diameter specimens, where only the specimens cured 8 and 14 days showed similar moisture loss profiles. Figure 3.25 shows that though the mass of water absorbed in 24 hours decreased with increasing curing time in general, the mass of water lost in a 24-hour

period leveled off at 8 days of curing. As mentioned earlier, the latter values are the most accurate predictors of the level of hydration within the concrete specimens.

Based on the absorption-desorption data, it would appear that there is no substantial increase in hydration levels of concrete containing Type I cement on curing beyond 8 days, and there is very limited increase in hydration levels of concrete containing Type I/II cement and fly ash on curing beyond 8 days.

3.1.5 Tests to Determine Effects of Varying Thickness of Size-Effect Specimens

The compressive strengths of the concrete used in this analysis were found to be 6554 psi and 6345 psi at 31 days of age for 15-day curing, and 37 days of age at 4-day curing, respectively. The nominal stresses at failure of the specimens are shown in Table 3.21 and Table 3.22 for specimens cured for 15 days and 4 days respectively. The average nominal stresses at failure are also shown in Figure 3.26 and Figure 3.27. It should be remembered that, as detailed in the chapter on experimental procedures, one set of cylinders with 4 in., 8 in., and 16 in. diameter were cast with lengths of 4 in., while supplementary cylinders of 8 in. and 16 in. diameter were cast with shorter lengths ensuring that uniform curing and drying took place unlike cylinders of 4 in. length. In the tables and figures, data corresponding to the cylinders with lengths varied as described above are labeled "varied length."

Table 3.21. Nominal Stresses at Failure for Specimens Cured for 15 Days.

Diameter	Spec. 1	Spec. 2	Spec. 3	Average
	Nominal Stress at Failure (psi)			
4in.	456	406	408	423
8in. Varied Length	342	354	378	358
8 in. Constant Length	385	356	368	370
16 in. Varied Length	347	321	345	337
16 in. Constant Length	276	336	338	316

Table 3.22. Nominal Stresses at Failure of Specimens Cured for 4 Days.

Diameter	Spec. 1	Spec. 2	Spec. 3	Average
	Nominal Stress at Failure (psi)			
4in.	369	307	392	356
8in. Varied Length	315	343	333	331
8 in. Constant Length	370	282	391	348
16 in. Varied Length	307	316	341	321
16 in. Constant Length	326	326	336	329
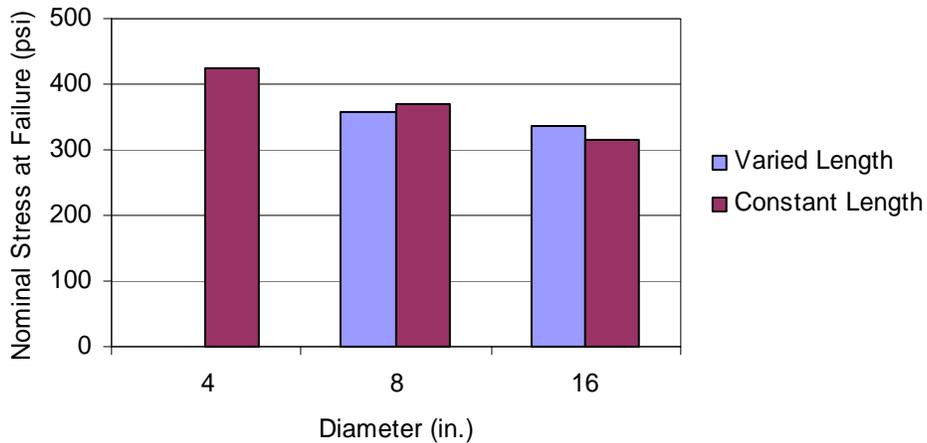
Figure 3.26 Average Nominal Stresses at Failure of Specimens Cured for 15 Days.
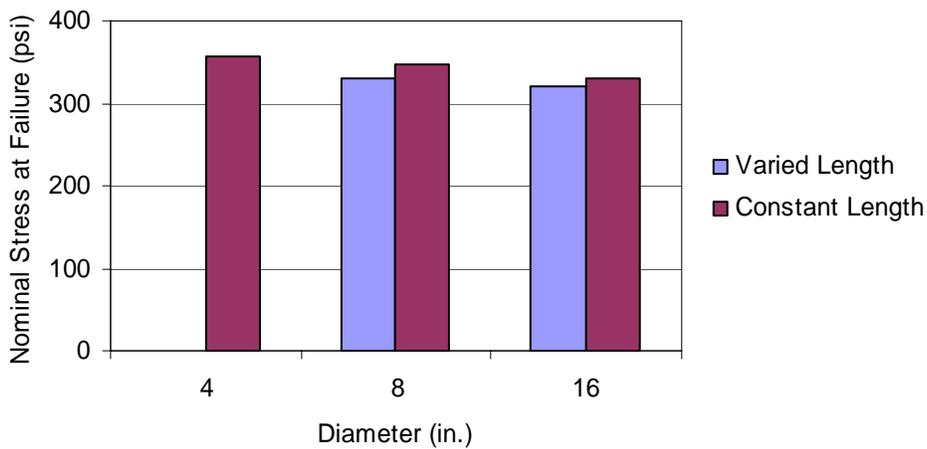
Figure 3.27 Average Nominal Stresses at Failure of Specimens Cured for 4 days.

Examining Figure 3.26, it can be seen that the hypothesis that the nominal failure stresses of specimens cured for extended periods of time are independent of their lengths seems to be correct. Though there are slight differences in the nominal stresses at failure of the cylinders with constant lengths and shorter lengths, the deviations are not systematic. It is surprising though, that the nominal stresses at failure of the specimens cured for 4 days were not affected significantly by varying the lengths of the specimens. It is possible that the concrete chosen to carry out this testing is not sensitive to the slight variations in the moisture conditions due to changes in lengths of specimens, at least as far as fracture properties go. However, when examining the fracture surfaces of the cylinders cured for 4 days, it was apparent that indeed the specimens with the varied lengths had similar hydration products, unlike the specimens with uniform length. This phenomenon is shown in Figure 3.28.

Figure 3.28 Differences in Hydrated Products Shown on Fractured Surfaces.

It is obvious that the products of hydration of the small cylinder are similar to the products of hydration of the thinner specimen on the left, whereas the specimen on the right with the same length as the small specimen is darker in color, probably due to it losing less moisture and hydrating to a relatively high degree upon being taken out of the curing environment.

It is thus established that there is no systematic error of thinner specimens failing at smaller loads due to buckling-type effects. Testing was carried out thereafter to prove that differential drying does lead to differences in the nominal stresses at failure of some types of concrete for some curing durations and ages. Specimens manufactured with the El Paso mix design, with the aggregate from Lubbock mix substituted for the aggregate from El Paso mix, were used, with specimens of 8 in. diameter being cured for 2 days and tested at 7 days of age. Two sets of notched specimens were manufactured; one with a nominal thickness of 4 in., and another with nominal thickness of 2.5 in. Three specimens were manufactured of each length. The nominal stresses at failure are shown in Table 3.23 and Figure 3.29.

Table 3.23 Ultimate Stresses Exhibiting Length Effects.

Length (in)	Specimen	Stress (psi)	Average (psi)
2.5 in.	Spec. 1	299	293
	Spec. 2	316	
	Spec. 3	264	
4 in.	Spec. 1	209	238
	Spec. 2	265	
	Spec. 3	240	
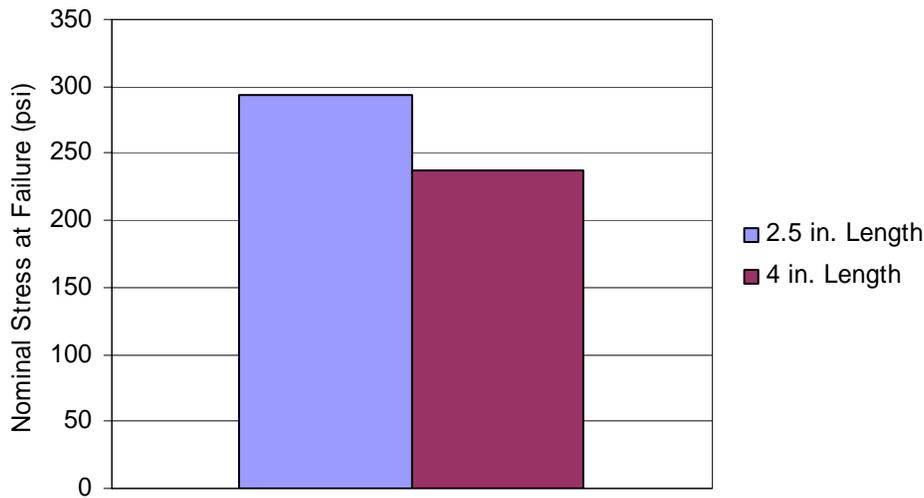
Figure 3.29 Ultimate Stresses Exhibiting Length Effects.

Obviously, the shorter cylinders lost relative humidity faster than the longer cylinders. It is not unexpected that the failure stresses of the longer specimens were lower, as specimens of 8 in. diameter cured for 7 days manufactured from El Paso mix concrete were weaker than specimens cured for only 4 days, i.e., for this combination of age and concrete type, better hydration leads to lower failure loads for the smaller sizes of cylinders tested. To conclude from the testing on effects of varying lengths of cylinders, it seems that the modified test procedure is highly desirable because it requires less concrete, requires lower capacities of loading machines, allows more specimens to be manufactured from a single batch of concrete, and specimens cure and dry more uniformly.

3.1.6 Tests for Comparison of Jenq-Shah Model and Size-Effect Law

The tests were carried out under COD control, in such a manner that both the Jenq-Shah model parameters and size-effect law parameters could be obtained from them. The specimen sizes were reported in Table 3.9., while the nominal stresses at failure for these tests were reported in Table 3.21 and Table 3.22. The fracture parameters at 28-day age as defined by Bazant's model, obtained from considering all specimens with constant length, and all specimens with varying length, are shown in Table 3.24.

Table 3.24 Fracture Parameters as Defined by the Size-Effect Law.

Duration of Curing (days)	Specimens with Varied Length		Specimens with Constant Length	
	K_{Ic} (psi.in$^{1/2}$)	c_f (in)	K_{Ic} (psi.in$^{1/2}$)	c_f (in)
15	1066	3.0	852	1.6
4	1503	9.2	1816	13.6

It is immediately apparent that, though the differences of the average nominal stresses at failure for specimens of constant length and specimens of varied length for each curing age was in the order of 4%, the variations in the fracture properties obtained are much larger. This is due to the very small differences between the nominal stresses at failure of the different sizes of cylinders used in testing. The fall-off in nominal stresses at failure with increasing size of notched beams is larger than in the case of notched cylinders, and the fracture parameters calculated have more precision as it is the *differences* between the nominal stresses at failure of the smaller and larger specimens that determine their numerical values. However, from the above data it can be stated with confidence that the concrete cured for 4 days is less brittle than the concrete cured for 14 days.

An attempt was made to determine the fracture parameters as predicted by the two parameter model thereafter. It was immediately found that the notched cylinder geometry does not permit the accurate determination of these parameters. It was confirmed by a leading authority on the subject that it is exceedingly difficult to use the compliance method on notched cylinders to determine the fracture properties of concrete (Tang, 2003). To demonstrate the difficulties, consider the fact that the Young's modulus of the concrete cured for 4 days, as determined by the initial compliance of four specimens using Equation 2.19 to be 22.45×10^6 psi, and from independent tests carried out on 6 in. diameter 12 in. length cylinders to be 5.75×10^6 psi. It may be wondered as to what the differences are between notched beams, on which it is quite easy to perform the two parameter model test, and notched cylinders. It should be remembered that (1) the knife edges are fixed a finite distance from the crack line (2) more importantly, in the case of notched beams, the crack mouth opening displacement is uniform along the length of the crack, whereas in notched cylinders, the crack mouth opening is variable along the length of the crack. For these reasons, a comparison between the parameters obtained from the two models cannot be carried out on notched cylinders.

It was thus concluded that the objectives (1), (2), and (5) as described in section 1.1.3 of the introduction cannot be fulfilled using notched cylinders as specimens, though objectives (3) and (4) were adequately dealt with. Therefore, though the methodology for obtaining the fracture parameters of concrete as defined by the two-parameter model has been laid out, it cannot be used in reality because of the difficulties described above.

3.2 FLEXURE

3.2.1 Flexural Strength Tests

The average flexural strengths for each mix design at 7-day age, obtained from testing three replicate specimens, are shown in Table 3.25. To facilitate further discussion, the data is also shown in Figure 3.30 and Figure 3.31, with the former figure limited to the data from the mix designs that portray clearer trends. The flexural strength obtained from every replicate is given in the Appendix.

Table 3.25 Flexural Strength of Bridge Deck Concrete Mixes.

Duration of Curing (days)	Lubbock (psi)	San Antonio (psi)	Atlanta (psi)	Pharr (psi)	Fort Worth (psi)	El Paso (psi)
0	508	628	585	439	564	458
2	536	556	622	438	535	499
4	531	636	661	517	566	419
7	555	652	693	628	539	573
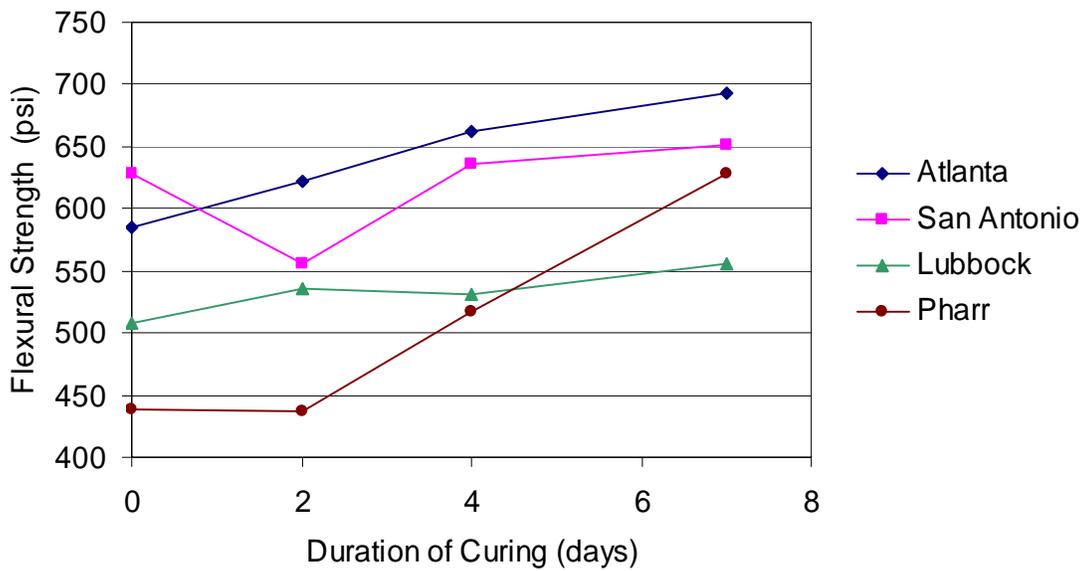
Figure 3.30 Average Flexural Strengths of Atlanta, San Antonio, Lubbock, and Pharr Concretes.
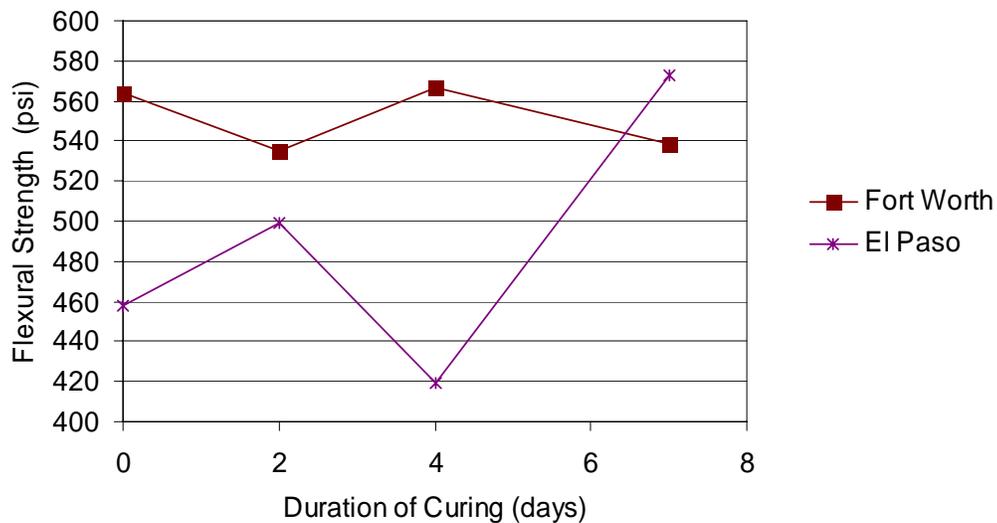
Figure 3.31 Average Flexural Strengths of Fort Worth and El Paso Concretes.

On examining Figure 3.30, it can be seen that data from the two lab-cast mixes, Atlanta mix and Pharr, show a trend of increasing flexural strength with increasing duration of curing. San Antonio mix and Lubbock mix could perhaps be said to have a weak trend of increasing flexural strength with increasing curing duration, notwithstanding the rather large scatter found in the

flexural strengths of San Antonio mix. It can also be observed that, in general, San Antonio mix and Atlanta mix seem to have the higher flexural strengths, while Figure 3.36 shows the El Paso mix seems to have a relatively lower flexural strength for most durations of curing. Since 50% of El Paso's cementitious material is slag, it can be deduced that concretes containing relatively large amounts of slag have lower flexural strengths at 7-day age.

There could be several reasons why there is fairly large scatter in the flexural strength data from field-cast specimens; dew could have formed on the specimens from time to time, or the lower face of some of the specimens could have retained surface moisture. According to a survey of the State Departments of Transportations (DOT), carried out at Texas Tech University as part of the research project this dissertation was generated from, many DOTs use flexural strength as an acceptance criterion (Garcia, 2002). It would appear that such a policy is not advisable given the variability in the field-cast data, and moving over to the compressive strength test as an acceptance criterion is preferable. Furthermore, the findings presented in this dissertation show that there are considerable influences of specimen size in comparisons of fracture or tensile strength data, and the flexural strength test could also be affected by specimen size, as will be discussed in subsequent sections.

3.3 SHRINKAGE

3.3.1 Free Linear Shrinkage Tests (Modified ASTM C 157-3)

3.3.1.1 Discussion of Results

Based on the free linear shrinkage data obtained from different district mixes an attempt has been made to compare the effect of different curing durations on the free shrinkage. Also the drying shrinkage and internal relative humidity data obtained for 3 district mixes is used to compare them. The results obtained are discussed in this section.

3.3.1.2 Free shrinkage with respect to day-1 length

Free shrinkage with respect to day-1 length has been made using Eq. 2.27. Due to lack of surface temperature data for Atlanta, El Paso, San Antonio and Houston district mixes temperature corrections were not made. Temperature corrections using Eq. 2.27 were made for Pharr, Fort Worth and Lubbock district mixes. Tables 3.30, 3.31, and 3.32 give the free shrinkage strain values in micro strains ($\mu\varepsilon$) for Pharr, Fort Worth and Lubbock district mixes, the values shown in the table are temperature corrected. Tables 3.26, 3.27, 3.28, and 3.29 give the free shrinkage strain values in micro strains ($\mu\varepsilon$) without temperature corrections for Atlanta, Houston, El Paso and San Antonio, respectively.

Figures 3.22 through 3.38 show age (day of reading) versus shrinkage strain (in $\mu\varepsilon$) plots, showing different curves for different curing durations for Atlanta, Houston, El Paso, San Antonio, Pharr, Fort Worth and Lubbock, respectively.

Looking at the shrinkage strain values obtained in this section, it can be said that increased curing duration is able to delay the shrinkage strain of concrete. However, additional information regarding the strength and stiffness of the mixes is necessary to understand the significance of this delay. Thus, shrinkage strain values in correlation with the modulus of elasticity values obtained in chapter 4 are used to estimate the shrinkage tensile stress developed due to 100% restraint. The splitting tensile strength values obtained in Chapter 2 will be used to compare the tensile strength and shrinkage tensile stress development, to estimate the age of first crack. Comparing the age of first crack for different curing durations, optimum curing period will be predicted.

Table 3.26 Free Shrinkage for Atlanta District Mix, 24 h (with respect to day-1 length)

Average Shrinkage strain in (after 24hours)								
	Shrinkage on Day							
Curing	1	2	4	7	10	14	21	28
Days	~	D1-D2	D1-D4	D1-D7	D1-D10	D1-D14	D1-D21	D1-D28
0 day	0.0	-3	-7	33	73	117	153	210
2 day	0.0	-67	-33	17	67	117	150	197
4 day	0.0	-67	-93	-13	37	110	143	193
7 day	0.0	-67	-93	-117	-23	47	107	163
10 day	0.0	-67	-93	-117	-140	-20	45	125
14 day	0.0	-67	-93	-117	-140	-97	23	123
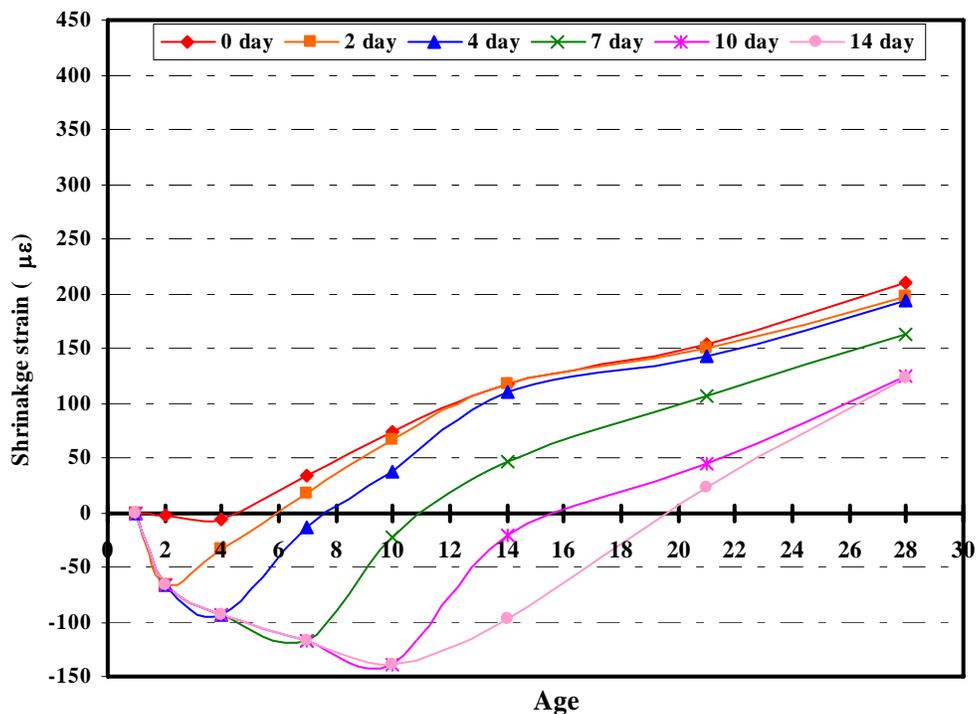
Figure 3.32. Free shrinkage strain (24 h) for Atlanta district mix

Table 3.27 Free Shrinkage for Houston District Mix, 24 h

Average Shrinkage strain in (after 24hours)								
	Shrinkage on Day							
Curing	1	2	4	7	10	14	21	28
Days	~	D1-D2	D1-D4	D1-D7	D1-D10	D1-D14	D1-D21	D1-D28
0 day	0.0	30	97	223	263	347	347	363
2 day	0.0	-47	20	130	187	283	310	353
4 day	0.0	-47	-83	40	120	240	287	343
7 day	0.0	-47	-83	-57	3	120	200	273
10 day	0.0	-47	-83	--	-97	27	143	247
14 day	0.0	-47	-83	--	-97	-95	80	215
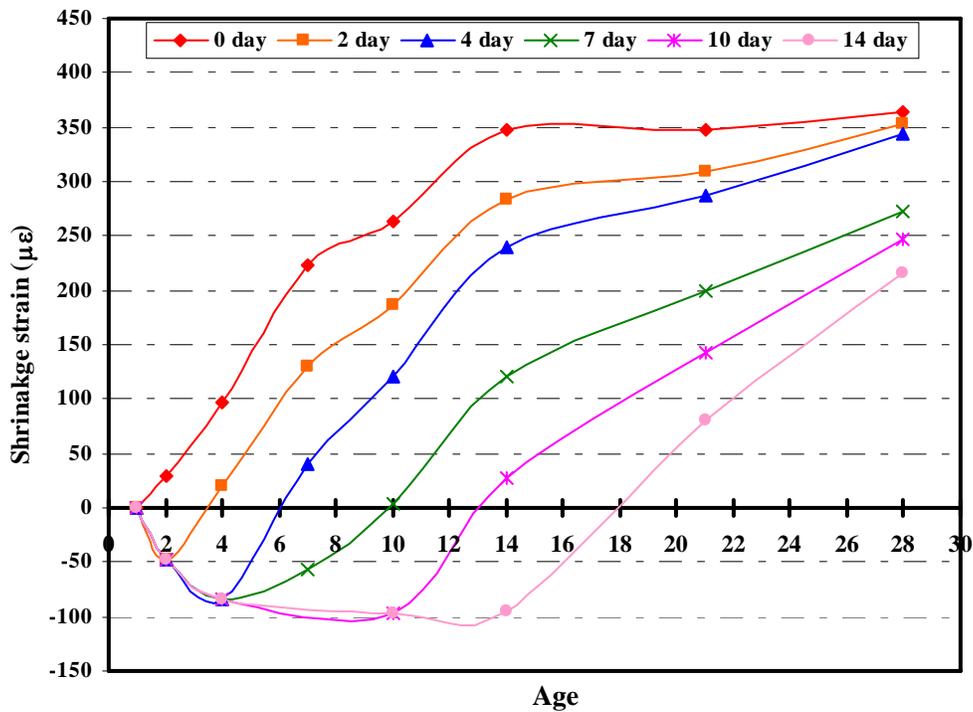
Figure 3.33 Free Shrinkage Strain (24 h) for Houston District Mix

Table 3.28 Free Shrinkage for El Paso District Mix, 24 h

Average Shrinkage strain in (after 24hours)							
	Shrinkage on Day						
Curing	1	4	7	14	16	21	28
Days	D1-D1	D1-D4	D1-D7	D1-D14	D1-D16	D1-D21	D1-D28
0 day	0.0	170	317	337	370	390	433
4 day	0.0	-47	120	173	207	253	300
7 day	0.0	-47	-13	77	137	177	243
14 day	0.0	-47	--	-60	-23	73	143
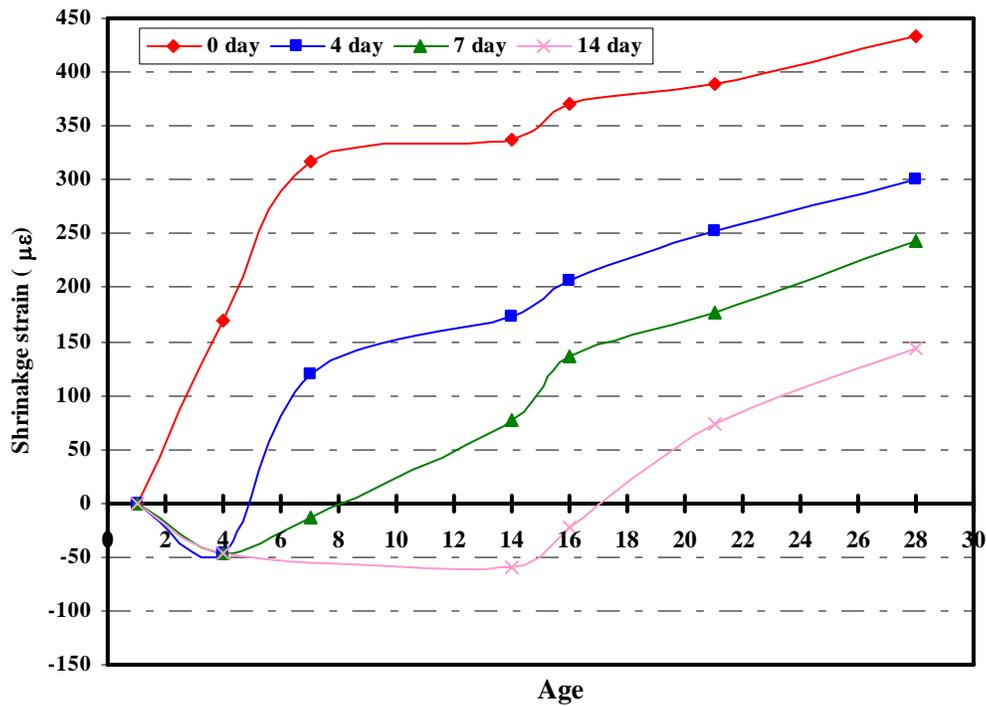
Figure 3.34. Free shrinkage strain (24 h) for El Paso district mix

Table 3.29 Free shrinkage for San Antonio district mix, 24 h

Average Shrinkage strain in (after 24hours)							
	Shrinkage on Day						
Curing	1	4	7	14	16	21	28
Days	D1-D1	D1-D4	D1-D7	D1-D14	D1-D16	D1-D21	D1-D28
0 day	0.0	77	133	200	227	263	280
4 day	0.0	-50	63	163	203	253	263
7 day	0.0	-50	-57	107	147	213	220
14 day	0.0	-50	-57	-57	-3	130	173
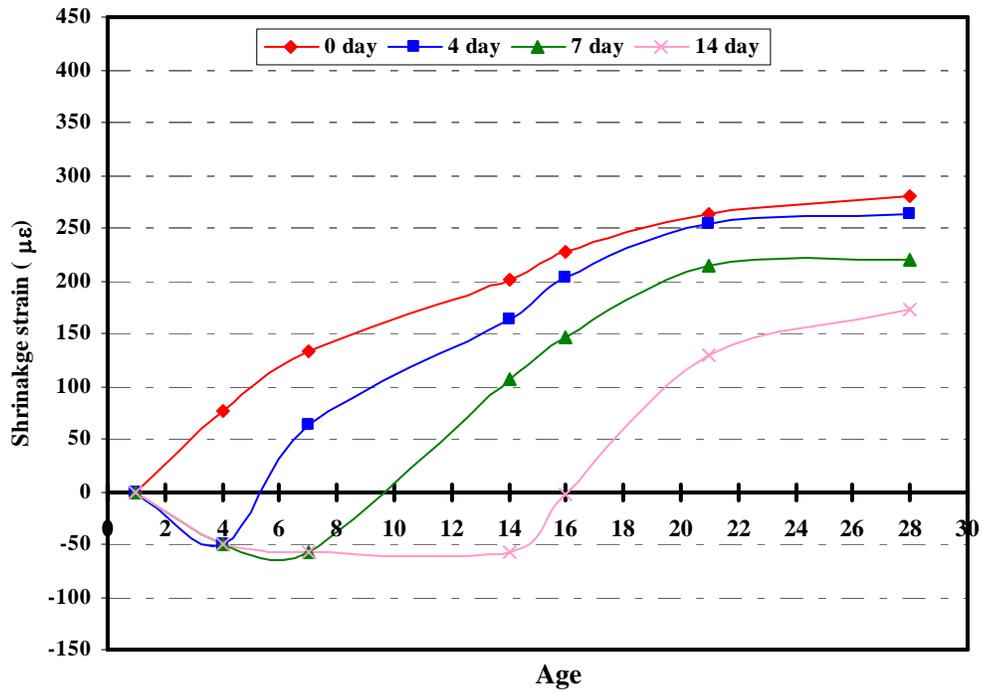
Figure 3.35 Free shrinkage strain (24 h) for San Antonio district mix

Table 3.30 Free shrinkage for Pharr district mix, 24 h

Average Shrinkage strain in (after 24h) using 70^{0}F as reference								
	Shrinkage on Day							
Curing	1	2	4	7	10	14	21	28
Days	~	D1-D2	D1-D4	D1-D7	D1-D10	D1-D14	D1-D21	D1-D28
0 day	0.0	34	93	142	182	209	242	258
2 day	0.0	-31	63	122	169	203	249	261
4 day	0.0	-31	-19	85	132	179	219	241
7 day	0.0	-31	-19	-16	79	133	192	218
10 day	0.0	-31	-19	-16	-27	83	155	188
14 day	0.0	-31	-19	-16	-27	-21	102	153
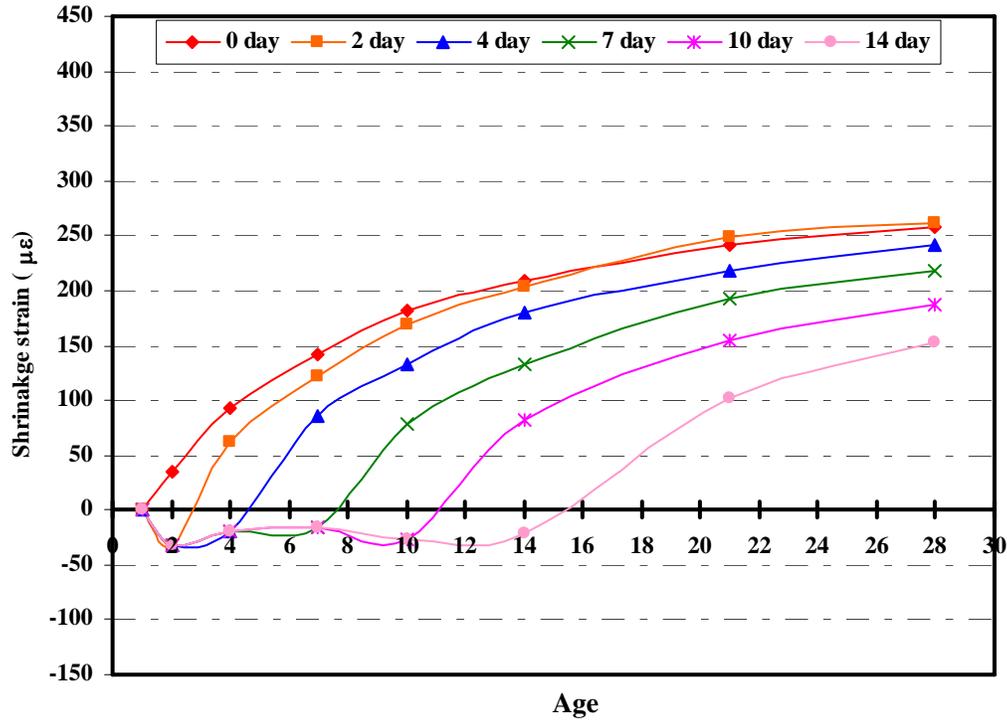
Figure 3.36 Free shrinkage strain (24 h) for Pharr district mix

Table 3.31 Free shrinkage for Fort Worth district mix, 24 h

Average Shrinkage strain in		(after 24hours) using 70⁰F as reference							
	Shrinkage on Day								
Curing	1	4	6	7	9	10	12	21	28
Days	~	d1-d4	d1-d6	d1-d7	d1-d9	d1-d10	d1-d12	d1-d21	d1-d28
0 day	0.0	87	148	178	226	237	267	350	369
4 day	0.0	-19	85	121	173	191	227	323	349
7 day	0.0	-19	--	-47	87	111	160	273	309
10 day	0.0	-19	--	-47	--	-51	57	213	256
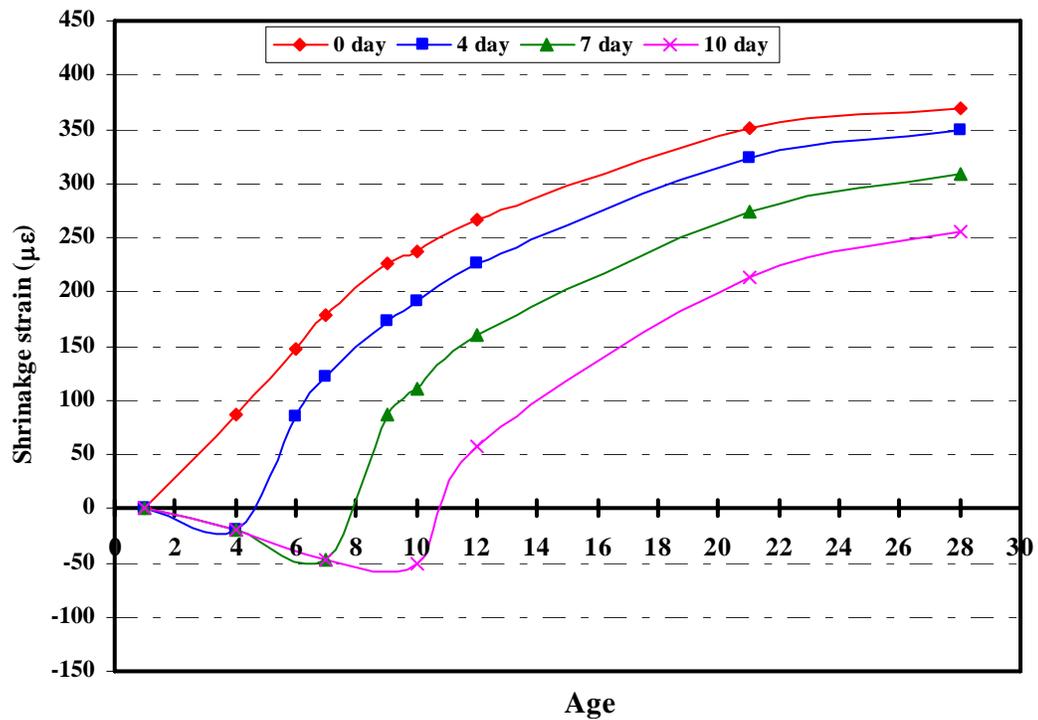
Figure 3.37 Free shrinkage strain (24 h) for Fort Worth district mix

Table 3.32 Free shrinkage for Lubbock district mix, 24 h

Average Shrinkage strain in		(after 24hours) using 70^{0}F as reference							
	Shrinkage on Day								
Curing	1	4	6	7	9	10	12	21	28
Days	~	d1-d4	d1-d6	d1-d7	d1-d9	d1-d10	d1-d12	d1-d21	d1-d28
0 day	0.0	142	181	203	253	273	299	375	388
4 day	0.0	-39	81	113	173	200	236	329	355
7 day	0.0	-39	--	-60	73	107	156	279	311
10 day	0.0	-39	--	-60	--	-64	46	215	268
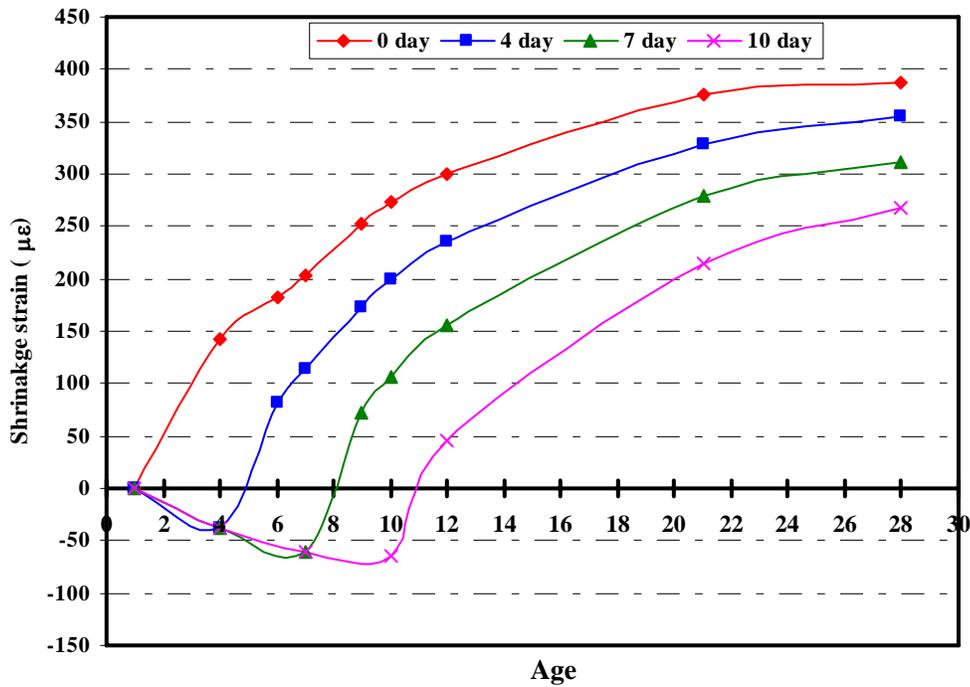
Figure 3.38 Free shrinkage strain (24 h) for Lubbock district mix

3.3.1.3 Drying Shrinkage

Drying shrinkage of the concrete, from the day the specimens are taken out of the water bath is calculated using Eq. 2.25. This drying shrinkage is not being used to estimate the tensile stress developed due to 100% restraint, as the stress development due to restraint begins right from the age when concrete is completely set (assumed as 24 h). However, drying shrinkage values using Eq. 2.25 in correlation with the internal relative humidity values using Eq. 2.26 can be used to compare different mixes. Due to the lack of availability of the surface temperature and relative humidity values for Atlanta, Houston, El Paso and San Antonio, only Pharr, Fort Worth and Lubbock district mixes will be compared, and are shown in Figures 3.39 through 3.41.

Temperature variations make a significant difference in the drying shrinkage values therefore making it necessary to make temperature corrections using Eq. 3.5. As the surface temperature data is not available for all the district mixes, Pharr, Fort Worth and Lubbock district mixes will only be discussed for drying shrinkage.

Table 3.33 Free drying shrinkage for Pharr district mix

Average Shrinkage strain in (drying shrinkage; *after taking out of bath*) using 70^0F as reference								
Curing Days	Drying shrinkage on Day							
	1	2	4	7	10	14	21	28
0 day	0.0	34	93	142	182	209	242	258
2 day	--	0.0	94	153	200	234	280	293
4 day	--	--	0.0	105	151	199	238	261
7 day	--	--	--	0.0	95	149	208	234
10 day	--	--	--	--	0.0	109	182	215
14 day	--	--	--	--	--	0.0	123	174
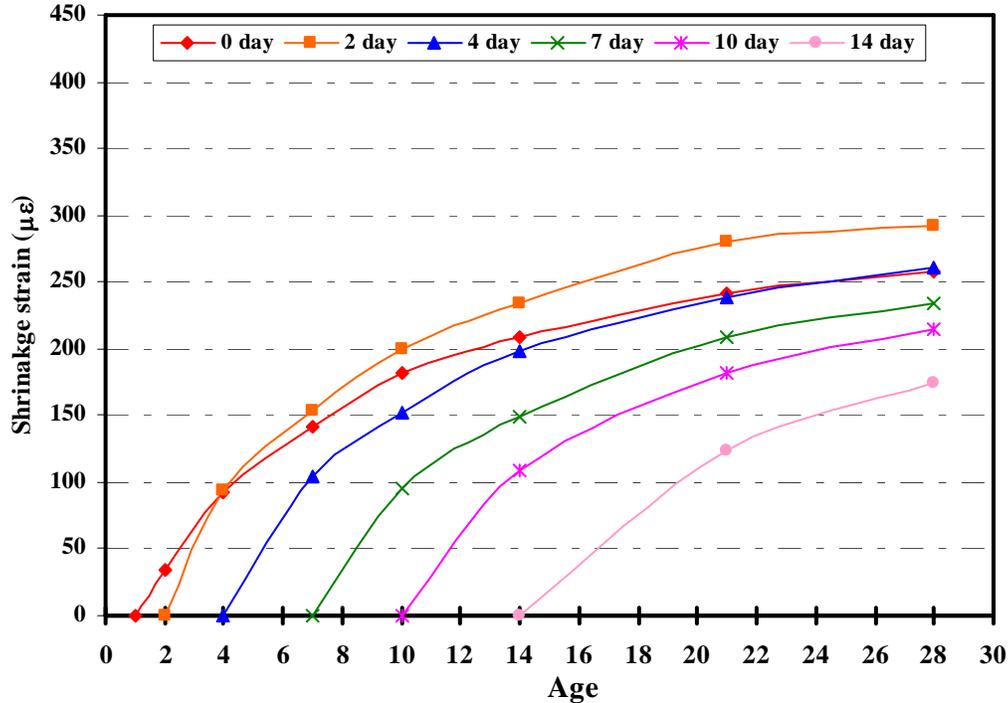
Figure 3.39 Free drying shrinkage strain for Pharr district mix

Table 3.34 Free drying shrinkage for Fort Worth district mix

Average Shrinkage strain in using 70⁰F as reference	(drying shrinkage; *after taking out of bath*)							
Curing	**Shrinkage on Day**							
Days	1	4	6	7	9	10	12	21	28
0 day	0.0	87	148	178	226	237	267	350	369
4 day	--	0.0	104	141	193	210	246	343	369
7 day	--	--	--	0.0	133	157	207	320	356
10 day	--	--	--	--	--	0.0	107	264	307
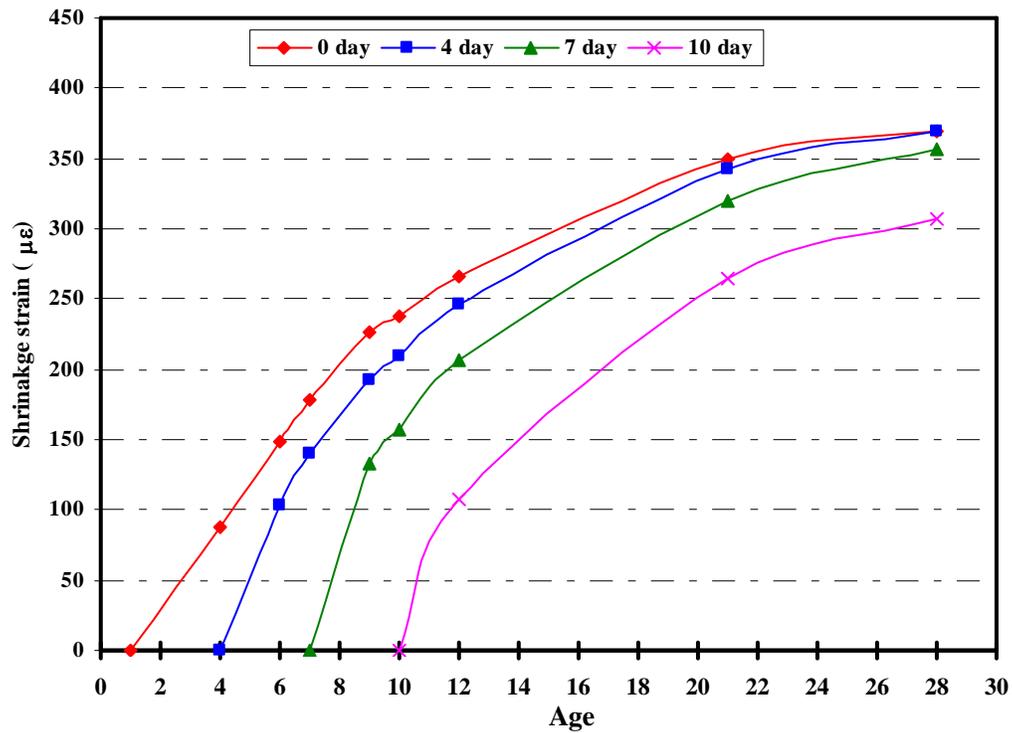
Figure 3.40 Free drying shrinkage strain for Fort Worth district mix

Table 3.35 Free drying shrinkage for Lubbock district mix

Average Shrinkage strain in (drying shrinkage; *after taking out of bath*) using 70^{0}F as reference									
Curing Days	**Shrinkage on Day**								
	1	4	6	7	9	10	12	21	28
0 day	0.0	142	181	203	253	273	299	375	388
4 day	--	0.0	120	152	211	239	275	367	393
7 day	--	--	--	0.0	133	167	216	339	371
10 day	--	--	--	--	--	0.0	110	279	332
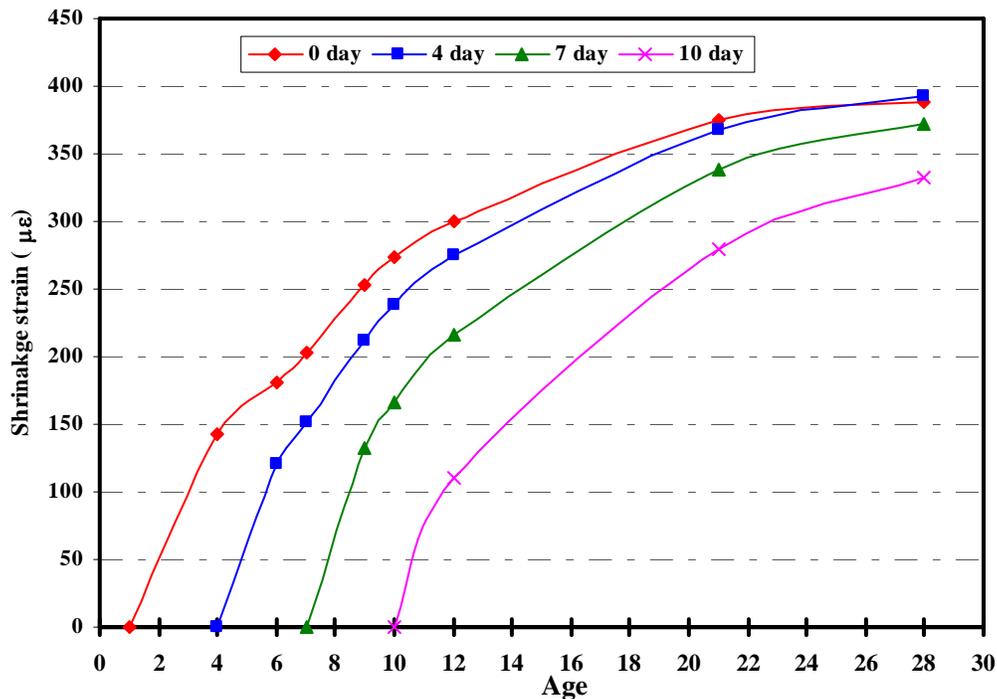
Figure 3.41 Free drying shrinkage strain for Lubbock district mix

3.3.1.4 Internal Relative Moisture Content

As discussed earlier, tracking internal moisture content helps compare different mix designs. The comparison of different mix designs is done in section 3.3.1.5. Here in this section the loss of internal moisture content will be discussed for 3 different district mixes.

Relative moisture content with respect to the moisture content on day-1 increases as the concrete is being cured in the water bath and it later drops during the drying process, as shown in Figures 3.42, 3.44 and 3.46 for Pharr, Fort Worth and Lubbock district mixes respectively. However, the

relative moisture content with respect to the moisture content on the day when concrete is taken out of the water bath is used to compare different mixes. This relative moisture content is referred to as drying relative moisture content and is shown in Figures 3.43, 3.45 and 3.46 for Pharr, Fort Worth and Lubbock district mixes.
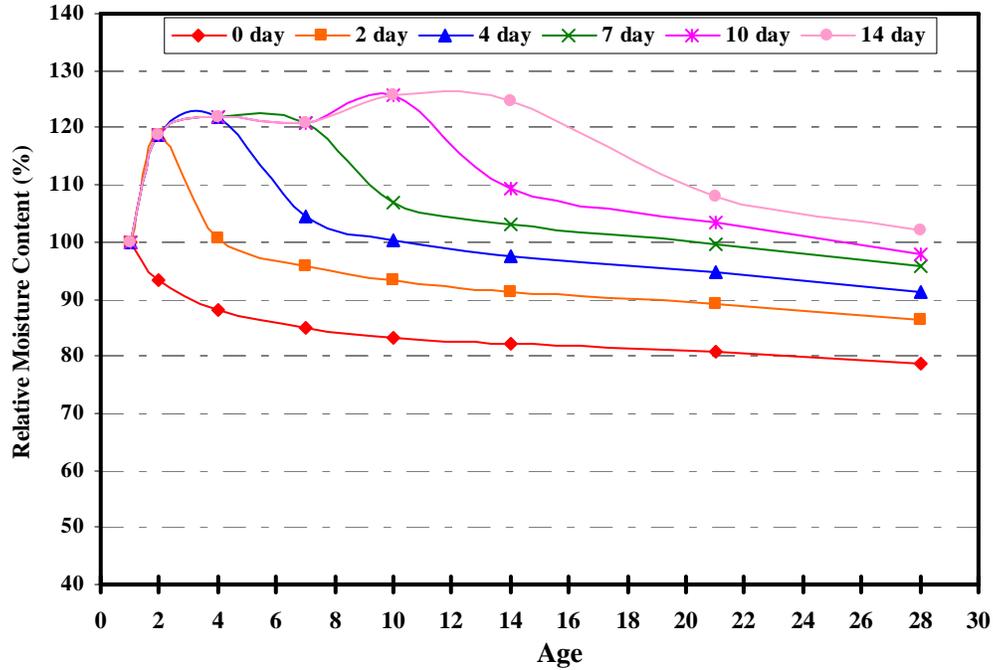
Figure 3.42. Moisture content relative to day-1 for Pharr district mix
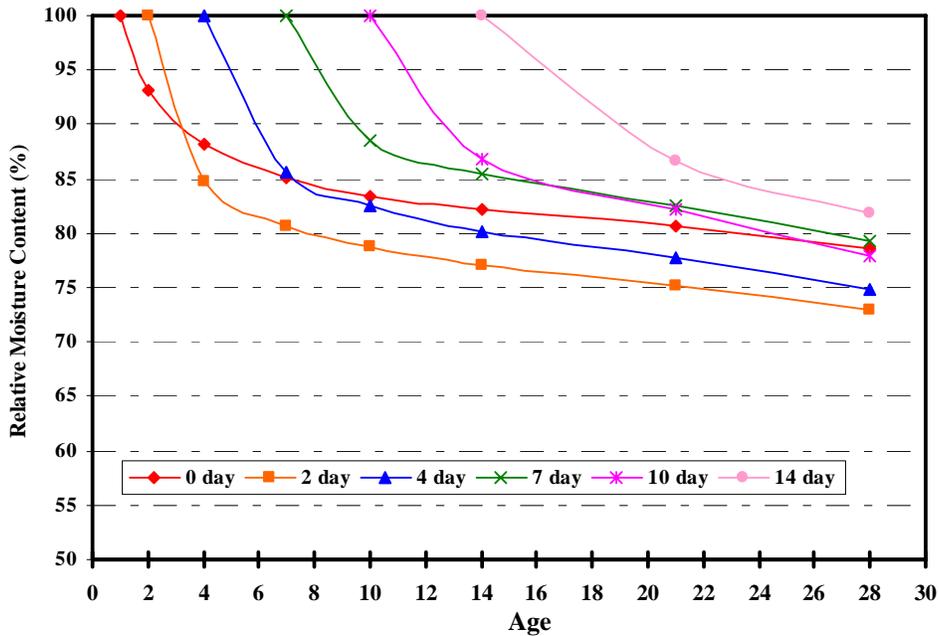
Figure 3.43 Relative moisture content (drying) for Pharr district mix
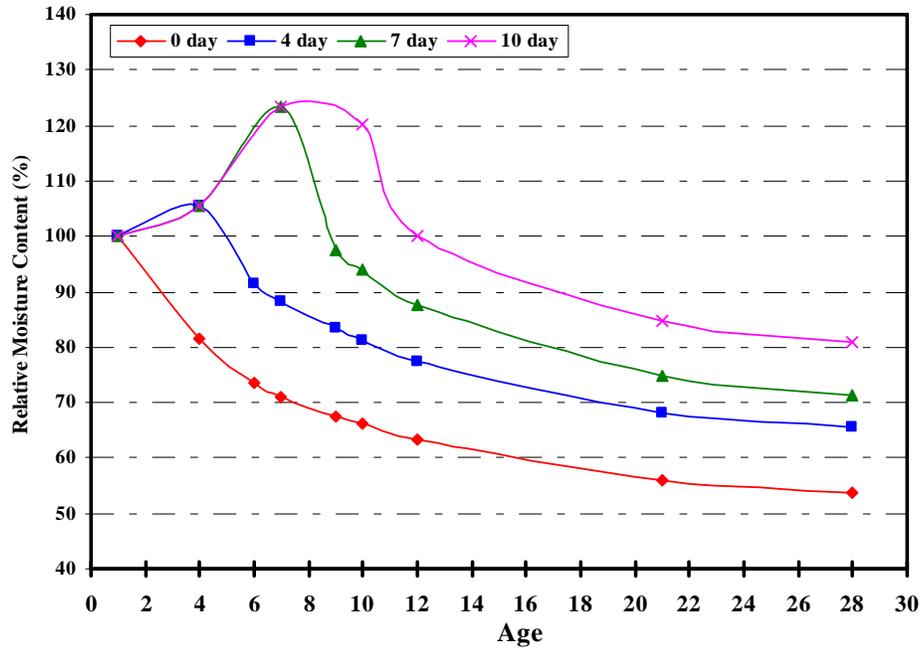
Figure 3.44 Moisture content relative to day-1 for Fort Worth district mix
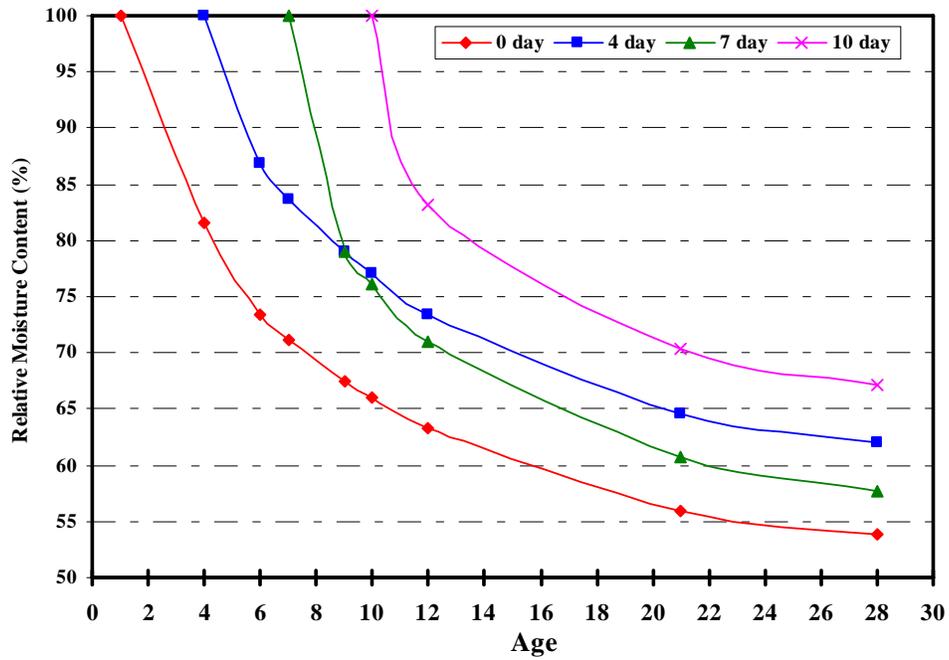
Figure 3.45 Relative moisture content (drying) for Fort Worth district mix
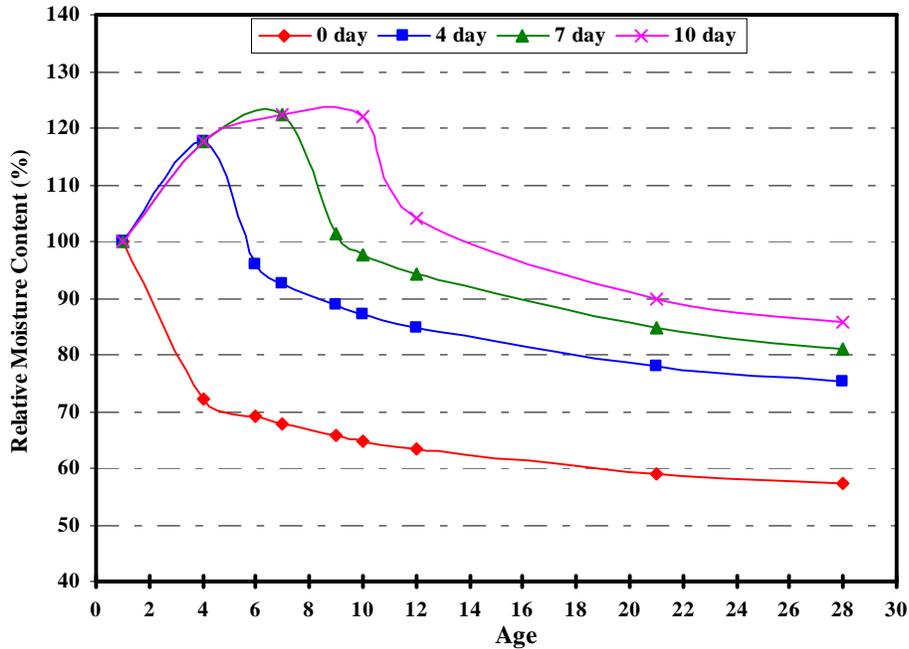
Figure 3.46 Moisture content relative to day-1 for Lubbock district mix
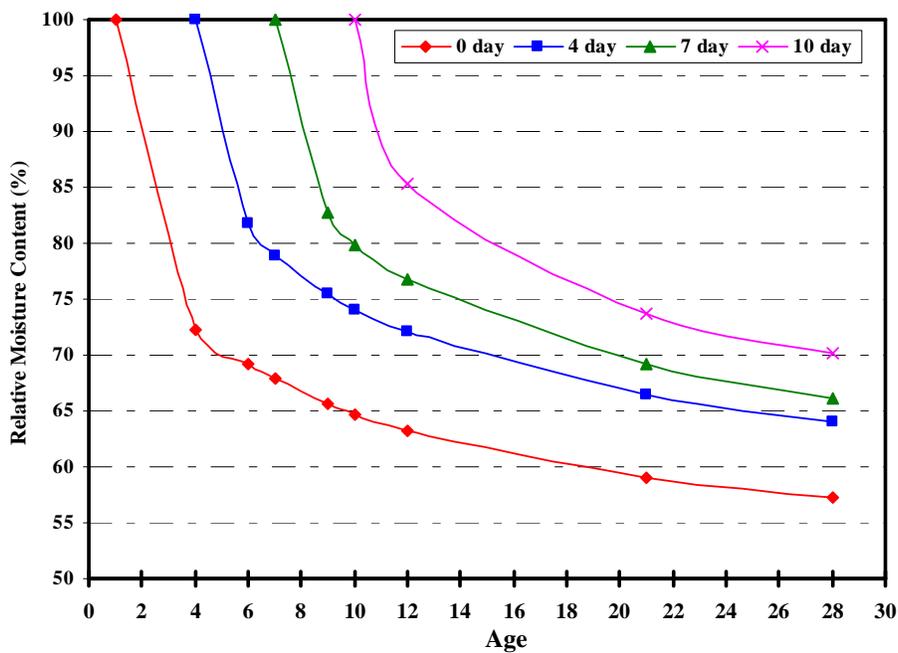
Figure 3.47 Relative moisture content (drying) for Lubbock district mix

3.3.1.5 Comparison of Different Mixes

Using the drying relative moisture content data obtained from section 3.3.1.4 and the drying shrinkage data obtained from section 3.3.1.3, a comparison is made between the behaviors of three different district mixes, i.e., Pharr, Fort Worth and Lubbock. For this comparison, relative moisture content vs. drying shrinkage strain plots have been made for different curing durations.

Here, if for a particular loss in moisture content, if one the mix shows a greater shrinkage strain, that suggests that the material properties of that mix have a greater tendency to shrink compared to the other. Using this approach the three district mixes have been compared. Figures 3.48 and 3.49 show the relative moisture content vs. drying shrinkage plots for 4 and 7 days curing duration respectively for Pharr, Fort Worth and Lubbock district mixes. The ambient R.H. for Pharr mix was around 70% and for Fort Worth and Lubbock mix it was around 50%.
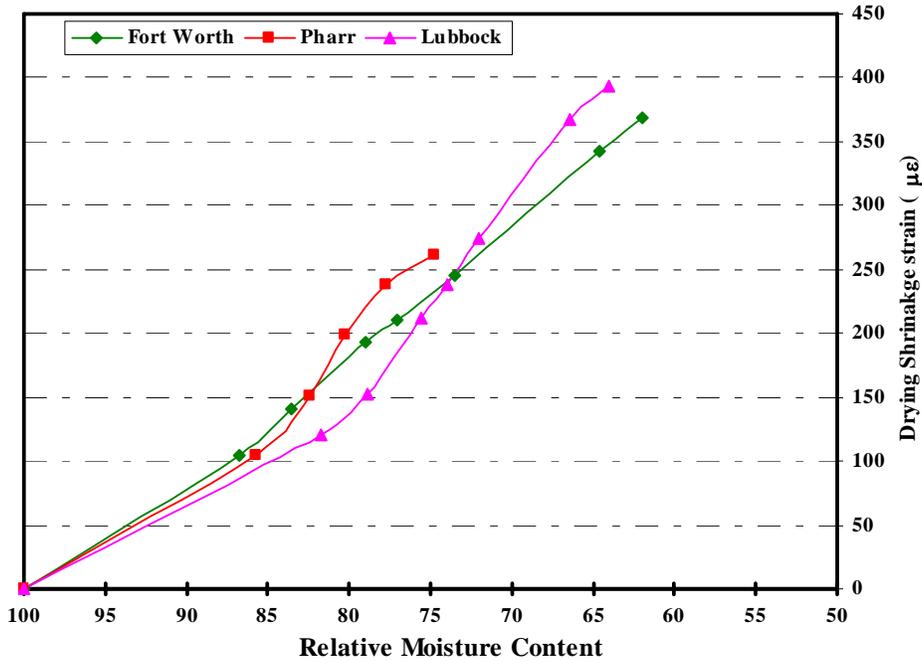
Figure 3.48 Relative moisture content (drying) vs. drying shrinkage strain for 4-day cure
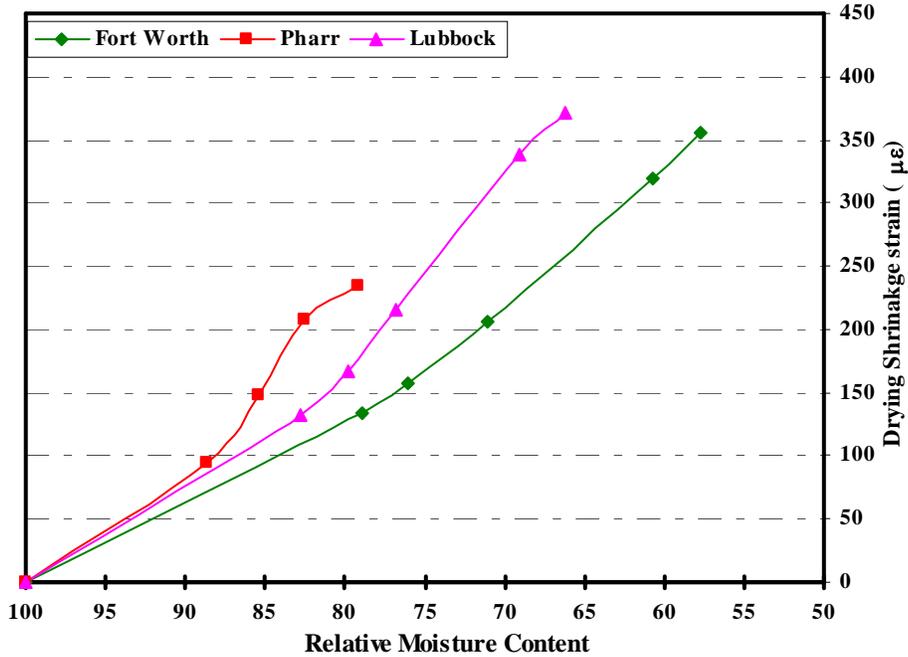
Figure 3.49 Relative moisture content (drying) vs. drying shrinkage strain for 7-day cure

Apart from plotting relative moisture content versus drying shrinkage strain for comparison, age vs. shrinkage strain (24 h) was also plotted to compare the three district mixes. The age vs. shrinkage strain (24 h) plots comparing Pharr, Fort Worth and Lubbock district mixes are shown in Figures 3.50 and 3.51 for 4 and 7 days of cure, respectively. However, it should be noted that Pharr was dried at around 70% ambient relative humidity and Fort Worth and Lubbock were dried at around 50% ambient relative humidity.

Fort Worth and Lubbock district, showed similar free shrinkage strain values for both 4 and 7 days of curing. Pharr showed less shrinkage strain (24 h) compared to Fort Worth and Lubbock but it can however be due to the high ambient relative humidity at which it was dried.
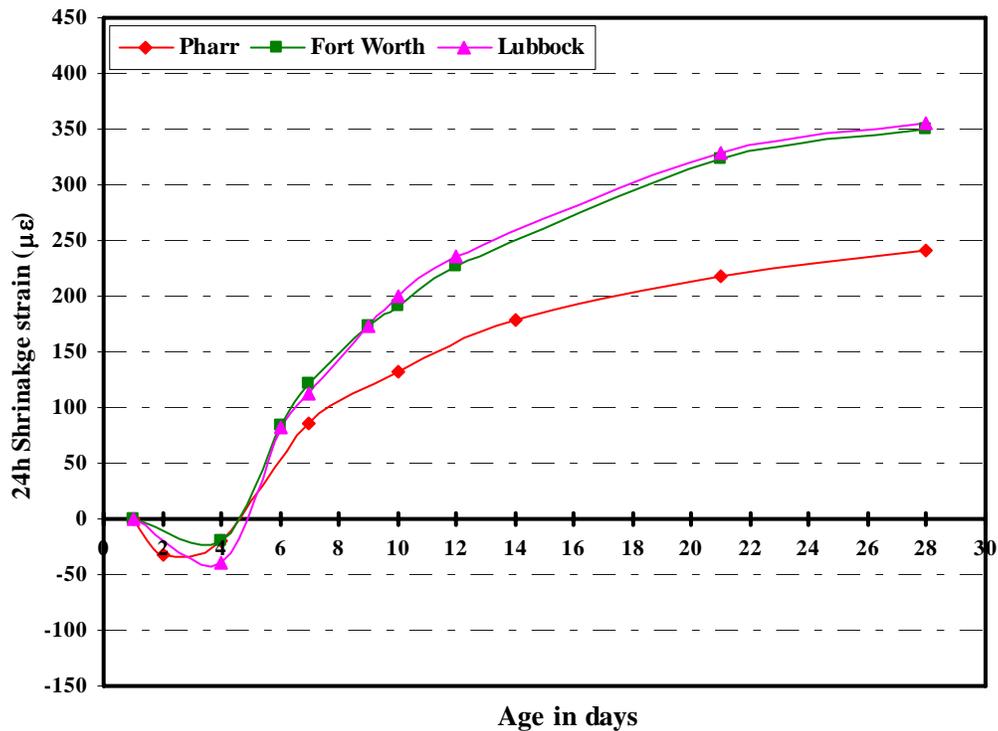
Figure 3.50 Age versus shrinkage strain (24 h) for 4-day cure
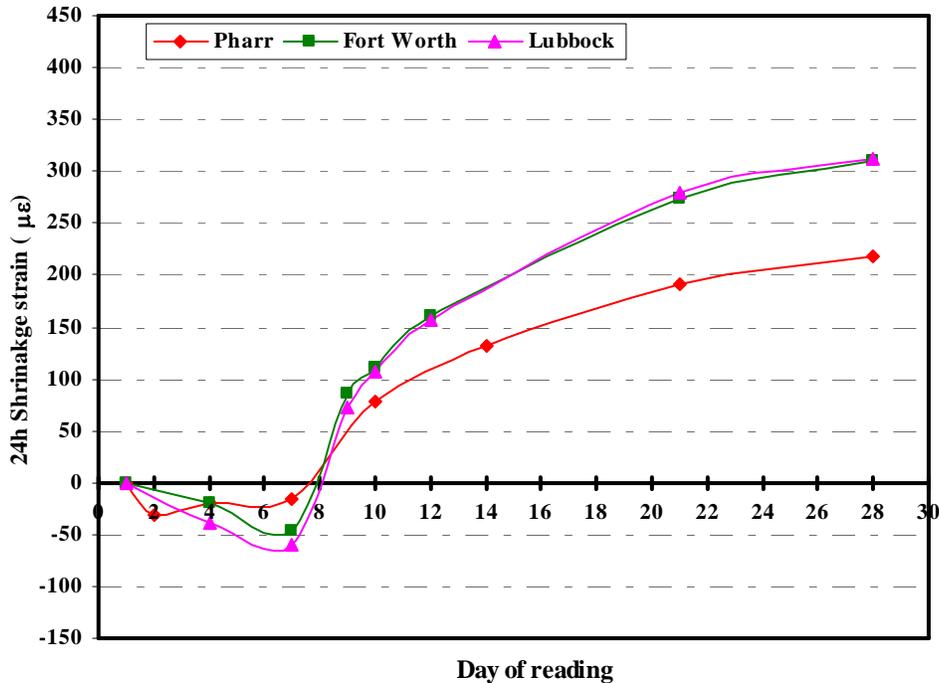
Figure 3.51 Age versus shrinkage strain (24 h) for 7-day cure

3.3.1.6 Summary and Conclusions

The observations made from the free linear shrinkage tests, without considering the stress development due to restraint or the tensile strength will be summarized in this section and the conclusions thus far will be discussed.

Figures 3.32, 3.33 and 3.34 show the comparison of 0, 2, 4, 7, 10 and 14 days curing duration for Atlanta, Houston, and Pharr district mixes, respectively. The curves for 0-day and 2-day cure for these mixes do not show a significant difference in the shrinkage strain values, suggesting that 2-day cure does not help much compared to 0-day. Therefore, 2-day cure was eliminated from the tests conducted on other district mixes. For the tests conducted on all the mixes excluding Fort Worth and Lubbock district mix, 14-day cure was also tested. However, 14- day cure was not considered for comparison in Lubbock and Fort Worth district mixes.

There was no significant difference between 0 and 4 day cure for the free shrinkage strain for all the district mixes except El Paso mix (Figure 3.29). The possible reason for this could be the use of 50% GGBS (slag) in the El Paso mix design which takes longer than Portland cement to hydrate [Section 2.4.1]. In the 0-day cure, the drying begins immediately after demolding. In the case of El Paso mix, where hydration of slag starts much later, no water is available to replace the water taken by the process of hydration of slag. This leads to self-desiccation of concrete resulting in an increased shrinkage strain compared to the concrete cured at least for 4 days.

Free shrinkage strain (24 h) for various curing durations for different district mixes from Figures 3.12 to 3.18 and drying shrinkage strain values for various curing durations for Pharr, Fort Worth and Lubbock district mixes from Figures 3.39, 3.40 and 3.41 respectively, were compared. From

the comparison, no significant decrease in the shrinkage strain with increase in the curing duration was observed. However, Houston and El Paso show a noticeable decrease in shrinkage strain with increase in curing duration but free shrinkage strain alone is not enough to understand the significance of this decrease.

From Figures 3.48 and 3.49, no significant difference between drying shrinkage strain values for different mixes was observed for 4 and/or 7 day cure. Figures 3.50 and 3.51 showing the shrinkage strain (24 h) versus age of concrete for 4 and 7 day cure respectively do not show much difference in the shrinkage strain (24 h) values for Fort Worth and Lubbock mixes. They show low shrinkage strain (24h) values for Pharr district mix but this low free shrinkage strain is perhaps due to high ambient relative humidity of 70% while drying. Therefore, from Figures 3.48 and 3.50 for 4 day curing it can be concluded that ambient relative humidity had a greater effect on the free shrinkage strain compared to the material properties.

From this discussion, it is clear that free shrinkage strain test is effective enough to compare different mix designs but to understand the effect of curing duration, additional testing is necessary to estimate the development of shrinkage tensile stresses and tensile strength. Therefore, modulus of elasticity and splitting tensile strength tests were conducted to estimate the age of first shrinkage-induced crack.

3.3.2 Modulus of Elasticity Tests (Modified ASTM C 469-94)

3.3.2.1 Discussion of Results

Modulus of elasticity was calculated using Eq. 2.29. The modulus of elasticity values in ksi. for El Paso, San Antonio, Fort Worth and Lubbock district mixes are given in Tables 3.36, 3.37, 3.38, and 3.39, respectively. Modulus of elasticity versus age of concrete, plots for El Paso, San Antonio, Fort Worth and Lubbock are shown in Figures 3.52, 3.53, 3.54, and 3.55.

Table 3.36 Modulus of elasticity in ksi for El Paso

Curing days	Age in days			
	0	4	7	16
0	0	5409*	5115	4835
4	0	5368	5293	5371
7	0	5368	5516	5291
14	0	5368	5516	5778

* Represents the values that are an average of two specimens

Table 3.37 Modulus of elasticity in ksi for San Antonio

Modulus of elasticity in KSI				
Curing days	Age in days			
	0	4	7	16
0	0	5627*	5699*	5937*
4	0	6028*	6118*	6042*
7	0	6028*	5618*	6313*
14	0	6028*	5618*	5801*

* Represents the values that are an average of two specimens

Table 3.38 Modulus of elasticity in ksi for Fort Worth

Modulus of elasticity in ksi									
Curing	Age in days								
Day	0	1	4	6	7	9	10	12	21
0	0	4176*	4756	--	4831	--	--	5097	5402
4	0	4176*	5102	5140	--	5286	--	5370	5472
7	0	4176*	5102	--	5295	5374	--	5448*	5565
10	0	4176*	5102	--	5295	--	5611	5617	5634

* Represents the values that are an average of two specimens

Table 3.39 Modulus of elasticity in ksi for Lubbock

Modulus of elasticity in ksi									
Curing	Age in days								
Day	0	1	4	6	7	9	10	12	21
0	0	4012	4807	--	4789	--	--	4885	4717
4	0	4012	5151	5100	--	5164	--	4986	4970
7	0	4012	5151	--	5348	5163	--	5417	4957
10	0	4012	5151	--	5348	--	5248	5245	5149

* Represents the values that are an average of two specimens
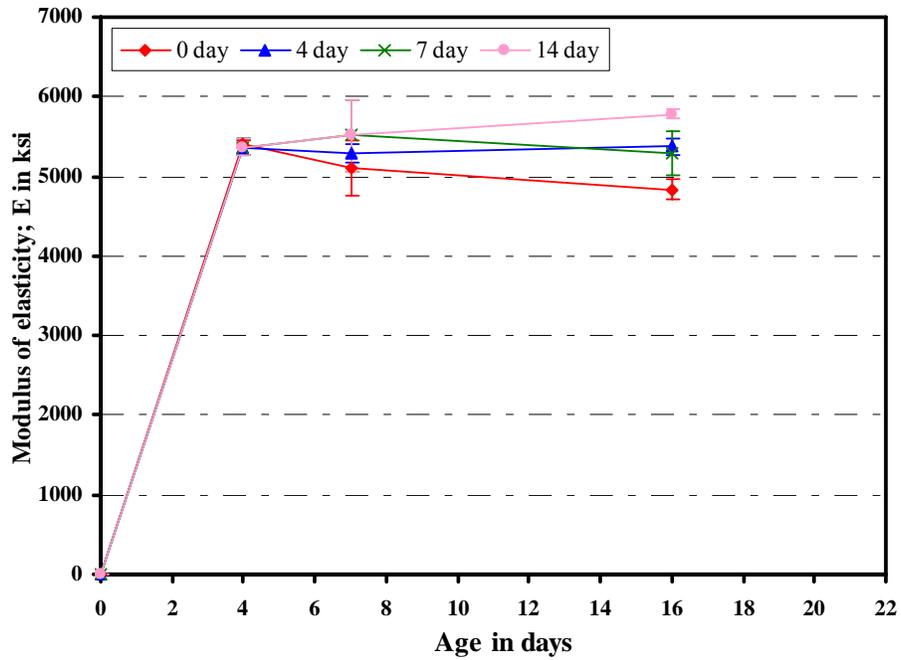
Figure 3.52 Modulus of elasticity in ksi versus age in days for El Paso district mix
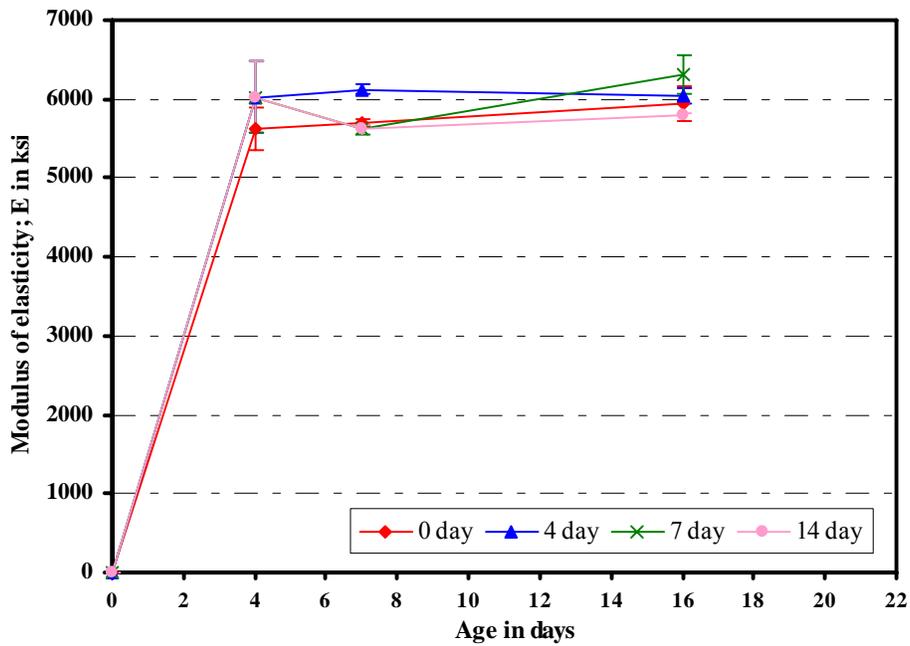
Figure 3.53 Modulus of elasticity in ksi versus age in days for San Antonio mix
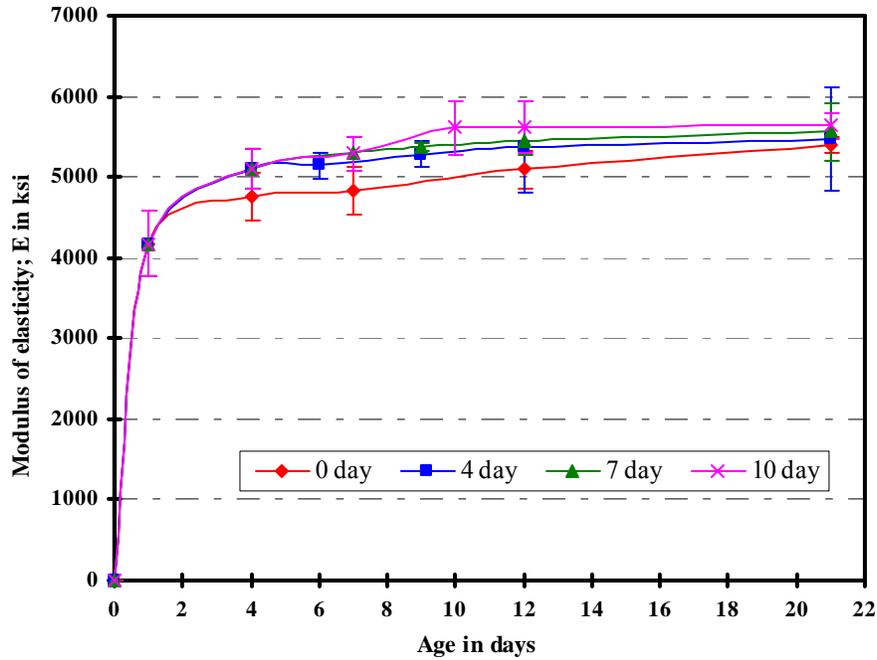
Figure 3.54 Modulus of elasticity in ksi versus age in days for Fort Worth district mix
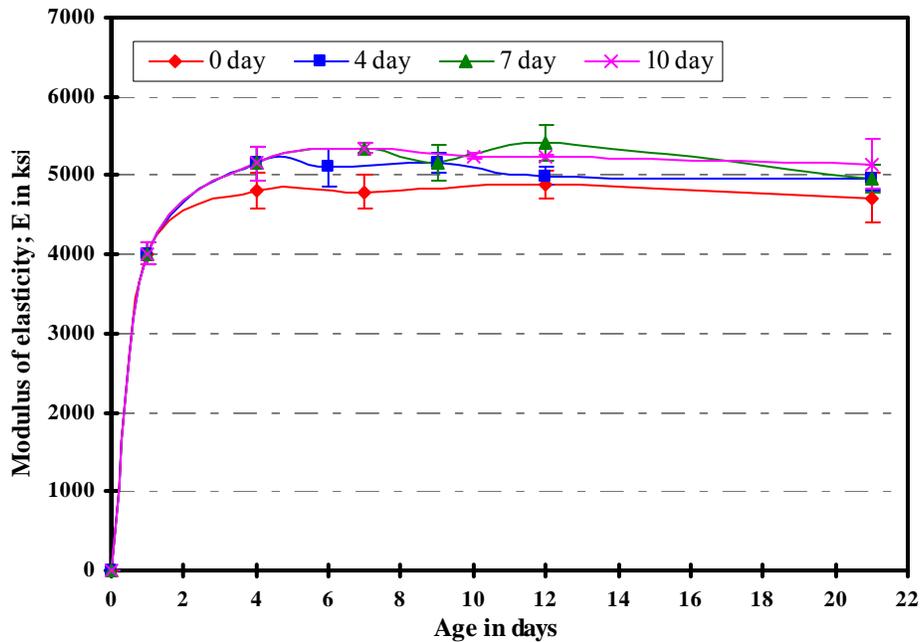
Figure 3.55 Modulus of elasticity in ksi versus age in days for Lubbock district mix

3.3.2.2 Summary and Conclusions

From the modulus of elasticity values obtained for different curing durations for all district mixes, it can be observed that curing duration did not have a significant effect on the modulus of elasticity. It can also be observed that for all curing durations, there is no significant increase in the modulus of elasticity after day 4.

3.3.3 Split Tensile Strength Tests

3.3.3.1 Discussion of Results

Split tensile strength values are calculated using Eq. 2.30. These values in lbf/sq.in. for El Paso, San Antonio, Fort Worth and Lubbock are given in Tables 3.40, 3.41, 3.42, and 3.43, respectively. Split tensile strength versus age of concrete, plots are for El Paso, San Antonio, Fort Worth, and Lubbock mixes are shown in Figures 3.51, 3.52, 3.53, and 3.54.

Table 3.40 Split tensile strength in psi for El Paso district mix

Splitting tensile strength in psi				
Curing days	Age			
	0	4	7	16
0	0	243*	346*	382*
4	0	346	415	464*
7	0	346	417*	520*
14	0	346	417*	409*

* Represents the values that are an average of two specimens

Table 3.41 Split tensile strength in psi for San Antonio district mix

Splitting tensile strength in psi				
Curing days	Age			
	0	4	7	16
0	0	357*	302*	336*
4	0	417*	439*	337*
7	0	417*	372*	574*
14	0	417*	372*	403*

* Represents the values that are an average of two specimens

Table 3.42 Split tensile strength in psi for Fort Worth district mix

Splitting tensile strength in psi									
Curing days	Age								
	0	1	4	6	7	9	10	12	21
0	0.0	307.3*	335.2	--	320.4*	--	--	336.1	318.0
4	0.0	307.3*	352.0	344.3	--	384.3	--	399.4	383.8
7	0.0	307.3*	352.0	--	356.7*	386.3	--	407.1	381.2
10	0.0	307.3*	352.0	--	356.7*	--	358.5*	372.7	418.3*

* Represents the values that are an average of two specimens

Table 3.43 Split tensile strength in psi for Lubbock district mix

Splitting tensile strength in psi									
Curing	Age								
days	0	1	4	6	7	9	10	12	21
0	0.0	213.9	283.9*	--	329.5	--	--	348.1	332.5
4	0.0	213.9	320.8	316.3*	--	333.2	--	367.3	409.1
7	0.0	213.9	320.8	--	331.7	356.6*	--	395.8	396.7
10	0.0	213.9	320.8	--	331.7	--	338.3	371.3*	366.5

* Represents the values that are an average of two specimens
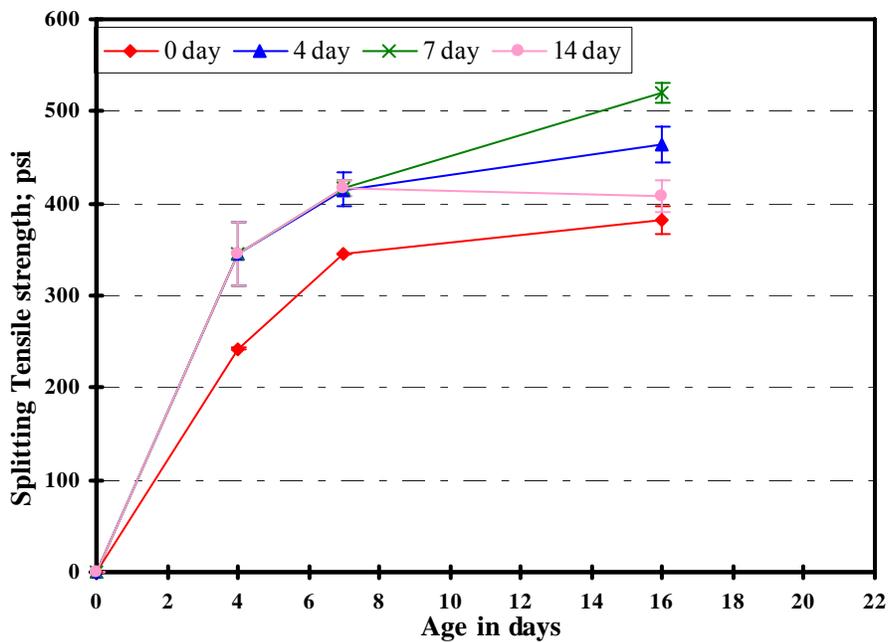
Figure 3.56 Split tensile strength in psi versus age in days for El Paso district mix
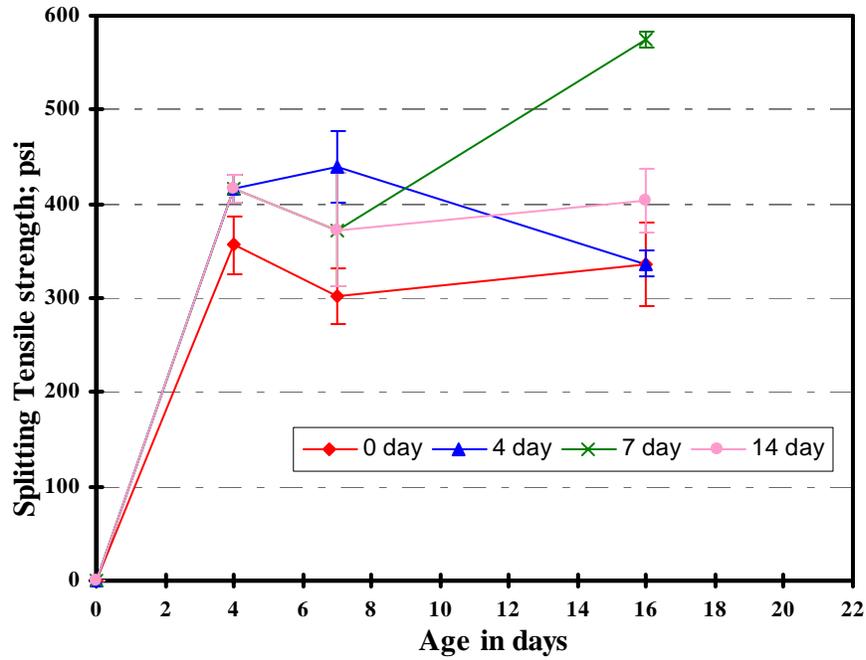
Figure 3.57 Split tensile strength in psi versus age in days for San Antonio mix
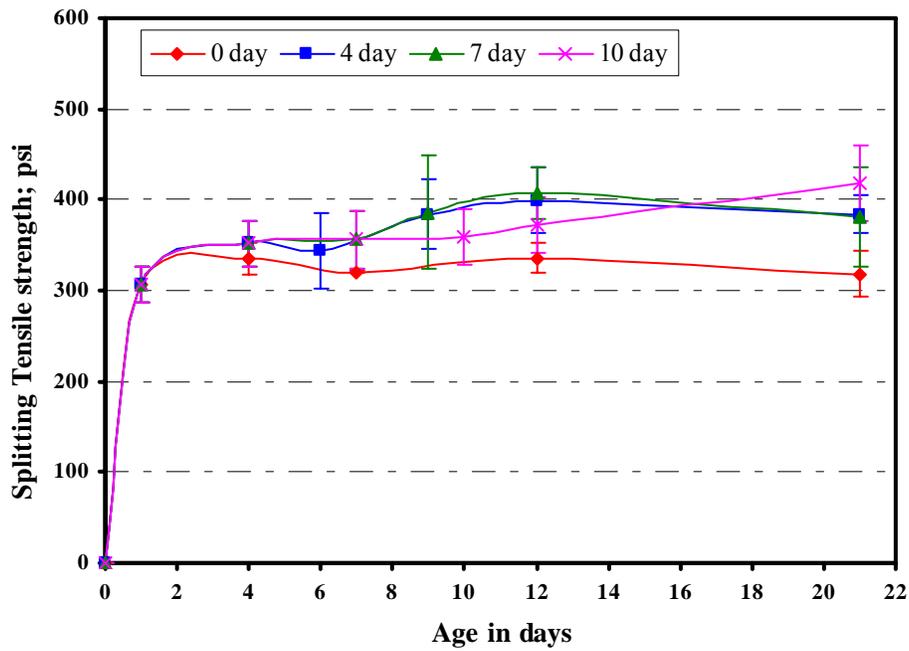
Figure 3.58 Split tensile strength in psi versus age in days for Fort Worth district mix
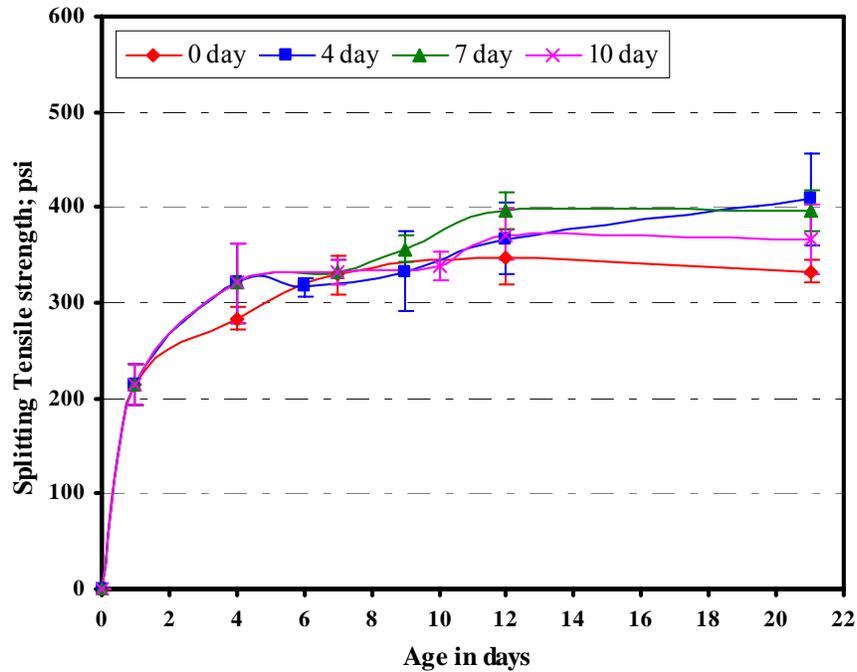
Figure 3.59 Split tensile strength in psi versus age in days for Lubbock district mix

3.3.3.2 Summary and Conclusions

The split tensile strength plots for El Paso and San Antonio show a large amount of variability. However, they do not show any significant effect of curing duration. The split tensile strength plots for Fort Worth and Lubbock district mixes are in a range of 300 to 450 psi, showing no significant effect of curing duration. Split tensile strength values do not show a significant development in strength after day 4 for any curing duration, similar to modulus of elasticity values for these mixes.

CHAPTER IV

CONCLUSIONS AND RECOMMENDATIONS

4.1. CONCLUSIONS

4.1.1 Fracture

4.1.1.1 Field-Cast Notched Cylinders

From the data obtained by testing field-cast notched cylinders, it is apparent that the concrete gets more brittle with increased duration of curing, at least at the test age of 28 days. The gain in strength with increased curing is not significant beyond 4 days of curing for this size of specimen, and the trends are much sharper than those obtained in the field-cast flexural beam tests. Furthermore, it would be erroneous to conclude from the data obtained that concrete, in general, is getting stronger in fracture with increased duration of curing, as tests on cylinders of larger diameter may have resulted in entirely different trends.

4.1.1.2 Size-Effect Tests at 16-Day Age and 7-Day Age

Size-effect testing at 16-day age and 7-day age shows that concretes with relatively large amounts of slag, or possibly, fly ash, take a long duration to cure, and have smaller fracture strengths than other types of concretes. Concretes made from Type I cement that do not contain any fly ash are more brittle than concretes containing Type I/II cement and fly ash. Since strengths of mix designs are heavily influenced by the compatibilities of the ingredients, statements about the effects of class of fly ash, or the relative amounts of fly ash within the ranges examined, are not made.

At 7 days of age, most concretes tested seem to have gained fracture strength and increased in size of fracture process zone upon increased duration of curing. However, at 16 days of age, concretes that produce specimens with larger failure loads have started to become more brittle and lose fracture toughness when the duration of curing is increased. The clear exception to the above is the concrete with a relatively large (50%) slag content, which is still gaining fracture toughness and becoming less brittle upon increased duration of curing. It is highly probable that for some concretes there is an optimal level of hydration beyond which the fracture toughness starts to drop.

The dissimilar trends in the fracture loads found for different sizes of cylinders tested brings doubts to the validity of conclusions made in published research based on one size of specimen, and surprisingly, these include recently published studies. The invalidity of testing methods which cannot separate the two controlling parameters of fracture toughness and size of fracture process zone is thus stressed. Furthermore, it appears that both the implications and magnitudes of size-effects are under-estimated, considering that most structural codes have restrictions on tensile stress levels of concretes, and the tensile strengths of concretes are determined on relatively small specimens and extrapolated to larger structures. It would be desirable to include size-effects in design codes, though a careful evaluation first has to be carried out to determine whether the added complications are compensated by more accurate estimates of safety factors.

4.1.1.3 Fatigue Testing

It was found that there is a distinct upward trend in the number of cycles to failure of cylinders as duration of curing is increased for data generated at the testing age of 28 days. A less marked increase in the number of cycles to failure with increased duration of curing was observed at 10-day age. It should be pointed out that for many concretes, the cylinders tested under static loading at 7-day age showed decreased failure loads with increased duration of curing, while the trend was reversed at 16-day age. The test data generated at the age of 10 days reflect the static loads to failure of the cylinders at this age, because there is a strong correlation between static failure loads and fatigue strength. As in section 5.1.1.2, a statement that the fatigue strength of concretes increases with increased duration of curing based on the data from 28-day age testing would be inaccurate, and it is believed that some previous studies in fatigue have made similar mistaken conclusions.

4.1.1.4 Absorption-Desorption Tests

Concretes containing Type I cement and no fly ash show smaller increases in hydration levels from curing beyond 8 days, while concretes containing Type I/II cement and fly ash show small improvements in hydration levels from curing beyond 8 days. Testing on larger specimens delivered absorption-desorption data that was less sensitive to curing duration than data generated from smaller specimens, and it seems logical to conclude that bridge decks are less sensitive to curing durations as far as hydration levels are concerned, because of their relatively large size when compared to specimens. It is possible to use the desorption characteristics of specimens conveniently to develop accurate estimates of relative hydration levels without resorting to the oven drying of specimens.

4.1.1.5 Tests to Determine Effects of Varying Thickness of Size-Effect Specimens

It has been proven that buckling type effects do not significantly affect the nominal stresses at failure of fracture specimens cured to the same hydration levels but are of different lengths, though specimens cured for shorter durations hydrate to different levels depending on lengths of specimens. The differences in hydration levels of specimens of different lengths can lead to differences in fracture strengths for certain combinations of concretes, curing durations, and testing ages, as demonstrated. The logical conclusion would be that it is desirable to change lengths of cylinders in such a manner that differential curing and drying is minimized. The current philosophy of curing test specimens for long duration until the time of tests leads test specimens to be non-representative of structures, especially ones with large surface areas like bridge decks. Even concrete in structures that are relatively thick are affected by self desiccation, and as test specimens used in fracture tests can be as thin as 2 inches, continued curing of specimens leads to hydration levels beyond what is found in structures. Comparison of concretes based on such specimens is inaccurate as curing seems to affect different concretes to different levels, and specimens are usually tested in a saturated condition, whereas structures are usually not permanently saturated. Studies have shown that saturated specimens behave differently to air-dry specimens in fracture and fatigue. The only way to effectively address these shortcomings is to dimension the specimens according to the scheme proposed in this dissertation, and curtail curing at a point in time to ensure that hydration levels of the specimens and the structure the concrete is being tested for are similar at the age the testing is carried out.

4.1.1.6 Comparison of Jenq-Shah Model and Size-Effect Law

Though there are publications detailing how the two-parameter model can be used in experimentation carried out on notched-cylinders to determine the fracture properties of concrete, the procedures outlined are flawed because of the practical difficulties experienced in measuring the CMOD accurately. However, it has been shown in studies that size-effect in the case of notched cylinders can be successfully predicted by the two-parameter model.

4.1.2 Flexure

Based on the results obtained in the flexural strength tests, it is concluded that, in general, flexural strength seems to increase with increased duration of curing. The scatter in the data obtained from field-cast specimens is rather high, and the practice of having a flexural strength test as an acceptance criterion by DOTs seems to be questionable. Largely from the work carried out in subsequent sections of this dissertation, it seems highly probable that testing of flexural strengths from specimens of different size may lead to different trends in the variation of flexural strengths with duration of curing being obtained.

4.1.3 Shrinkage

It is concluded from results of free shrinkage tests presented in Chapter 3 that a certain amount of decrease in free shrinkage strain was observed with increase in curing duration. However, other tests were conducted to understand the significance of this decrease in free shrinkage. The decrease in free shrinkage with increase in curing duration was more profound in El Paso district mix with 50% GGBS. This could be attributed to the slow hydration of GGBS, increasing the autogenous shrinkage of concrete due to continued hydration of cement and GGBS even after concrete is allowed to dry.

From the weight measurements taken to compare three different district mixes, i.e., Pharr, Fort Worth and Lubbock mixes it has been observed that the ambient relative humidity made a greater effect on the free shrinkage strain than any particular material properties.

Modulus and split tensile strength tests have been conducted to assist in the prediction of age of first shrinkage-induced crack to better understand the effects of curing duration on restrained shrinkage cracking. Moduli of elasticity results discussed in Chapter 4 do not indicate a significant difference with an increase in curing duration in controlled lab conditions. It is also observed that there is no noticeable increase in the modulus of elasticity after an age of 4 days for any curing duration. However, the moduli of elasticity values being used for predicting tensile stresses were calculated from compression tests assuming that modulus of elasticity of concrete is same for both tension and compression.

Split tensile strength results discussed in Chapter 3 also did not show any significant increase with increase in curing duration. Thus, it can be said that no significant improvement in the tensile strength can be achieved by an increase in curing duration over 4 days. The split tensile strength results also indicate that there is no noticeable increase in the split tensile strength after an age of 4 days for any curing duration.

Prediction of age of first shrinkage-induced crack, with and without creep considerations, was discussed in Chapter 3. From the prediction of the age of first shrinkage-induced crack without creep considerations, no noticeable delay in the age of first crack was observed from an increase in curing duration. However, when creep relaxation is considered, a noticeable delay in the age of first crack from an increase in curing duration was observed.

When creep relaxation was considered a significant increase in the age of first shrinkage-induced crack was observed from an increase in curing duration from 4 days to 10 days. However, the difference between the effects of 4 day and 7 day curing duration on shrinkage-induced cracking is not significant as indicated by the age of first shrinkage-induced crack values.

Based on the above discussion it can be concluded that 4 day cure from shrinkage perspective, is sufficient for bridge decks with mixes using Type I or III cements without fly ash, as these bridge decks are currently being cured for 8 days in Texas. However, conducting restrained tests would be beneficial the change in curing duration can be implemented

It can also be concluded that from shrinkage perspective 4 day cure can also be used for bridge deck mixes with Type II or I/II cements or for bridge deck mixes with fly ash as cement type or fly ash content is not expected to make any significant effect on shrinkage of concrete. However, additional parametric study on cement types and fly ash contents from shrinkage perspective would be beneficial before the change in curing duration is implemented for these mixes.

4.2 RECOMMENDATIONS

4.2.1 Fracture and Flexure

It appears that there cannot be significant improvements in the fracture properties of medium-strength bridge-deck concrete beyond 4 days of curing, excepting perhaps concretes containing relatively large amounts of slag. In fact, there could be negative effects from curing beyond 4 days, because the creep capabilities of concretes are adversely affected, and stiffness is increased, making it hard for brittle concretes to withstand the effects of restrained shrinkage. It is therefore recommended that bridge decks made from medium-strength concretes be cured for approximately 4 days, with the exception of those containing large amounts of slag, with the note that further testing on such concretes be carried out to determine the variations of the other durability characteristics with duration of curing.

It has been shown that there are many shortcomings in the current testing philosophies of fracture properties of concrete, and the lack of consideration of size-effects in design, and it is recommended that these practices be closely evaluated to produce better designs of structures and to aid in the choice of concrete materials.

4.2.2 Shrinkage

While the approach used in this thesis to predict the age of first shrinkage-induced crack to comparing different curing durations is considered accurate enough to comparatively predict the restrained shrinkage crack density in bridge decks, further work on restrained shrinkage tests is warranted. Concrete slabs can be cast and a restraint can be applied to simulate the restraint experienced by the bridge decks from the structure.

Additional study to understand the tensile stress development behavior considering creep relaxation would be beneficial. Further work can be performed to better assist in the understanding the effect of shrinkage reducing admixtures on reducing the detrimental effects caused by shrinkage. The use of different types of fibers can also be studied as a method to reduce the overall bridge deck crack density. Tests can be performed to understand the effects of fibers on tensile strength of concrete.

REFERENCES

Abendroth, R. E. (1995), "Nominal Strength of Composite Prestressed Concrete Bridge Deck Panels," *Journal of Structural Engineering*, Vol. 121, No. 2, February, ASCE. pp. 307-318.

ACI (1992), "*318/318R-85*, Building Code and Commentary", American Concrete Institute, Farmington Hills, Mich 1992, quoted in Haque, M.N., 1998, "Give it a Week: 7 Days Initial Curing," *Concrete International*, September, ACI. pp. 45-48.

Altoubat S. A., Lange D. A. (2001). Creep, shrinkage, and cracking of restrained concrete at early ages. *ACI Materials Journal*, Vol. 98, No. 4, pp. 323 – 331.

ASTM (2000a), "C150-99: Standard Specification for Portland Cement," *Annual Book of ASTM Standards*, Vol. 04.01, Philadelphia, Pennsylvania.

ASTM (2000b), "C 618-99: Standard Specification for Coal Fly Ash and Raw or Calcined Natural Pozzolan for Use as a Mineral Admixture in Portland Cement Concrete," *Annual Book of ASTM Standards*, Vol. 04.02, Philadelphia, Pennsylvania.

ASTM (2000c), "C 496-96: Standard Test Method for Splitting Tensile Strength of Cylindrical Concrete Speciemens," *Annual Book of ASTM Standards*, Vol. 04.02, Philadelphia, Pennsylvania.

ASTM (2000d), "C 192/C 192M: Standard Practice for Making and Curing Test Specimens in the Laboratory," *Annual Book of ASTM Standards*, Vol. 04.02, Philadelphia, Pennsylvania.

ASTM (2000e), "C 78-94: Standard Test Method for Flexural Strength of Concrete (Using Simple Beam with Third Point Loading)," *Annual Book of ASTM Standards*, Vol. 04.02, Philadelphia, Pennsylvania.

ASTM (2000f), "C 469-94: Standard Test Method for Static Modulus of Elasticity and Poisson's Ratio of Concrete in Compression," *Annual Book of ASTM Standards*, Vol. 04.02, Philadelphia, Pennsylvania.

Bazant, Z. P.; Kazemi, M. T.; Hasegawa, T., and Mazars, J. (1991), "Size Effect in Brazilian Split-Cylinder Test: Measurement and Fracture Analysis," *ACI Materials Journal*, Vol. 88, No. 3, May-June.

Bazant, Z. P.; Ozbolt, J., and Eligehausen, R. (1994), "Fracture Size Effect: Review of Evidence for Concrete Structures," *Journal of Structural Engineering*, Vol. 120, No. 8, August, ASCE, pp. 2377-2398.

Bazant, Z., and Planas, J. (1998), *Fracture and Size Effect in Concrete and Other Quasibrittle Materials*, CRC Press, New York.

Bazant, Z.P., and Schell, W. F. (1993), "Fatigue Fracture of High-Strength Concrete and Size Effect," *ACI Materials Journal*, American Concrete Institute, V. 90, September - October.

Bazant Z. P. and Wittmann F. H. (1983). *Creep and Shrinkage in concrete structures.* John Wiley & Sons Ltd, New York.

Bazant, Z.P., and Xu, K. (1991), "Size Effect in Fatigue Fracture of Concrete," *ACI Materials Journal*, V. 88, No. 4, July-August 1991.

Broek, D. (1986), *Elementary Engineering Fracture Mechanics*, 4th ed., Martinus Nijhoff Publishers, Dordrecht, p. 501., quoted in Ramsamooj, D.V. (2002), "Analytical Model for Fatigue Crack Propagation in Concrete," *Journal of Testing and Evaluation*, JTEVA, V. 30, No. 4, July, pp. 340-349.

Carden A. C., and Ramey G. E. (1999). Weather exposure and its effect on bridge deck curing in Alabama. *Practice Periodical on Structural Design and Construction*, Vol. 4, No. 4, pp. 139 – 146.

Chen, W. F., and Yuan, R. L. (1980), "Tensile Strength of Concrete: Double-Punch Test," *Journal of the Structural Division*, ASCE, V. 106 ST8, Aug., pp. 1673-93., quoted in, Bazant, Z. P.; Kazemi, M. T.; Hasegawa, T., and Mazars, J. (1991), "Size Effect in Brazilian Split-Cylinder Test: Measurement and Fracture Analysis," *ACI Materials Journal*, V. 88, No. 3, May-June.

Csagoly, P., Holowka, M., and Dorton, R. (1978), "The True Behavior of Thin Concrete Bridge Slabs," *Transportation Research Record 664*, Transportation Research Board, pp. 171-174.

Darwin, D.; Barham, S.; Kozul, R., and Luan S. (2001), "Fracture Energy of High-Strength Concrete," *ACI Materials Journal*, V. 98, No. 5, September-October, pp. 410-417.

French C., Eppers L., Quoc Le, and Hajjar J. F. (1999). Transverse cracking in concrete bridge decks. *Transportation Research Record*, No. 1688, pp. 21 – 29.

Garcia H. M. (2003). *Maturity of concrete – strength* development. M.S. thesis, Department of Civil Engineering, Texas Tech University.

Garcia, H. (2002), Personal Communication, Texas Tech University, Lubbock, Texas.

Garcia, H. (2003), Personal Communication, Texas Tech University, Lubbock, Texas.

Gettu, R.; Bazant, Z. P., and Karr, M. E. (1990), "Fracture Properties and Brittleness of High-Strength Concrete," *ACI Materials Journal*, V. 87, No. 6, November - December, pp. 608-618.

Haque, M.N. (1998), "Give it a Week: 7 Days Initial Curing," *Concrete International*, September, ACI, pp. 45-48.

Hondros, G. (1959), "Evaluation of Poisson Ratio and the Modulus of Materials of Low Tensile Strength Resistance by the Brazilian (Indirect Tensile) Strength Test with Particular Reference to Concrete," *Australian Journal of Applied Science,* V.10, No. 3, 1959, pp.243-268. quoted in Bazant, Z. P.; Kazemi, M. T.; Hasegawa, T.; and Mazars, J., 1991, "Size Effect in Brazilian Split-Cylinder Tests: Measurement and Fracture Analysis," *ACI Materials Journal*, V. 88, No. 3, May-June.

Jenq, Y., and Shah, S.P. (1985), "Two Parameter Fracture Model for Concrete," *Journal of Engineering Mechanics*, V. 111, No. 10, October, pp. 1227-1241.

Issa M. A. (1999). Investigation of cracking in concrete bridge decks at early ages. *Journal of Bridge Engineering*, Vol. 4, No. 2, pp. 116 – 124.

Issa M.A., Shafiq, A.B. (1999), "Fatigue Characteristics of Aligned Fiber Reinforced Mortar," *Journal of Engineering Mechanics*, V. 125, No. 2, February, ASCE, pp. 156-164.

Koenders E. A. B. (1997). *Simulation of volume changes in hardening cement-based materials.* PhD dissertation, Civil Engineering Department, Delft University of Technology.

Kwak H. -G., Seo Y. -J., Jung C. -M. (2000). Effects of slab casting sequences and the drying shrinkage of concrete slabs on the short-term and long-term behavior of composite steel box girder bridges. Part 2. *Engineering Structures*, Vol. 22, No. 11, pp. 1467 – 1480.

Li, Q., and Ansari, F. (2000), "High-Strength Concrete in Uniaxial Tension," *ACI Materials Journal* V. 97, No.1, January-February, pp. 49-57.

MacGregor, J.G. (1996), *Reinforced Concrete Mechanics and Design*, Third Edition, Prentice Hall, Upper Saddle River, New Jersey 07458.

Manning D. G. (1981). Effect of traffic induced vibrations on bridge deck repairs. *N.C.H.R.P. Synthesis of highway practice*, No. 86, pp 40

Mufti, A.A., and Newhook, J.P. (1999), "On the Use of Steel-Free Concrete Bridge Decks in Continuous Span Bridges," *Canadian Journal of Civil Engineering*, Vol. 26, No. 5, October, National Research Council of Canada, Ottawa, pp. 667-72.

Murakami, Y. (1987), Editor-in-Chief, *Stress Intensity Factors Handbook*, Pergamon Press, New York., quoted in Gettu, R.; Bazant, Z. P; and Karr, M. E. (1990), Fracture Properties and Brittleness of High-Strength Concrete, *ACI Materials Journal*, V.87, No. 6, November-December, pp. 608-618.

Navalurkar, R.K.; Hsu, C.T.; Kim, S.K., and Wecharatana M. (1999), "True Fracture Energy of Concrete," *ACI Materials Journal*, V.96, No.2, March-April, pp. 213-224.

Neville, A.M. (1996), *Properties of Concrete*, Fourth and Final Edition, John Wiley & Sons, Inc, Malaysia, VVP, pp. 649-666.

Ojdrovic, R.P.; Stojimirovic, A.L., and Petroski, H.J. (1987), "Effect of Age on Splitting Tensile Strength and Fracture Resistance of Concrete," *Cement and Concrete Research*, V 17. Pergamon Press, pp. 70-76.

Ojdrovic, R. P., and Petroski, H. J. (1986), "Fracture Behavior of Notched Concrete Cylinder," *Journal of Engineering Mechanics*, V 113, No.10, October, pp. 1551-1563.

Okada, K.; Okamura, H., and Sonoda, K. (1978), "Fatigue Failure Mechanism of Reinforced Concrete Bridge Deck Slabs," *Transportation Research Record 664*, Transportation Research Board, pp. 136-144.

Parrott, L.J. (1991), "Factors Effecting Relative Humidity in Concrete," *Magazine of Concrete Research*, British Cement Association, V. 43, No. 154, pp. 45-52.

Petrou, M. F.; Harries, K. A., and Schroeder, G. E. (2001), "Field Investigation of High Performance Concrete Bridge Decks in South Carolina," *Transportation Research Record 1770*, Transportation Research Board.

Popovics, S. (1992), *Concrete Materials: Properties, Specifications and Testing*, Noyes Publications, Park Ridge, New Jersey.

Raithby K.W., and Galloway J.W. (1974), "Effects of Moisture Condition, Age, and Rate of Loading on Fatigue of Plain Concrete," *SP 41-2*, American Concrete Institutue, Detroit, pp. 15-33.

Ramachandran V. S. (1995). *Concrete Admixtures Handbook; properties, science, and technology,* 2nd edition. Noyes Publications, New Jersey.

Ramakrishnan V. (2001). Concrete plastic shrinkage-reduction potential of synergy fibers. *Transportation Research Record*, n1775, pp. 106 – 117.

Ramsamooj, D.V. (1994), "Prediction of Fatigue Life of Plain Concrete Beams from Fracture Tests," *Journal of Testing and Evaluation*, American Society for Testing and Materials, 1994.

Reed, R.L. (1978), "Application and Design of Prestressed Bridge Deck Panels," *Transportation Research Record 664*, TRB, pp. 164-167.

RILEM (1990a), "Size Effect Method for Determining Fracture Energy and Process Zone Size of Concrete," *Materials and Structures*, 23, pp. 461-465.

RILEM (1990b), "Determination of Fracture Parameters (K^s_{Ic} and $CTOD_c$) of Plain Concrete Using Three-Point Bend Tests," *Materials and Structures*, 23, pp. 457-460.

Rogalla E. A., Krauss P. D., McDonald D. B. (1995). Reducing transverse cracking in new concrete bridge decks. *Aberdeen's Concrete Construction*, Vol. 40, No. 9, pp. 735 – 738.

Sabnis, G.M., and Mirza, S.M. (1979), "Size Effects in Model Concretes?" *Journal of the Structural Division*, ASCE V. 106, ST6, 1979, pp.1007-1020., quoted in Bazant, Z,P.; Kazemi, M.T.; Hasegawa, T., and Mazars, J., (1991), "Size Effect in Brazilian Split-Cylinder Tests: Measurement and Fracture Analysis", *ACI Materials Journal*, V. 88, No. 3, May-June.

Schmitt T. R., Darwin D. (1999). Effect of material properties on cracking in bridge decks. *Journal of Bridge Engineering*, Vol. 4, No. 1, pp. 8 – 13.

Shah S. P., Marikunte S., Yang W., and Aldea C. (1997). Control of cracking with shrinkage- reducing admixtures. *Transportation Research Record*, No.1574, pp. 25 – 36.

Standards Australia (1994), "Concrete Structures-AS-3600," p.156, quoted in Haque, M.N. (1998), "Give it a Week: 7 Days Initial Curing," *Concrete International*, September, ACI. pp. 45-48.

Sule M. S. (2003). *Effect of reinforcement on early-age cracking in high strength concrete.* PhD dissertation, Civil Engineering Department, Delft University of Technology.

Tada, H.; Paris, P.C., and Irwin, G.R. (1985), *Stress Analysis of Crack Handbook*, 2nd Edition, Paris Productions St. Louis., quoted in Gettu, R.; Bazant, Z. P., and Karr, M. E. (1990) , "Fracture Properties and Brittleness of High-Strength Concrete," *ACI Materials Journal*, V.87, No. 6, November – December, pp. 608-618.

Tang, T. (2003), Personal Communication, Houston, Texas.

Tang, T. (1994), "Effects of Load Distributed Width on Split Tension of Unnotched and Notched Cylindrical Specimens," *Journal of Testing and Evaluation*, Vol. 22, No. 5, September, pp. 401-409.

Tang, T.; Ouyang, C., and Shah, S. P. (1996), "A Simple Method for Determining Material Fracture Properties from Peak Loads," *ACI Materials Journal* V. 93, No.2, March-April.

Tang, T.; Shah, S. P., and Ouyang, C. (1992), "Fracture Mechanics and Size Effect of Concrete in Tension," *Journal of Structural Engineering*, V. 118. No. 11. November, pp. 3169-3185.

Tang, T., Yang, S., and Zollinger, D. G. (1999), "Determination of Fracture Energy and Process Zone Length Using Variable-Notch One-Size Specimens," *ACI Materials Journal* V. 96, No.1, January-February.

Texas Department of Transportation (1993a), *Standard Specifications for Highways and Bridges*, Austin, Texas.

Texas Department of Transportation (1993b), *Special Specification 420,* web site - http://www.dot.state.tx.us/apps/specs/ShowAll.asp?year=1&type=SP&number=420

TxDOT (1993). *Standard specifications for construction of highways, streets and bridges.* Texas Department of Transportation, Austin, TX.

TxDOT (1998). *Special Provisions to Item 420 Concrete Structures.* Texas Department of Transportation, Austin, TX.

Wang K., Shah S. P., and Phuaksuk P. (2001). Plastic shrinkage cracking in concrete materials – influence of fly ash and fibers. *ACI Materials Journal*. Vol. 98, No. 6, pp. 458 – 464.

Weiss W. J., Yang W., and Shah S.P. (1998). Shrinkage cracking of restrained concrete slabs. *Journal of Engineering Mechanics*, Vol. 124, No.7, pp. 765 – 774.

Weiss W. J. (1999). Prediction of early-age shrinkage cracking in concrete. PhD dissertation, Civil Engineering, Northwestern University.

Weiss W. J., Yang W., and Shah S.P. (2000). Influence of specimen size/geometry on shrinkage cracking of rings. Journal *of Engineering Mechanics*, Vol. 126, No. 1, pp. 93 – 101.